Assessing the ramping behavior and system impact of wind-based hybrid power plants

Rohit Thota

TU Delft

Assessing the ramping behavior and system impact of wind-based hybrid power plants

by

Rohit Thota

in partial fulfillment of the requirements for the degree of Master of Science in
Sustainable Energy Technology at the Delft University of Technology,
to be defended publicly on September 20, 2021

Student number:	5005493	
Project duration:	November, 2020 – September, 2021	
Thesis committee:	Prof. dr. D. A. von Terzi,	TU Delft, Supervisor
	Prof. dr. Peter Palensky,	TU Delft
	Mihir Mehta,	TU Delft

Wind Energy Group, Faculty of Aerospace Engineering, Delft University of Technology
Faculty of Electrical Engineering, Mathematics and Computer Science, Delft University of Technology

Keywords: power ramp events, wind based hybrid power plant

Cover photo: Vestas

An electronic version of this thesis is available at `http://repository.tudelft.nl/`.

TU Delft

Acknowledgements

It seems like only yesterday that I arrived in Delft to begin my masters studies, but I happily look back at the wonderful time I had here and all the wonderful people I met along the road. The thesis project has been a challenging endeavor that has been both exhausting and rewarding. I am glad to be concluding my time as a TU Delft student with this project, but it wouldn't have been possible without the help of a number of people, and I would want to thank them for their assistance throughout the completion of my graduation project.

First, I would like to thank my supervisor, Professor Dominic von Terzi, for his guidance through each stage of the process. Your insightful feedback and suggestions pushed me to sharpen my thinking and brought my work to a higher level. Secondly, I would like to thank my second supervisor, Mihir for the support, numerous discussions, meticulous feedback, and engagement in the project. Their patience and abundance of knowledge were instrumental in the success of this thesis and it has been a pleasure working with them.

I am indebted to my housemates and neighbors in Prof. Schermerhornstraat for the parties, chai, and for always making me feel at home. Moreover, I want to express my gratitude to Abhishek, Amith, and Sushanth for their unwavering support and encouragement. Finally, I want to express my appreciation to Hima for motivating me and providing stimulating discussions as well as happy distractions to rest my mind outside of my research.

As my time as a student draws to a close, I'd like to express my gratitude to my parents and family for their unwavering support during my journey toward graduation. I feel grateful to know that you are always there.

Rohit Thota
Delft, September 2021

Summary

Renewable energy sources have become a cost-competitive and green option for supplying power to the grid in recent years. Nonetheless, their variable nature poses a problem to the regular operation of the electrical grid by introducing severe fluctuations of large magnitudes and/or short-duration known as ramps. There is a lack of research in the literature on characterizing ramp events induced by wind-based hybrid power plants. The main research question of this study is *how to characterize the ramping behaviour of wind-based hybrid power plants and what impact they have on the system.* The application of the different methods to detect and assess the implications of ramps on sizing were presented in this thesis using wind and solar power based on the reference location.

Due to dependence on threshold values that vary across the literature and the limitations associated with calculating thresholds as a percentage of installed capacity, it was demonstrated that binary ramp definitions are not ideal and result in under-reporting. On the other hand, the wavelet approach extracts ramp events from the generation using statistically determined threshold values. As a result, the problem of under-detection of ramp events is mitigated. The proposed approach of "significant ramps" allows the evaluation of which ramp events are important and which are far less disruptive and may be ignored.

It is frequently mentioned in the literature that wind-PV hybrid plants have the advantage of a more stable power output due to the anti-correlation of wind and solar energy. However, it was demonstrated that anti-correlation alone is not adequate to promise a smoother output as it does not provide sufficient information about ramp events. Anti-correlations at shorter time resolutions, such as 15 minutes or one hour, could be preferable. While seasonal anti-correlation may benefit national system adequacy, it does not benefit daily ramping events.

The optimal wind-PV capacity size for decreasing the total number of ramps was such that wind turbines filled the grid capacity, as solar power would result in extra ramps. It was observed that solar over-planting leads to a significantly increased number of ramp events, whereas wind over-planting results in a minimal change in ramp events. A penalty price was proposed to internalize the severity of ramp events, which could influence the choice between wind and solar over-planting. A solution was presented to mitigate ramp incidents in a hybrid power plant using a battery. When compared to solar over-planting, the addition of a battery was found to be more effective and/or more economical in minimizing ramps.

The proposed "significant wavelet ramp approach" is shown to be a useful metric for characterizing wind-based hybrid power plant ramp occurrences. For a future in which variable renewable energy sources account for a substantial portion of the energy mix, it is proposed that demand information be considered when defining ramp events. More attention has to be paid to power ramp occurrences, either by penalizing ramps or enforcing tougher grid codes, as ramp events grow more frequent and dangerous. The ramp events must be taken into account at the initial site sizing and development process, with the possibility of including a ramp-reducing battery strategy. A thorough examination of ramp events in hybrid power plants demonstrates the importance of minimizing and managing ramp events for both the system operator and the producer.

Contents

Nomenclature

Abbreviations

AEP	Annual Energy Production
IRR	Internal rate of return
NPV	Net present value
$OpSDA$	Optimized Swinging Door Algorithm
SDA	Swinging Door Algorithm
SOC	State of Charge
STC	Standard Test Conditions

Symbols

a	Scaling coefficient
A_{rotor}	Area of the rotor
b	Translation coefficient
Cap	Installed capacity
CF	Capacity factor
E_{nom}	Nominal battery energy
G_{TI}	Global tilted irradiance
k_b	Boltzmann constant
L	Demand
P	Power
$P_{\%}$	Ramp threshold as a percent
P_{aero}	Aerodynamic wind power
$P_{curtail}$	Curtailed power
$P_{grid\ cap}$	Grid connection
P_{Hybrid}	Total hybrid power
P_{module}	Module solar-PV power
P_{PV}	Total solar-PV power
P_{rated}	Rated power
P_{th}	Ramp threshold
P_{wind}	Total wind power
PRR_{th}	Ramp rate threshold

r	Pearson correlation coefficient
R_b	Ramp function
R_D	Ramp duration
R_M	Ramp magnitude
R_R	Ramp rate
R_{ST}	Ramp start time
t_e	End time of ramp
t_s	Start time of ramp
U_{10m}	Wind speed at 10m
U_{60m}	Wind speed at 60m
U_{cut-in}	Cut in wind speed
$U_{cut-out}$	Cut out wind speed
U_{hub}	Wind speed at hub
W_H	Wavelet transform
W_i^*	Wavelet transform of surrogate
W_T^*	Wavelet transform threshold
x	Battery power

List of Figures

List of Tables

1

Introduction

This chapter introduces the concept of the wind-based hybrid power plants and the ramp events in the generation in Sections 1.1 and 1.2 respectively. Further, the research gap in the literature is presented in Section 1.3. Next, the objectives of the research are presented in Section 1.4. Finally, Section 1.5 gives an overview of the chapters in the report.

1.1. Hybrid wind-solar plants

Over the last years, renewable energy sources have become a cost-competitive and clean option to supply power to the grid all around the world. Nonetheless, their variable nature challenges the daily operation of the electrical grid. With the transition towards a sustainable energy future, new technologies and solutions are being developed in order to handle the variable nature of renewable energy. Hybrid renewable power plants are considered to be one possible solution that can provide significant value to the electrical grid by having a stable power supply [1].

Hybrid power plants are a combination of various generation assets such as wind, solar, storage, and/or other renewable sources. Figure 1.1 shows a simple schematic diagram of a hybrid power plant with wind turbines, solar PV panels and a battery storage system connected to the grid. Hybrid systems combine the advantageously complementary renewable sources in a region to provide a more reliable and stable power profile compared to individual renewable sources.

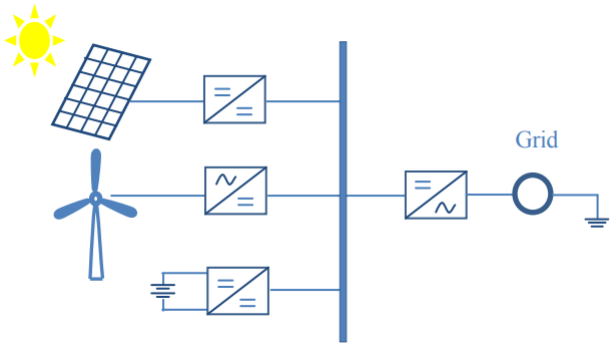

Figure 1.1: Schematic diagram of a simple Hybrid Wind-PV System [2]

A common advantage that is stated for hybrid power plants is that it can reduce investments for infrastructure as just one grid connection point is required to be set up in most cases. This could reduce the overall grid investment costs as well as the tariffs paid by the end-user. Furthermore, the energy that is produced per a unit area is higher since the land is used more efficiently compared to standalone wind or solar plants. The hybrid power plants could hence have a lower levelized cost of energy due to better utilization of the infrastructure and resources of the site.

With the planned eventual phasing out of conventional power plants, hybrid renewable plants offer a higher capacity factor and better stability in terms of power output compared to wind only or solar only power plants. The reason behind this benefit is the anti-correlation or the complementary nature of wind speed and solar irradiation that exists at suitable sites. It is often stated that the system becomes more economical to operate since the weakness of one source is complemented by the strength of the other source [2]. However, it is still unclear whether the hybrid wind-PV power plants can always be competitive in terms of reliability and cost against conventional fossil fuel systems or standalone wind-only plants.

1.2. Ramp events

One of the biggest challenges associated with the integration of large amounts of renewable energy into the energy mix is the ability to handle severe fluctuation incidents with large magnitudes and short duration known as ramps [3]. Wind power ramping events are usually caused due to atmospheric phenomena such as thunderstorms, gusts, cyclones, or low-level jets. In a solar-PV generation, the ramp events are predominantly caused due to passing clouds other than the diurnal variability. Down ramps in the generation while there is an increase in the load can cause severe damage and possible failure of the grid in a renewable energy dominant future. In order to ensure system reliability and dispatchability, it is essential for the power system operators and providers to better understand the ramping features.

Ramping events are generally defined using features such as ramp duration, magnitudes, start/end and ramp rates. The definition of a ramp event depends on the application of utilities and the system operators. Several different definitions are available in the literature that consider the power change or ramp rate above a significant percent of the rated power with or without a defined time-span. Up ramps in generation are sometimes defined with a higher threshold than down ramps due to the severity of down ramps [4]. Based on the definition, the ramp events are detected using an optimized swinging door algorithm [5] or simple sliding window calculations.

In Hybrid power plants, since the solar irradiation and wind speed are negatively correlated, the power output could have a comparatively stable nature. The instantaneous peaks are reduced since solar power compensates for the reduction in wind power during low wind time instances.

1.3. Research gap

At present, the number of existing wind-based hybrid power plants, in development or operation is very low and this makes accessing reliable data very difficult. This is mainly due to the early age of the projects and since the business cases are still under evaluation or development making developers or operators reluctant to sharing information [6].

The concept of complementarity of renewable sources for hybrid power plants is often mentioned but the clear practical application of the analysis is not provided in the literature. The statistical relationship i.e. the complementarity of power generation is not sufficient to define the benefits of the hybrid plants since it does not consider the effect of variability of the load and the effect on the grid [7]. Although there might be a seasonal anti-correlation between wind speed and solar irradiation, the daily correlation may not be always as distinct. The correlation indices need to be verified with other parameters such as ramp events to study the system security.

In the current literature, the study of ramp events caused during the operation of hybrid power plants is very limited and not thorough. In the cases that are studied, the ramps are considered mainly for islanded and microgrid operations and not for utility-scale hybrid power plants. There is a lack of studies on whether the ramp events in hybrid power plants are sufficient and meet the grid code requirements. There is a lack of analysis of the role of wind turbine technology choices in the analysis of correlation and ramps in hybrid systems.

Various definitions of ramps are considered in different situations without a standard that can be followed universally. A metric that quantifies the smoothening of the power profile to verify the advantages of the inclusion of hybrid power plants is unavailable. There is a lack of research in the changes in ramp duration, magnitudes and rates and their impacts with the increase in renewable and hybrid systems [3]. Based on the current review on the ramp events of hybrids, the knowledge gap is to identify an effective way to gauge the impact of hybrid renewable energy plants on reliability and dispatchability in terms of ramp events.

1.4. Objectives

In this section, the objectives of the research are discussed by explaining the main objective of the thesis along with sub-objectives that are to be answered.
The main objective of this research project is to ***characterize the ramping behaviour and system impact of wind-based hybrid power plants.*** With the research gap discussed in Section 1.3 it is evident that there is a lack of research in characterizing and describing ramp events that are caused by wind-based hybrid power plants. There are several methods and definitions for discriminating ramp events from incoherent variations. With the growing market share of variable renewable energy sources, the detection of ramp events becomes more important. Further, the impact of these events on the reliability and sizing of the wind-based hybrid system needs is to be addressed.

The main objective of the research can be broken into four research questions.

- *What is the most effective metric to characterize the ramp features of a wind-based hybrid power plant?* The current literature consists of several definitions and methods of classifying and detecting ramp events in the power profile. However, there is no universally accepted or recommended definition and method. The first research question is to find the most effective metric to characterize a ramp event in the case of a wind-based hybrid power plant.
- *How do the results of complementarity on different time scales and ramp events compare* Although it is commonly stated that the hybrid power plants have a benefit of stable power output due to the complementary nature, there is no research reported on how the ramp events are affected and if the severity is increased or decreased with the inclusion of solar for a whole year. The objective is to check if a complementarity analysis of the site is sufficient or if the ramp event analysis gives results that are not desirable for a plant.
- *What role does the installed wind to PV ratio play on the ramp events of the hybrid plant?* The next research question is to explore how the ramp event features change with varying the installed capacities of the wind and PV components of the plant. In the case of a very high PV generation while a high wind generation already exists could lead to high ramp magnitudes.
- *How will the inclusion of battery storage in wind-based hybrid power plants impact the ramp events?* The last research question is to explore how the inclusion of a battery storage system in the hybrid power plant would affect the ramp events. Further, a battery control strategy based on the ramp events is to be explored.

1.5. Report overview

The layout of this work is as follows:

- *Chapter 1:* Introduction to the concepts of hybrid wind-based power plants and power ramp events and an overview of the research gap and objectives.
- *Chapter 2:* Overview of the current research and literature on ramp events and detection of ramp events.
- *Chapter 3:* Modeling of the wind, PV and battery components and reference case for the analysis .
- *Chapter 4:* Methodology of detection of ramps using various methods and selection of most suitable method.
- *Chapter 5:* Complementarity analysis between wind and solar and the relation with ramp events.
- *Chapter 6:* Sizing and over-planting based on the number of ramps, capacity factor, IRR and penalties.
- *Chapter 7:* Battery control strategy and functionality for ramp reduction.
- *Chapter 8:* Conclusions of the research and recommendations for future research.

2

Literature Survey

This chapter highlights the current research and literature available on complementarity and ramp events. Section 2.1 gives an overview of the complementary nature of wind and solar energy. Sections 2.2 and 2.3 give an explanation of what ramps events are and the different definitions that are used in literature.

2.1. Complementary nature of wind and solar

In order to evaluate the potential of a hybrid power plant, it is very important to consider the complementarity of the renewable energy sources at the location [1]. Both spatial and temporal complementarity exist between wind and solar resources. There are some regions in a country where the solar irradiation is strong while the wind speeds are low and within the same country, there may be locations with high wind speeds and low solar irradiation. This is known as complementarity over spatial scales. However, there are some locations where there is high irradiation as well as high wind speeds. With the solar irradiation following a diurnal cycle, that is high irradiation during the day and no irradiation during the night, it is possible that in a location the wind is complementary to the solar power. This type of complementary nature exists in a time scale and is hence called temporal complementarity. It can also occur in a larger time period owing to the annual patterns of wind and solar [7].

Since the co-located hybrid plants have wind turbines and PV modules located in the same location, temporal complementarity will be focused on for the purpose of the study. The purpose of evaluating complementarity is to determine whether the hybrid plant can provide a more stable power production than stand-alone wind or solar farms.

Figure 2.1 shows the hourly averaged normalized wind and solar resources along with the normalized demand for the year 2010 for a location in the state of Victoria, Australia discussed in [8]. The complementary nature of wind and solar can be observed with solar dominating in the daytime when the wind is minimum while the wind is dominating in the night when the solar is low. During the day it can also be seen that the load is peaking along with the solar resource. During the night, the wind begins to increase complementing for the unavailability of solar resources.

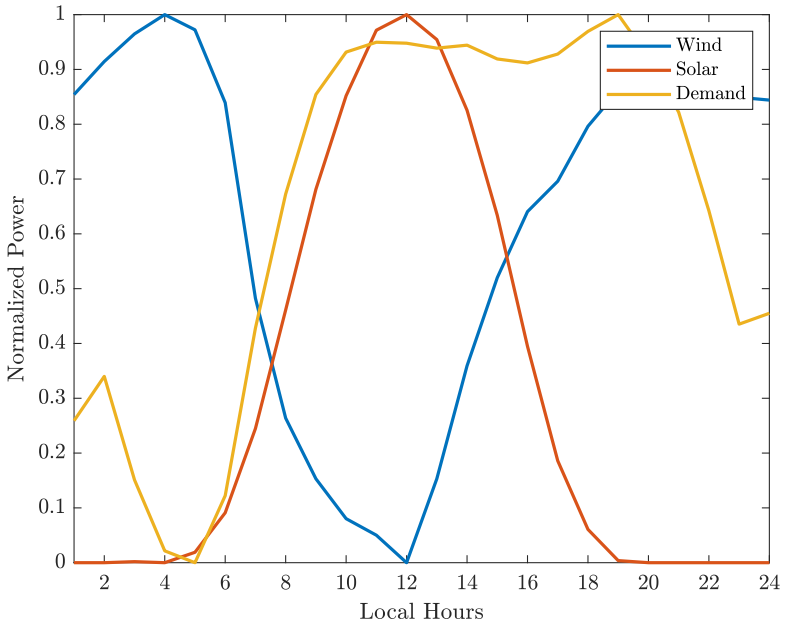

Figure 2.1: Illustration of relationship of hourly averaged solar and wind resource with peak demand for the year 2010 for a reference grid point in the state of Victoria.

To quantify the complementarity of wind and solar sources, it is important to evaluate the correlation between the two sources at different time scales. Irrespective of the availability of the resource over the year, wind speed and solar irradiation have different correlations at different timescales. There is no standard metric for the complementary analysis that is defined in the literature [9]. As seen in the case of Figure 2.1, there is a high anti-correlation or inverse correlation between wind and solar resource. There exists a trend of inverse-diurnal correlation between the wind and solar profiles for the location. Similarly, in most locations, there is a seasonal inverse correlation where there is higher wind energy produced in the winter and higher solar generation in the summer. However, there are instances where there is a strong correlation between the sources. In such a case instead of providing the benefit of smoothing the profile, both wind and solar would peak at the same time [1].

Correlation is the measure of the degree to which two different variables move in relation to one another or how they are linearly related [10]. The Pearson correlation coefficient or the simple correlation coefficient measures the association strength between the two variables, in this case, the wind and solar resources. The value of the coefficient ranges from +1 to -1. A positive value implies that when one variable increases or decreases, the behavior of the second variable is similar. A negative value implies that when one variable increases or decreases, the behavior of the other variable is the opposite. In a case that the coefficient is zero, no association exists between the two variables. The Pearson correlation coefficient between two sets of x and y is usually denoted by r_{xy} where a sample of paired data is given as $\{(x_1, y_1), \ldots, (x_n, y_n)\}$. Equation 2.1 is used to calculate the r_{xy} where n is the sample size and $\bar{x}$ and $\bar{y}$ are the means of the samples.

$$r_{xy} = \frac{\sum_{i=1}^{n} (x_i - \bar{x})(y_i - \bar{y})}{\sqrt{\sum_{i=1}^{n} (x_i - \bar{x})^2} \sqrt{\sum_{i=1}^{n} (y_i - \bar{y})^2}} \tag{2.1}$$

In the evaluation of complementarity for hybrid power plants, a r_{xy} value of -1 would be the most desirable as it would mean a full anti-correlation and hence the best complementarity for wind and solar resources. Similarly, a value of +1 would be the worst possible value since it implies that both the sources follow the same pattern and do not compensate for one another. However, a negative r_{xy} value for one timescale does not always imply the same behavior for smaller or larger time scales. A negative value for the seasonal correlation might exist but it may be that the daily correlation is not as desirable.

2.2. Ramp events

As we shift towards a sustainable future with wind and solar energy playing a larger role in the energy mix, there is a need for more research in the fields of understanding these variable sources of energy [11]. Large and sharp unscheduled fluctuations in the power output of renewable sources are known as ramp events. The generation suddenly increases or decreases due to the changes in the wind speeds or solar irradiation. The ramp events cause disruptions in the operations by making the task of balancing the demand and generation at all times challenging for the system operators.

Various meteorological factors cause ramp events in wind generation like thunderstorms, low-level jets, dew point fronts and cold fronts [12]. Although macro-scale conditions do lead to ramps in the power generation, local and mesoscale effects too play an important role in causing ramps. The terrain characteristics, roughness or land-sea breezes along with the layout of the farm may affect the occurrences of ramps. Solar ramping events on the other hand occur due to passing clouds beyond the diurnal nature of solar energy. When a cloud passes over the PV panel, the inverter output is ramped down suddenly [3].

In the case where a downward ramp event occurs, that is where there is a large decrease in the generation for a short time, back-up generators need to be used to meet the load due to the deficiency. Currently, gas and coal powered plants serve as the back up generators to maintain the balance between the load and generation [13]. A downward ramp is considered to be a serious problem since the system operator needs to closely monitor and plan other generators to meet the load during such a situation.

Upward ramps can also cause problems in case the transmission capacity in a region becomes full when supply from multiple producers is more than the grid capacity and cause congestion. The potential for this to occur increases as the wind and PV penetration increases but the demand does not change much [14]. The surpluses can be curtailed when the generated power is undesirable but is not a sustainable method, and over time these situations need to be avoided. Figure 2.2 shows ramp events that occur in a ten-day period for a wind power plant located in Haringvliet, the Netherlands. The green lines depict the ramp ups and the red lines depict the ramp downs.

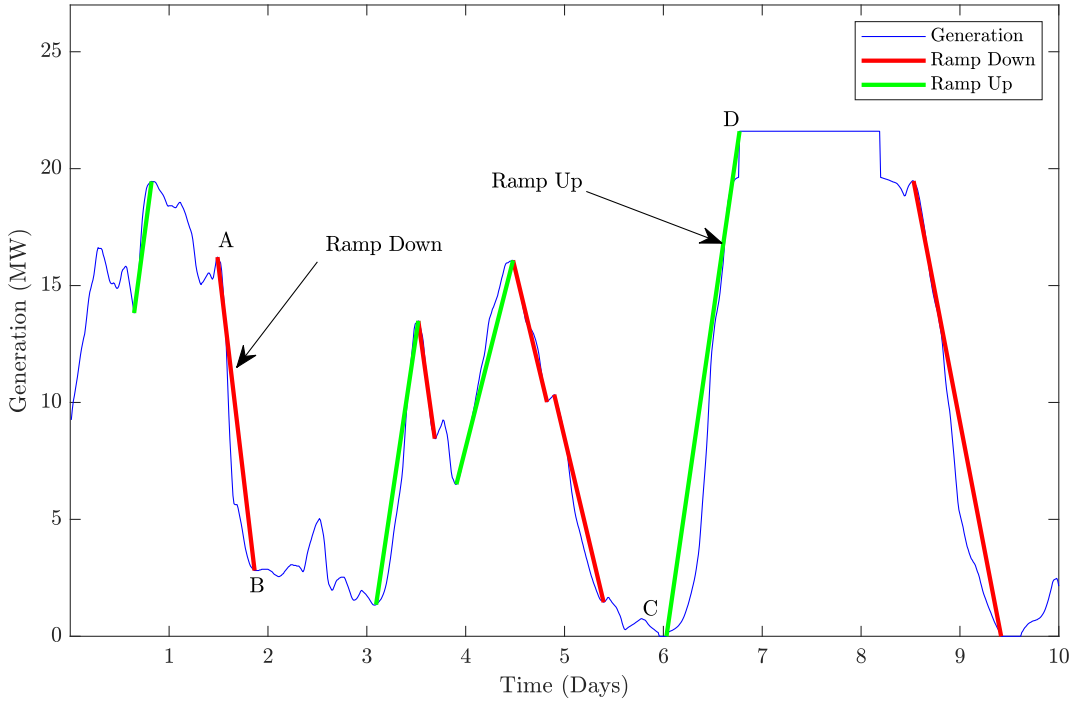

Figure 2.2: Ramp events in a wind power series

A ramp event is mainly parameterized by features such as ramp start time, ramp duration, ramp magnitude ramp rate, and ramp direction. Figure 2.3 shows the important features from an event in the wind power. The ramp start time is the time at which the ramp up or down begins, represented by R_{ST} in the figure. Ramp duration is the duration of time that ramp event lasts, given by R_D while the ramp magnitude is the amplitude of the event which is the difference between the generation at the end point and start point given by R_M. Ramp rate R_R is the slope of the ramp event that is occurring. The ramp direction specifies whether the generation is increasing or decreasing that is if the ramp is a ramp up or a ramp down.

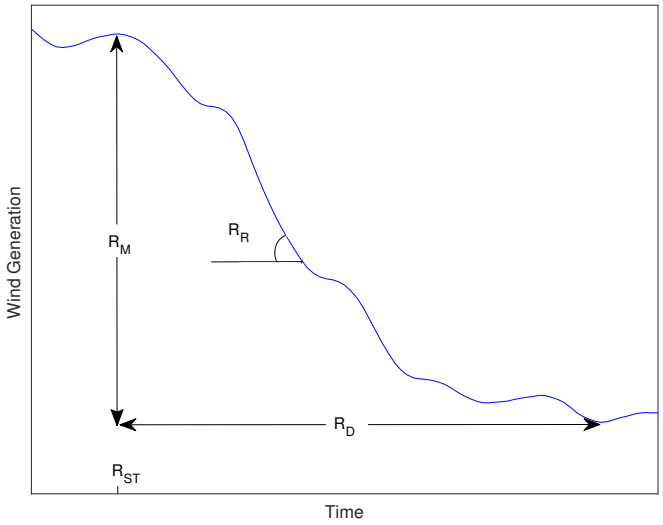

Figure 2.3: Features of a ramp Event

2.3. Ramp definitions

Although it is simple to identify ramps visually in the power output signal, there is no universally accepted definition for ramp events [11],[15]. Many definitions based on setting a threshold value for the ramp magnitude are available in the literature. These definitions known as binary definitions use pre-defined values as the discriminator between ramp and non-ramp events. Further, there are other methods such as ramp function which uses a wavelet transform of the power signal to discriminate ramp events. This section gives an overview of the commonly used definitions for ramp events.

The basic definitions given in **Definition 1 to 3** use two parameters Δt and P_{th} or PRR_{th} to define the ramp event. Δt is the time interval that is chosen to identify the ramp event, it is usually measured in minutes or hours. P_{th} is the magnitude threshold that is set to act as a cut-off for the ramp magnitude changes. It is set as a percentage of the installed capacity or a specific power value in megawatts. PRR_{th} is the threshold for the ramp rate above which the fluctuation in power is considered a ramp event.

Definition 1: In this definition, the ramp event in the generation P can be identified using Δt and P_{th}. A ramp event is considered to occur if the magnitude change (increase or decrease) in an interval of Δt is greater than the threshold value, P_{th} [11], [15].

$$|P(t+\Delta t) - P(t)| > P_{th} \tag{2.2}$$

If $P(t+\Delta t)$ is greater than P_{th} then the ramp is considered as a ramp up and if it is lesser it is a ramp down event. This definition ignores the magnitudes of the power between the t and Δt and considers only the difference between the start and end values. If consecutive ramps occur in different directions within the interval, the detection may be inaccurate [12].

Definition 2: The ramp event can be identified using Δt and P_{th} similar to Definition 1. A ramp event is considered to occur if the magnitude of the difference between the maximum and minimum power in the interval of Δt is greater than the threshold value, P_{th} [16].

$$max(P[t, t+\Delta t)]) - min(P[t, t+\Delta t)]) > P_{th} \tag{2.3}$$

Unlike the first definition, it is not straightforward to detect the direction of the ramp. In this case, if the maximum of the power series occurs after the minimum it is considered as a ramp up event. This definition addresses the issue of ignoring values from the middle of the interval from the previous definition.

Definition 3: A ramp event is identified if the ratio of the modulus of the difference between the power at the end and beginning of the time interval and the value of the time interval Δt is greater than the user-defined ramp rate threshold PRR_{th} [15].

$$\frac{|P(t+\Delta t) - P(t)|}{\Delta t} > PRR_{th} \tag{2.4}$$

Similar to Definition 1, if $P(t+\Delta t)$ is greater than $P(t)$ then the ramp is considered as a ramp up and if it is lesser it is a ramp down event. In this definition, the rate of change of the power over a time interval is considered. This slope or rate is known as the ramp rate. The units of the ramp rate are expressed with (MWm^{-1}) or (MWh^{-1}).

Typically, the time intervals Δt chosen for the ramp event definitions are 15 minutes, 30 minutes, and 1 hour. However, the choice of the values of the power threshold and the ramp thresholds are not direct. The value is system-dependent and is determined by the amount of power that is difficult to secure in the time interval set in order to maintain the balance between the load and generation [11]. This could be set as an absolute value of a certain MW for the time interval. However, such a value is always varying on a day-to-day basis and depending on generation from other plants.

The threshold can also be defined as a percentage of the installed capacity of the wind farm. The problem that arises in such an instance is that the installed capacity could be varying over time. New turbines or panels could be added or existing ones could be upgraded. The generators would also be disconnected for repairs and maintenance. In the case of higher installed capacity, a ramp event that is detected earlier would not be detected as one since the capacity is increased hence the threshold is increased. On the other hand, when the capacity is reduced, the ramps of lower magnitude are qualified which can be handled by the operator but are falsely detected. But the challenge of handling ramps of the same magnitude would be the same for either situation.

Author	P_{th}	Δt	**Rated Power** P_R
Cutler [17]	75%P_R	3 h	65 MW
Cutler [17]	65%P_R	1 h	65 MW
Freedman [18]	200 MW	30 min	1 GW
Truewind [19]	Ramp-Up 20%P_R	1 h	not specified
Truewind [19]	Ramp-Down 15%P_R	1 h	not specified
Potter [20]	10%P_R	1 h	1 GW
Greaves [21]	50%P_R	4 h	3-240 MW
Barbour [22]	20%P_R	30 min	200 MW
Collier [23]	50%P_R	4 h	not specified
Bradford [24]	20%P_R	1 h	not specified
Bossavy [25]	50%P_R	-	not specified
Kamath [11]	10 - 12%P_R	30 min	1 GW
Kamath [11]	15 - 20%P_R	1 h	1 GW
Bossavy [25]	30%P_R	-	8 MW
Yang [26]	15%P_R	1 h	not specified
Fernandez [27]	25%P_R	3 h	18 MW
Suzuki [28]	25%P_R	6 h	not specified
Revheim [29]	30%P_R	3 h	not specified

Table 2.1: Threshold values for binary ramp event definitions in literature

Table 2.1 gives a few threshold values set for the power and the corresponding time intervals along with the installed capacities of the power plant used in the studies. The high number of different values is due to the threshold being selected based on the input from system operators or end-user considerations [30]. This could vary highly with the considered regions and with the changes in the energy mix. Hence, there is no motivation behind selecting one particular value over another.

The definitions from Equation 2.2 to 2.4 have a common consideration of a fixed time interval and threshold value which affect the identification of the ramps in the power signal. These definitions are considered as a simple classification since the ramps are reported to have the same time duration that is pre-determined and hence do not show ramps of lower or higher time resolutions. An under-reporting of the ramps may occur since the ramps are not always of a fixed duration and can vary between 15 minutes to longer periods such as 10 hours. The detection is also subject to the noise in the power signal. Additionally, the ramp events that are identified are very sensitive to the selected values [30]. Further, all ramps are considered to be similar to one another with no distinctions based on their characteristics even if ramp events of different magnitudes and duration are present.

The ramp event definitions given in **Definition 4 to 7** are based on the change in the power magnitude, the direction and/or the duration of the ramp. The detection is dependent on user-predefined threshold values of $P_{\%}$. A Swinging Door Algorithm is used to identify such ramps in the power series [4],[31] discussed in detail in Chapter 4.2.

Definition 4: In this definition, a ramp event is said to occur if the change in the wind power is greater than a certain percentage of the installed capacity of the plant $P_{\%}$ without having any constraints on the duration of the ramp event [4].

$$|P(t_e) - P(t_s)| > P_{\%} \tag{2.5}$$

Here, t_s is the start time of the ramp event and t_e is the end time of the event and the duration is given by the difference between the two. The magnitude of the ramp is the absolute difference between the power, the left

side of the equation. The direction of the ramp is determined by the values of the power at the start and the power at the endpoint. In case the power at the end time is higher it is identified as a ramp up.

Definition 5: A ramp event is identified if the change in the wind power is greater than a certain percentage of the installed capacity of the plant $P_{\%}$ with a time constrain such that the change must occur within a time span of 4 hours or less [4].

$$|P(t_e) - P(t_s)| > P_{\%} \tag{2.6}$$

$$t_e - t_s \leq 4h \tag{2.7}$$

Similar to the previous definition, t_s is the start time of the ramp event and t_e is the end time of the event and the duration is given by the difference between the two. The magnitude of the ramp is the absolute difference between the power. The direction of the ramp is determined by the values of the power at the start and the power at the endpoint.

Definition 6: A ramp event is defined as the rate of change in the power that is greater than the value of a pre-defined percentage $P_{\%}$ of the installed capacity per hour [4].

$$\frac{|P(t_e) - P(t_s)|}{(t_e - t_s)} > P_{\%} \tag{2.8}$$

Similar to the previous definitions, t_s is the start time of the ramp event and t_e is the end time of the event and the duration is given by the difference between the two. The magnitude of the ramp is the absolute difference between the power. The direction of the ramp is determined by the values of the power at the start and the power at the endpoint.

Definition 7: A ramp up event is identified if the change in the wind power is greater than a certain percentage of the installed capacity of the plant $P_{\%1}$ and a ramp down event is identified if the change in the wind power is lower than a certain percentage of the installed capacity of the plant $P_{\%2}$ with a time constrain such that the change must occur within a time span of 4 hours or less [4]. The definition is similar to Equation 2.6, however, the percentage value is different for up and down ramps in this case. Since down ramps are considered to be more challenging and disruptive to the balancing of load, a lower threshold is set for down ramps.

$$P(t_e) - P(t_s) > P_{\%1} \tag{2.9}$$

$$P(t_e) - P(t_s) < P_{\%2} \tag{2.10}$$

$$t_e - t_s \leq 4h \tag{2.11}$$

$$P_{\%1} > P_{\%2} \tag{2.12}$$

Similar to the previous definitions, t_s is the start time of the ramp event and t_e is the end time of the event and the duration is given by the difference between the two. The magnitude of the ramp is the absolute difference between the power. The direction of the ramp is determined by the values of the power at the start and the power at the end point.

Author	Defintion Type	Definition	Δt
Cui [32]	Definition 4	$\lvert P(t_e) - P(t_s)\rvert > 20\%P_R$	-
Zhang [4]	Definition 4	$\lvert P(t_e) - P(t_s)\rvert > 30\%P_R$	-
Cui [32]	Definition 5	$\lvert P(t_e) - P(t_s)\rvert > 20\%P_R$	$\leq 4h$
Zhang [4]	Definition 5	$\lvert P(t_e) - P(t_s)\rvert > 25\%P_R$	$\leq 4h$
Zhang [4]	Definition 6	$\frac{\lvert P(t_e)-P(t_s)\rvert}{(t_e-t_s)} > 10\%P_R$	-
Cui [32]	Definition 7	$P(t_e) - P(t_s) > 20\%P_R$ Ramp Up $P(t_e) - P(t_s) < 15\%P_R$ Ramp Down	$\leq 4h$
Zhang [4]	Definition 7	$P(t_e) - P(t_s) > 20\%P_R$ Ramp Up $P(t_e) - P(t_s) < 15\%P_R$ Ramp Down	$\leq 4h$

Table 2.2: Threshold values for ramp event definitions in literature

The aforementioned definitions are based on setting threshold values for the power magnitude and in some instances threshold on the duration as well as shown in Table 2.2. However, **Definitions 8 and 9** provide methods to compare the ramp without using system-dependent threshold values that vary based on the operator and farm capacity. These methods of detection used are based on using wavelet transform. Wavelet transform is a method that allows the analysis of the time-frequency information of a signal [30]. Using a mother wavelet function, a series of data can be decomposed by varying the dilation and translation of the mother wavelet. A one-dimensional time series data can be mapped to a two-dimensional group of coefficients that give information on the scale as well as the location of specific events.

Thus the wavelet transform can localize the scales of a time series data which can be useful to detect the ramp events in the power series [33]. In both cases, the Daubechies level-1 (db1 or Haar) mother wavelet is used to decompose the power time series. The Haar wavelet is useful in detecting sudden changes in a level by providing information about the gradient in the signal in various time scales which can be attributed to occur during a ramp event. The mother wavelet function with scaling coefficient a and translation coefficient of b is given by Equation 2.13.

$$\psi_{a,b}(t) = \psi\left(\frac{t-b}{a}\right) \tag{2.13}$$

The wavelet transform $W_H(a,b)$ of a power signal $P(t)$ based on the mother wavelet function with a range of scale and translation coefficients is given by Equation 2.14.

$$W_H(a,b) = \frac{1}{\sqrt{a}}\int_{-\infty}^{\infty} P(t)\psi\left(\frac{t-b}{a}\right)dt \tag{2.14}$$

Figure 2.4 shows an example wind power signal for a period of 10 days. A wavelet transform of the normalized series of the example power signal using a Haar mother wavelet is given in Figure 2.5, where the wavelet coefficients W for each scale, a for the time is plotted as a scalogram.

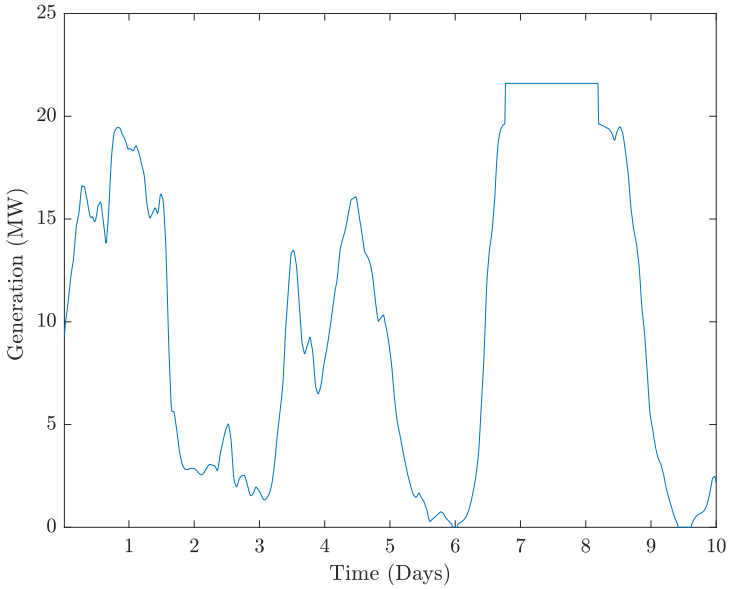

Figure 2.4: Wind power time series for 10 days

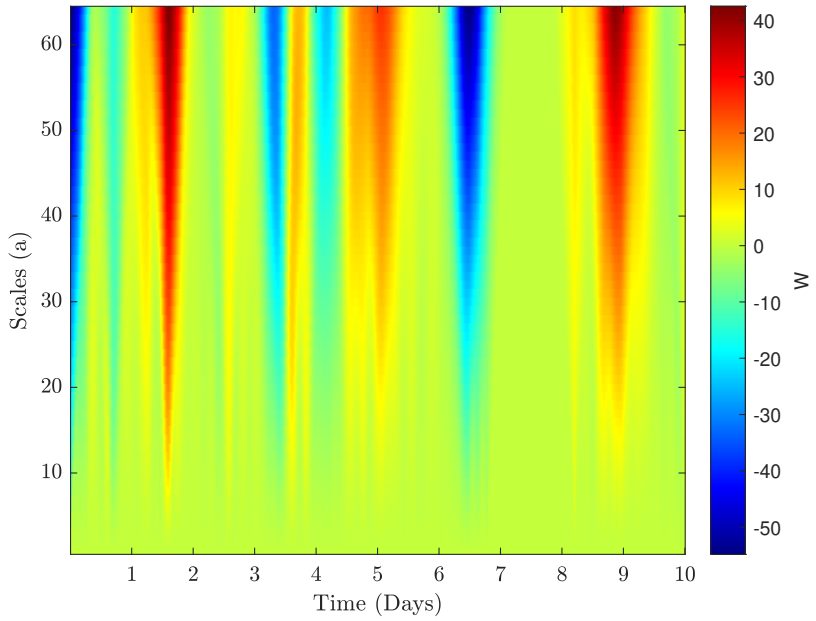

Figure 2.5: Wavelet transform of the wind power time series

Definition 8: This method of defining ramp events using wavelet transforms known as ramp function [30] allows comparison of the ramp intensities of different events without the need to force a binary decision that defines a ramp or non-ramp nature of an event. A wavelet transform is applied to the power time series from the farm and the coefficients are used in calculating the ramp function.

The ramp function R_b is defined as the summation of the wavelet coefficients $W_H(a,b)$ for the particular time position b for the scales of a_1 to a_N as shown in equation 2.15. The ramp function is re-scaled as a relative ramp function as given in 2.16 such that the values of the ramp events are in the range of -1 to 1.

$$R_b(a_1, a_N) = \sum_{a=a_1}^{a_N} W_H(a,b) \tag{2.15}$$

$$r_t = \frac{R_t}{\max(|R_t|)} \tag{2.16}$$

The difficulty that arises with using such a definition is that there is no particular method of discriminating the ramp events over unclear noise in the power generation time series. The ramp event time series gives values of the ramps over the entire time also giving a particular value to events that would not be considered as ramp events either due to their low magnitudes or long duration. It is unclear which magnitude of the $W_H(a,b)$ above which an event can be considered as a ramp event.

Definition 9: This method of detecting ramp events using wavelets, proposed by [33], works on an improved method to discriminate the ramps over incoherent noise. This method uses wavelets transform along with wind power surrogates in order to detect power ramps of various magnitudes and duration. Unlike the earlier definitions which rely on thresholds for magnitude and duration that are fixed, this method uses discrimination using thresholds that are statistically calculated.

Similar to **Definition 8**, a continuous wavelet transform is applied to the power time series of the farm. In order to approach the difficulty of discriminating the ramp events, randomly generated surrogates of the power time series are used. The largest 10% or 5% of the wavelet coefficient, W_{T}^* for each scale of the surrogates are used to set threshold values for the wavelets coefficients of the power series. In case the wavelet coefficients are greater than the threshold, the event is recorded as a ramp event. Else the value is considered to be zero. The discriminated values of the wavelet transform, W_{R} are then used to calculate the normalized ramps by the maximum resolved scale, $a_{\max}$ as given in 2.17. The method of detection is discussed in detail in Chapter 4.

$$\begin{aligned} &R(t) = \frac{1}{a_{\max}} \sum_{a=1}^{a_{\max}} W_{\mathrm{R}}(a,b), \\ &\text{where} \\ &W_{\mathrm{R}}(a,b) = W(a,b) \quad \text{when} \quad |W(a,b)| \geq W_{\mathrm{T}}^*(a) \\ &W_{\mathrm{R}}(a,b) = 0 \quad \text{when} \quad |W(a,b)| < W_{\mathrm{T}}^*(a) \end{aligned} \tag{2.17}$$

2.4. Problem with current definitions

As discussed in the previous section, the limitation of the definitions using fixed thresholds are dependent on the system and vary depending on the location as well as with time. There is no universally accepted threshold for the discrimination of a ramp event over non-ramp events. This problem is tackled in the methods that utilize wavelet transforms that do not depend on fixed thresholds that are system dependent or varying with different literature.

Although the problem of fixed thresholds is dealt with using wavelets, a common drawback still persists in all the definitions. In all the methods, the definition and identification of power ramp events are based solely on the power output from the farm and no importance is given to the information from the load side or the grid side. In order to effectively assess the ramp events and their significance, information from both the source as well as the load side needs to be considered in defining and detecting ramp events.

In the case of a ramp up event occurring in the instance when there is a ramp up in the load, it is not required to curtail the wind generation. Similarly, if there is a large ramp down occurring but it is consistent with the decrease in load or complementary to another renewable energy power output connected to the grid, the ramp down event may be desirable. Small variations in power can turn out to be undesirable in cases where is the trend is opposite of the load demand or is matching other renewable energy sources. Hence, such a comprehensive method for defining ramp events while combining both power from the source as well as the load information is required [34]. The thesis tries to address this gap in the literature by introducing an idea of significant ramp events.

3

Modeling

This chapter gives an overview of the models for the wind and PV power generation that are to be used for the analysis of the ramp events in the further chapters. Section 3.1 describes the wind turbine component while Sections 3.2 and 3.3 dive into the modeling of the PV component and battery component. The reference case and the modeling of the wind and solar power at the site are presented in Section 3.4.

3.1. Wind component

The wind power generation for the hybrid power plant is based on the BEM model power expression for wind turbines. The wind speed at 10 meter height is first expressed at a height of 60 meters using the logarithmic wind profile law given in Equation 3.1 where the surface roughness length, z_o is taken 0.03 m. Next, the wind speed at hub height is calculated using the power law, Equation 3.2 with the value of α being 0.143 since the plant is over land.

$$U_{60m} = U_{10m} \frac{\ln\left(\frac{h_{60}}{z_0}\right)}{\ln\left(\frac{h_{10}}{z_o}\right)} \tag{3.1}$$

$$U_{hub} = U_{60}\left(\frac{h_{hub}}{h_{60}}\right)^{\alpha} \tag{3.2}$$

The aerodynamic wind power over a range of wind speeds is calculated using Equation 3.3 with a drive train efficiency of 90%. The A_{rotor} is the total area swept by the rotor and ρ_{air} is taken as 1.225 kg/m^3. The aerodynamic power at partial load is given by the first equation whereas at rated wind speed, the aerodynamic power is given by the second equation.

$$P_{\text{aero}}\left(U_{hub}\right) = \begin{cases} \frac{1}{2} C_p \rho_{\text{air}}\, A_{\text{rotor}}\, U_{hub}^3 & \text{if } U_{\text{cut-in}} \leq U_{hub} < U_{\text{rated}} \\ \frac{P_{\text{rated}}}{\eta_{dt}} & \text{if } U_{\text{rated}} \leq U_{hub} < U_{\text{cut-out}} \\ 0 & \text{if } U_{hub} < U_{\text{cut-in}}\,, U_{hub} \geq U_{\text{cut -out}} \end{cases} \tag{3.3}$$

The total wind power generated considering the drive train efficiency is given by Equation 3.4. Further, the total wind power generated by the wind farm is calculated by multiplying the turbine power with the number of wind turbines in the plant given in Equation 3.5.

$$P_{\text{t}}(U_{hub}) = P_{\text{aero}}\left(U_{hub}\right) * \eta_{dt} \tag{3.4}$$

$$P_{Wind} = P_{\text{t}}(U_{hub}) * \text{Number of turbines} \tag{3.5}$$

3.2. Solar component

The modeling of the PV modules is dependent on parameters such as irradiance and temperature at the time period. The global tilted irradiance for the module is calculated using a fixed optimal tilt and azimuth based on the location of the site. The power output of the PV module is heavily dependent on the irradiance and temperature. Since the irradiance and temperature are not constant throughout the day, the power output varies accordingly. As the module receives solar energy, a fraction of the energy is converted to heat and thus results in an increase in the temperature of the module. This results in a reduction in V_{OC} of the module and hence the energy output is reduced.

The effective temperature at the module to be used for further calculations is modeled using the Faiman module temperature model [35]. The effective temperature of the module, T_m is calculated using Equation 3.6 using the global tilted irradiance G_{TI} denoted in units W/m^2. The T_a is the ambient air temperature and U_0 and U_1 are the constant heat transfer component and convective heat transfer component respectively. The values of U_0 and U_1 are taken as 26.9 W/m^2K and 6.2 W/m^2K since a crystalline silicon module is considered in the analysis [35]. The wind speed, WS is in the units m/s.

$$T_m = T_a + \frac{G_{TI}}{U_0 + (U_1 \times WS)} \tag{3.6}$$

The power output of the module reduces with the reduction in irradiance on the PV module. However, the variation of the efficiency of the PV module is not straightforward. The effect of irradiance on the solar module performance is modeled using the equations given in Equations 3.7 to 3.11 [36]. The open-circuit voltage, V_{OC}, which is the maximum voltage a solar cell can deliver at a temperature of 25°C is given by Equation 3.7 which uses the open-circuit voltage at STC (Standard Test Conditions) values which is the V_{OC} at 25°C and irradiance of 1000 W/m^2. The ideality factor, n is taken as 1.2, and charge of an electron, q is $1.6 * 10^{-19}$ C. The temperature T is in the units K and k_b, the Boltzmann constant is $1.38 * 10^{-23} m^2 kg s^{-2} K^{-1}$.

$$V_{\text{oc}}\left(25^\circ\text{C}, G_{TI}\right) = V_{\text{oc}}(\text{STC}) + \frac{n k_B T}{q} \ln\left(\frac{G_{TI}}{G_{\text{STC}}}\right) \tag{3.7}$$

$$I_{\text{sc}}\left(25^\circ\text{C}, G_{TI}\right) = I_{\text{sc}}(\text{STC}) \frac{G_{TI}}{G_{\text{STC}}} \tag{3.8}$$

$$FF = \frac{I_{\text{mpp}}(\text{STC})\, V_{\text{mpp}}(\text{STC})}{I_{\text{sc}}(\text{STC})\, V_{\text{oc}}(\text{STC})} \tag{3.9}$$

$$P_{\text{mpp}}\left(25^\circ\text{C}, G_{TI}\right) = FF \times V_{\text{oc}}\left(25^\circ\text{C}, G_{TI}\right) I_{\text{sc}}\left(25^\circ\text{C}, G_{TI}\right) \tag{3.10}$$

$$\eta\left(25^\circ\text{C}, G_{TI}\right) = \frac{P_{\text{mpp}}\left(25^\circ\text{C}, \text{G}_{TI}\right)}{G_{TI} A_M} \tag{3.11}$$

Further, the short circuit current, I_{sc} at 25°C and irradiance G_{TI} is calculated using Equation 3.8. The fill factor, FF for the module is calculated with Equation 3.9 and used in Equation 3.10 to find the maximum power at irradiance G_{TI}. The efficiency of the PV module at irradiance G_{TI} for a temperature of 25°C, $\eta(25^\circ\text{C}, G_{TI})$ is calculated according to Equation 3.11 where the area of the module is denoted by A_M.

The effect of the solar cell deviating from the STC temperature of 25°C to the effective module temperature T_M is expressed with Equation 3.12. Using this expression, the final efficiency of the module at every level of irradiance and temperature can be determined. The effects of both temperature and intensity of the irradiation are combined in this efficiency. The T_M is calculated from Equation 3.6 which was discussed earlier.

$$\eta\left(T_M, G_{TI}\right) = \eta\left(25^\circ\text{C}, G_{TI}\right)\left[1 + \kappa\left(T_M - 25^\circ\text{C}\right)\right] \tag{3.12}$$

The power output of each PV module is hence calculated by multiplying the $\eta(T_M, G_{TI})$ with the irradiance and area of the module as given in Equation 3.13. Further, the losses due to module mismatch, ohmic losses and soiling are assumed to be 5% and the inverter converter losses are taken to be 5%. Thus the system efficiency of the PV system is expressed as a product of the efficiencies as shown in Equation 3.14. Finally, the total power output of the PV system is calculated by multiplying the P_{module} with the number of PV modules installed in the plant and the system efficiency as given in Equation 3.15.

$$P_{module}(T_M, G_{TI}) = \eta(T_M, G_{TI}) * A_M * G_{TI} \tag{3.13}$$

$$\eta_{system} = \eta_{inverter} * \eta_{losses} \tag{3.14}$$

$$P_{PV} = P_{module}(T_M, G_{TI}) * \text{Number of modules} * \eta_{system} \tag{3.15}$$

3.3. Battery component

The state of charge (SOC) of an electric battery indicates its charge level in relation to its capacity. The SOC is generally expressed in percentages with 0 % implying empty battery and 100 % implying a full battery. The majority of rechargeable batteries are not intended to be completely depleted. Completely discharging some batteries might cause irreversible damage. Typically, the minimum state of charge is fixed to between 20% and 30% to avoid causing damage to the battery bank by excessive discharge. The minimum state of charge allowed (SOC_{min}) is assumed as 20 % and the maximum state of charge (SOC_{max}) as 100 %. A charge and discharge efficiency of 95% is assumed for the model. A simple battery model is used in this study as the goal of including storage is to present the functionality of battery storage in reducing the ramp events.

The battery energy charged or discharged at a time interval is calculated using Equation 3.16 and 3.17 respectively. The battery energy at any instance i is denoted by E_i while x_i is the battery power that is either given to or taken from the battery. E_{nom} is the nominal energy capacity of the battery storage system. The factor of 4 is included in the calculations since the time resolution of the power in the model is 15 minutes ($\frac{1}{4}$ of an hour) and the nominal capacity is in MWh. The battery control in order to reduce the ramp events is further explained in detail in Chapter 7.

$$E_{i+1} = E_i + \frac{x_i \eta_c}{4 * E_{nom}} \tag{3.16}$$

$$E_{i+1} = E_i - \frac{x_i}{4 * E_{nom} \eta_d} \tag{3.17}$$

3.4. Reference case

In order to model the wind and solar generation for the analysis of ramp events in the power profile, a reference case is chosen such that real data is available. The reference location and specifications are chosen based on the Energiepark Haringvliet Zuid located in the Netherlands.

Energiepark Haringvliet Zuid is a co-located hybrid energy park by Vattenfall that combines wind energy, solar energy and battery storage. It is located in the southern part of Haringvliet, in Van Pallandtpolder in Middelharnis. Figure 3.1 shows the location of the site on the map.

Figure 3.1: Location of Haringvliet Energy Park

The motivation for choosing the particular park as a reference is as follows:

- **Availability and accessibility of data**: For the analysis of the ramp events in the power generation of the hybrid plant it is essential to have a time series data for at least a year with a resolution of at least 1 hour or better. The wind speed, solar irradiation, and temperature used for the modeling can be obtained using Solcast API. Further, the yearly national load, wind and solar power time series for the Netherlands can be accessed through the Transparency platform of ENTSO-E [37] for a time resolution of 15 minutes.
- **Existing hybrid plant as a reference**: The Energiepark Haringvliet Zuid is one of the few hybrid power plants that are operational in Europe with specifications of the turbines, PV modules, and battery publicly available. Building a reference case based on a pre-existing plant would eliminate the need to design an optimal hybrid power plant as the study is focused on the analysis of the power generation rather than the design of the plant.

The averaged daily profiles of the wind speeds at hub height of 91 m and solar irradiation for each month for the year 2019 at the location are shown in Figure 3.2 and 3.3 respectively. As can be seen, solar irradiation is greater throughout the summer months, whereas wind speeds are lower during the same months. Similarly,

wind speeds are higher during the winter, while irradiance is lower. As can be observed in Figure 3.3, the solar profile exhibits a diurnal pattern, with no irradiance at night and a high irradiance throughout the day.

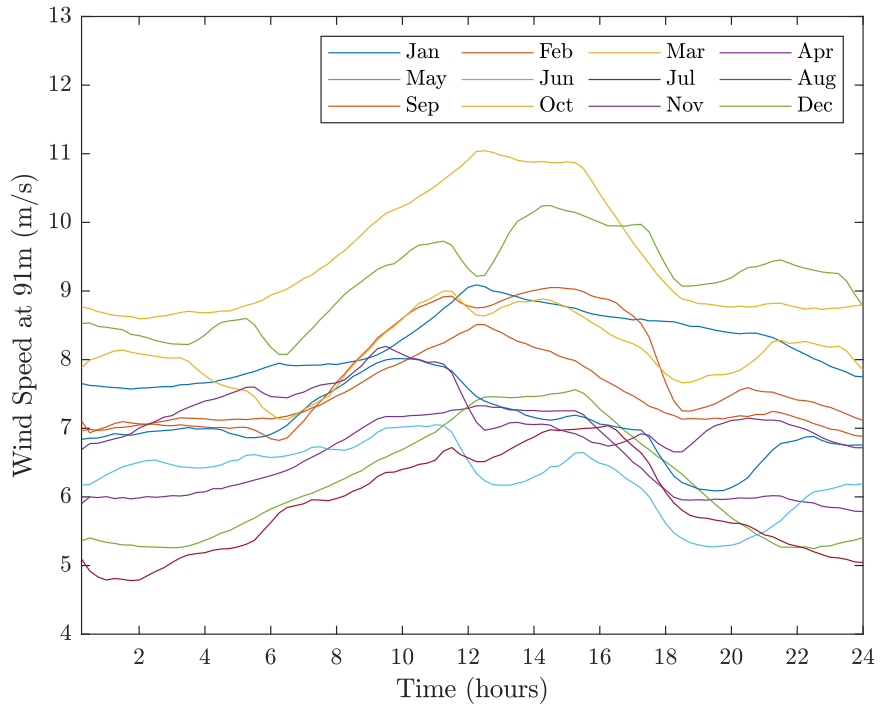

Figure 3.2: Average daily wind speed

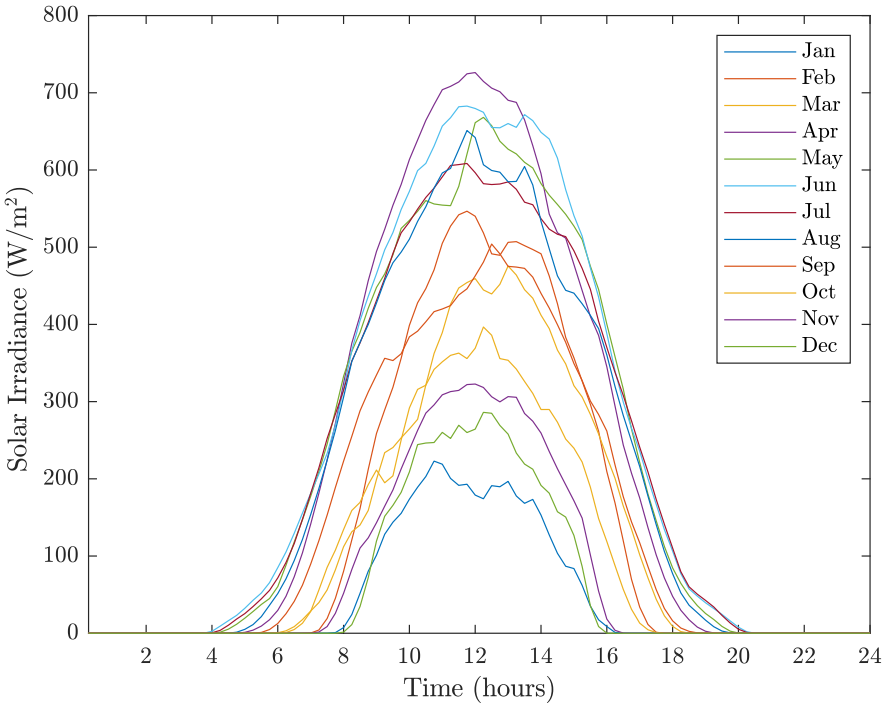

Figure 3.3: Average daily solar irradiation

The park consists of 6 Nordex N117/3600 wind turbines, 115,000 solar panels, and a storage system of 12 MWh with 288 BMW i3 batteries. The park has an installed wind capacity of 21.6 MW and an installed solar PV capacity of 38 MW. The construction of the park was started in 2019 and was commissioned in the fourth quarter of 2020. These specifications are taken as a reference and the modeling of the plant is executed with the models discussed in Section 3.1 and Section 3.2 for the year 2019.

The turbine used in the model is a Nordex N117/3600 which has a rated power of 3.6 MW and a rated speed of 13 m/s. The specifications and details of the turbine are given in Table 3.1 [38]. Figure 3.4 gives the power curve and the C_p curve with a step size of 1 m/s of the turbine that is considered. It can be seen that the rated power of the wind turbine is 3.6 MW at a wind speed of 13 m/s. Figure 3.5 gives the wind power generation profile for a period of 10 days in the month of March using the specifications of the Haringvliet energy park.

Description	**Specification**
Rated Power	3.6 MW
Rated Speed	13 m/s
Cut-in Speed	3 m/s
Cut-out Speed	25 m/s
Rotor Diameter	117 m
Hub Height	91 m
Hub Diameter	3 m

Table 3.1: Specifications of Nordex N117/3600 turbine

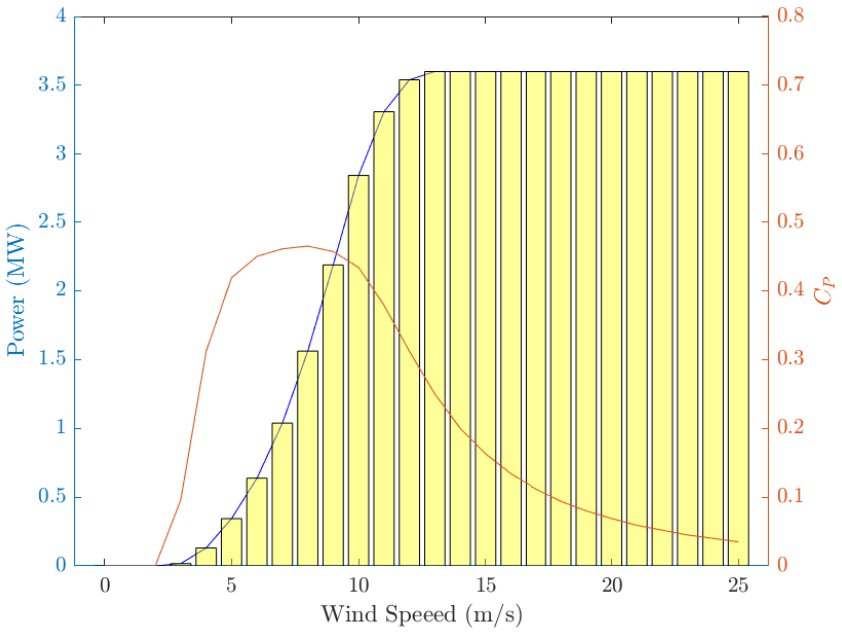

Figure 3.4: Power curve of the wind turbine

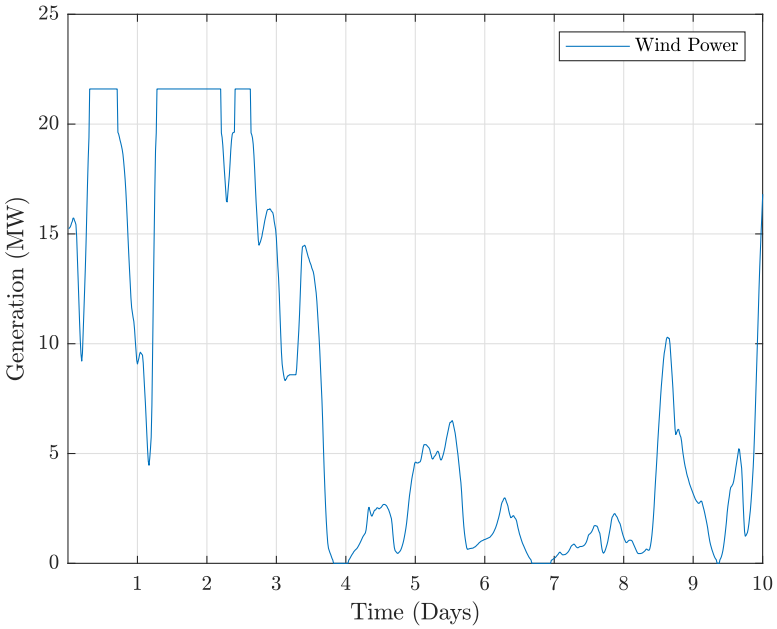

Figure 3.5: Wind generation for a period of 10 days

The specifications of the 345 W rated PV module used in the modeling based on the reference case are given in Table 3.2 [39]. Figure 3.6 gives the solar power generation profile for a period of 10 days in the month of March using the specifications of the Haringvliet energy park.

Description	**Specification**
V_{oc}(STC)	46.68 V
V_{mpp}(STC)	38.04 V
I_{sc}(STC)	9.55 A
I_{mpp}(STC)	9.07 A
P_{mpp}(STC)	345 W
A_M	1.971 m^2
k	-0.0035 /°C

Table 3.2: Specifications of 345 W PV Module

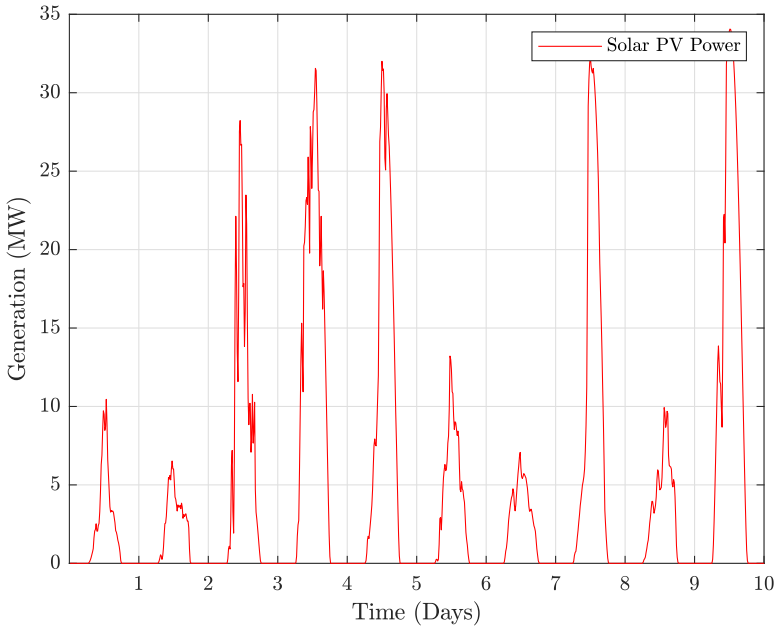

Figure 3.6: Solar generation for a period of 10 days

The total power generation of the hybrid plant is expressed as the sum of the power from the wind component and the power from the PV component expressed in Equation 3.18. Figure 3.7 gives the hybrid combined wind-PV power generation profile for a period of 10 days in the month of March using the specifications of the Haringvliet energy park.

$$P_{Hybrid} = P_{PV} + P_{Wind} \tag{3.18}$$

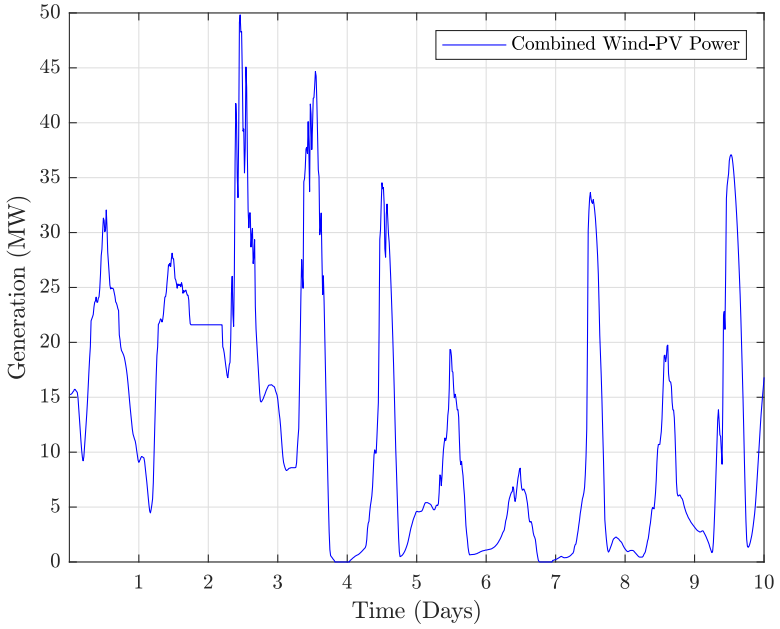

Figure 3.7: Combined wind-PV generation for a period of 10 days

The national demand load profile is accessed through the transparency platform of ENTSO-E for the year 2019. The demand is normalized since the trend is to be analyzed in the further sections and not the exact values of the demand. Figure 3.8 displays the average daily load for each month of the year. It can be noticed that the energy demand is lower in the summer months compared to the colder winter months. It can also be seen that the load profile follows a diurnal behavior.

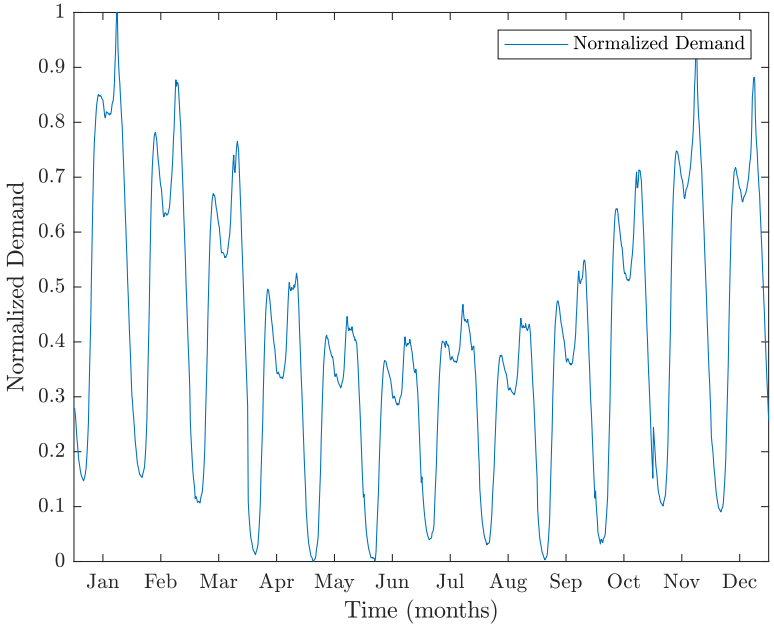

Figure 3.8: Average monthly demand

4

Ramp Detection Methodology

This chapter presents the methodologies used for the analysis and detection of ramp events in the power profile. Section 4.1 and 4.2 describe the detection of ramp events using simple and binary definitions. Section 4.3 gives an overview of detecting ramp events utilizing wavelet transform. Section 4.4 gives a method of defining ramp events by comparing the behavior of the load with the ramps. Finally, the objective of *the most suitable metric to characterize the ramp features of a wind-based hybrid power plant* is evaluated in Section 4.5

4.1. Ramp detection with basic definitions

The most simple and straightforward methods of discriminating ramp events from non-ramp events in a power generation time series are through Definitions 1 and 2 discussed in Section 2.3. Firstly, the first definition is considered, where a ramp event is identified when the power magnitude change is above a threshold value P_{th} within an interval Δt. Time windows of 4hr and 6hr are considered while the power thresholds considered are 50% and 25% as given by Greaves et al. [21] and Suzuki et al. [28] respectively.

Similarly, the second definition is analyzed which considers the difference of the maximum and the minimum power within the interval. If the difference is above the threshold value P_{th} within an interval Δt, the event is considered a ramp event. Time windows of 4hr and 6hr are considered while the power thresholds considered are 50% and 25% as given by Greaves and Suzuki respectively.

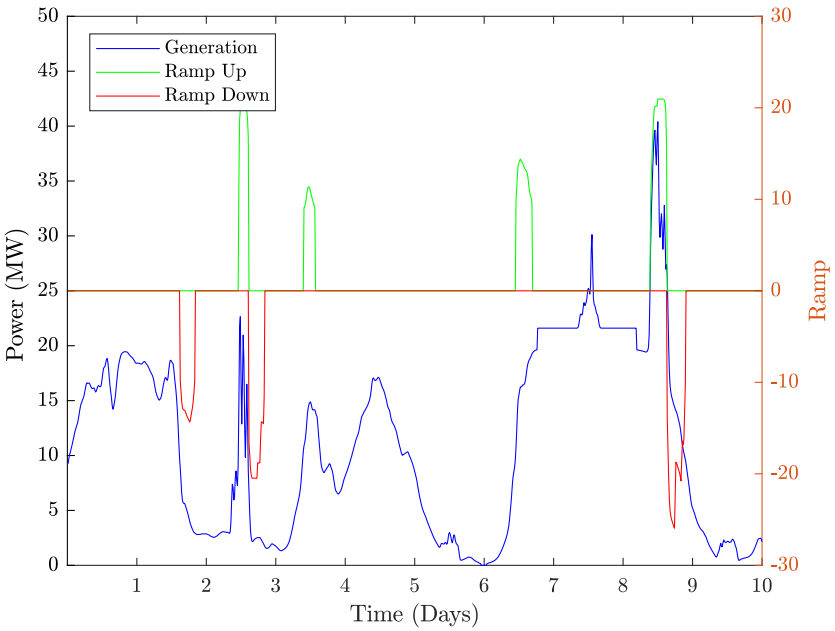

Figure 4.1: Ramp detection with definition 2 (Maximum - Minimum)

Once the power series is analyzed with different thresholds and time windows, the number of ramp ups and ramp downs are recorded. Hereinafter, this ramp detection method will be referred to as the **Basic Method**. The number of ramps is counted by each start time of the ramps. Figure 4.1 shows the detected ramps in the first 10 days of the power generation using Definition 2, with P_{th} of 25% of the installed capacity and Δt of 6 hours.

4.2. Ramp detection with binary definitions

The binary definitions discussed in Section 2.3, that is Definition 4 through 7 are based on the change in magnitude with or without constraints on the duration of the ramp events. The extraction of the ramp events is done by applying an optimized swinging door algorithm to the generation data.

4.2.1. Data pre-processing for binary definitions

In order to detect the ramp events in the generation, first, the time-series data is compressed using an archive compression method. The data compression is used in order to reduce the number of samples that are to be further evaluated. In an archive compression, the data is only stored when the change of the signal that is analyzed is beyond a user set limit.

The swinging door algorithm (SDA) is a data compression method that filters the signal according to the parallelogram rule which is based on adjustable door width parameter ϵ. The initial point and the endpoint of every portion of the data are detected as a piece-wise point while compressing the data in the signal that lies between the two points [5][40]. In Figure 4.2, multiple parallelograms are constructed from the first initial point A with a height of 2ϵ from length A to C and A to D. After every parallelogram is constructed, it is checked whether all the samples from the initial point lie within the parallelogram. In a case that the parallelogram does not cover all the data, such as in the case of A to F, the previous sample point, E is recorded as the endpoint of the segment and the initial point of the next segment. By doing so, the data points between the initial point and the endpoint are compressed into one segment. In the figure, the piece-wise points are A, E, I, and K while the points B, C, and D are compressed into the first segment, F, G, and H into the second and J into the third segment.

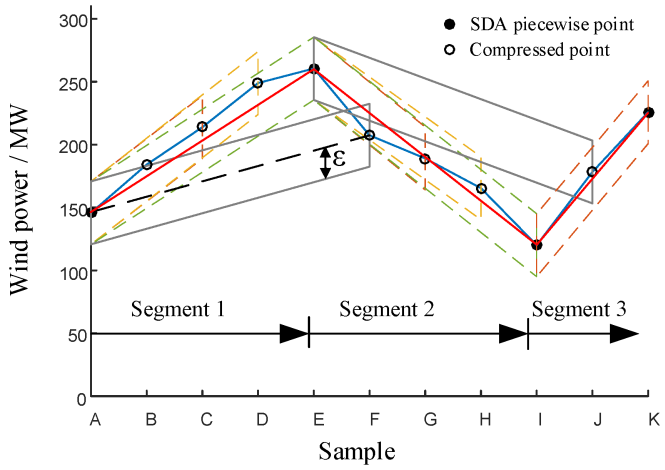

Figure 4.2: Basic principle of a Swinging Door Algorithm [40]

Using the swinging door algorithm and the user set limit for the door width as 0.03 as defined in [32], the generation data is compressed. Figure 4.3 gives the piece-wise points in the time series for a 10 day period after extraction with the Swinging Door Algorithm. However, ramps according to Definitions 4 to 7 can only be detected between the piece-wise points after data compression.

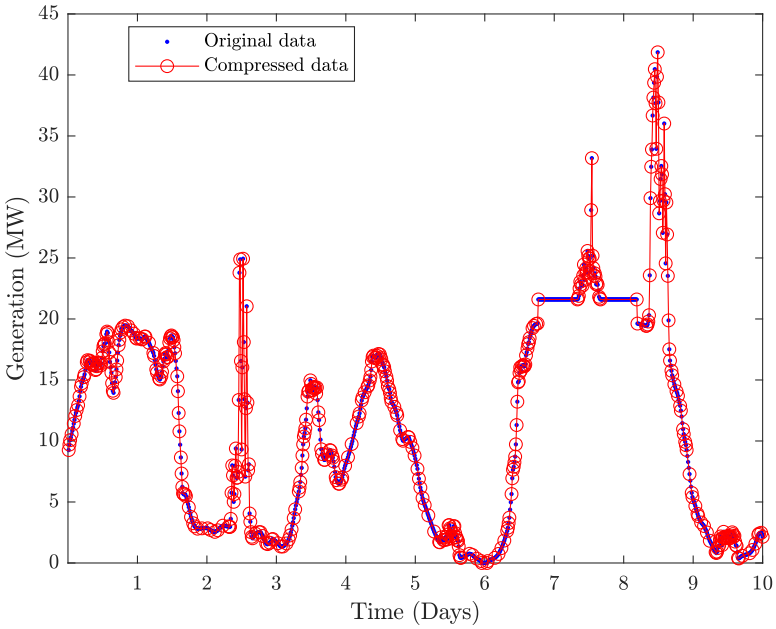

Figure 4.3: Compressed generation data with $\epsilon = 0.03$

4.2.2. Optimized swinging door algorithm

The objective of this method is to minimize the number of individual segments discriminated by the SDA while still approximating the generation signal as a ramp event [5]. Hence, adjacent segments with the same direction (either upwards or downwards) can be merged into a single segment. This method is applied to the original segments from the SDA that is applied to the data. Figure 4.4 shows the signal where the adjacent piece-wise points are merged if the direction is the same. It can be seen that the number of points has been reduced by a considerable amount.

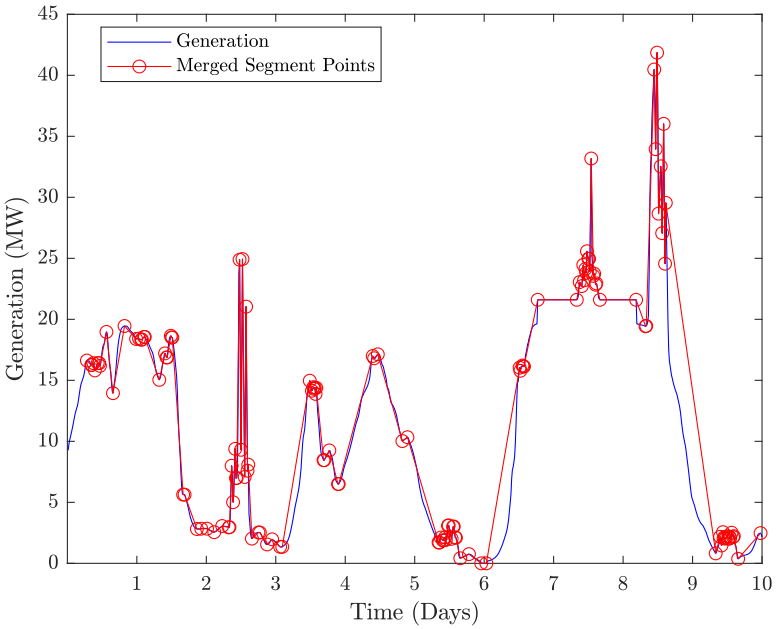

Figure 4.4: Event detection after merging adjacent same direction segments

Further, in order to improve the efficiency of the extraction of events, bumps in the generation signal are to be removed. Bumps are events of small magnitude and duration that occur between two ramps of the opposite direction [40]. In Figure 4.4 between the day 6 and 7, it can be seen that there is a small event that occurs in the downward direction that is in the middle of two events that occur in the upward direction. These bumps are removed from the segments by eliminating an event that occurs for less than 1 hour and has a magnitude of less than 1% of the installed capacity. Figure 4.5 gives the resulting segments by applying the OpSDA and removing the bumps superimposed on the original generation signal.

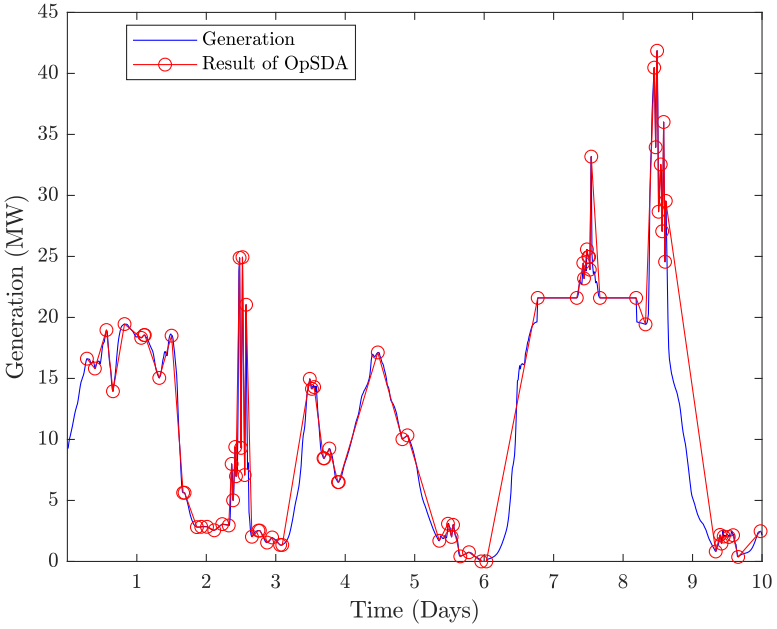

Figure 4.5: Extracted events with OpSDA after bump removal

4.2.3. Detection of ramp events

Once the OpSDA is applied to the time-series data of the generation, the events can be differentiated into ramp and non-ramp events. The OpSDA gives the start and end timings of each event segment along with the magnitude of the generation at the two timings. This information can be used along with Equations 2.5 to 2.10. The power thresholds, $P_{\%}$ that are considered in the analysis are 20% for both up and down ramps, 20% for up ramps, and 15% for down ramps. Ramp events are detected depending if they satisfy the conditions and the features such as the number of ramps, start time, end time, duration, direction and magnitude are returned. The ramps detection method using these definitions will be referred to as **Binary Method** in the report. Figure 4.6 shows the ramp ups and ramp downs detected in the 10 day period that is analyzed. Figure 4.7 gives the overall framework of the binary ramp detection methodology.

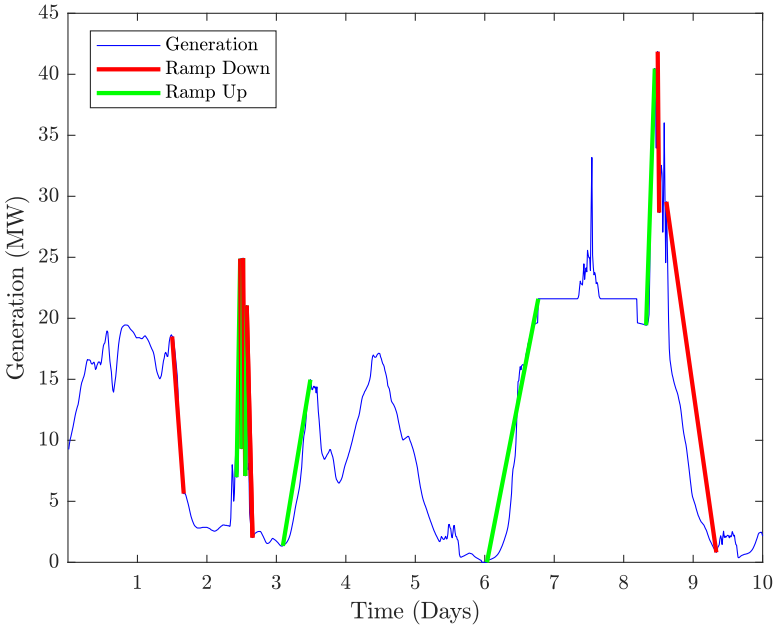

Figure 4.6: Ramp detection with binary definition

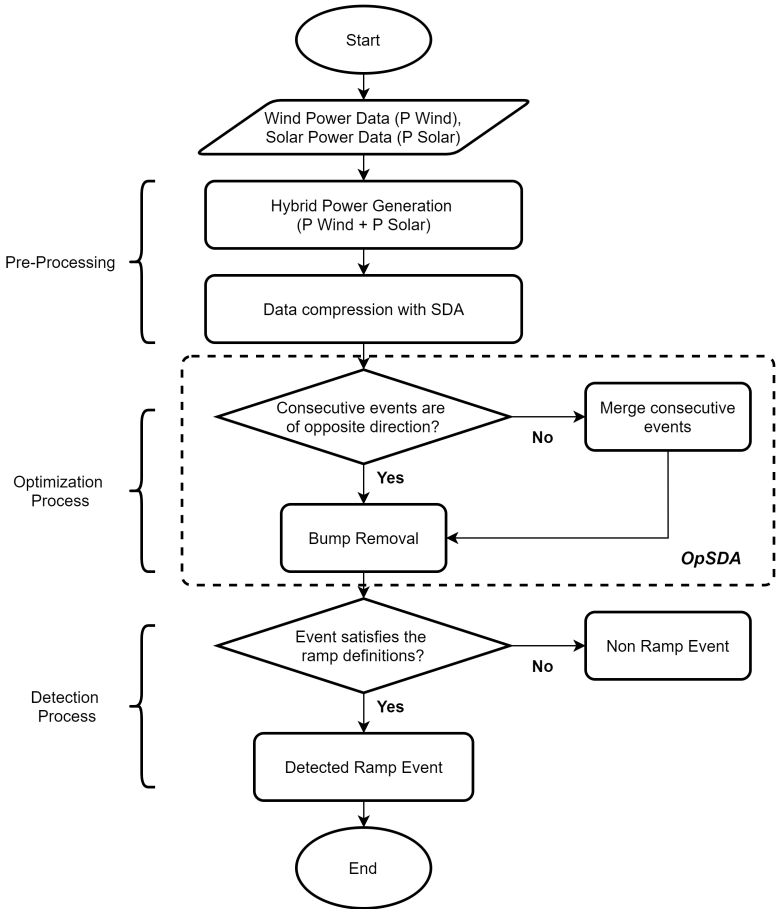

Figure 4.7: Overall framework of ramp detection using binary method

4.3. Ramp detection with wavelet transform

This section explains the ramp detection method from the generation signal, utilizing the reference site defined in Section 2.3. Unlike the previous methods that depend on the fixed power change and duration thresholds, this method depends on the detection of ramps based on statistical thresholds as presented by [33]. The ramp event threshold values are generated statistically using randomly randomized surrogate signals.

4.3.1. Wavelet transform

The power signal is decomposed using a wavelet transform utilizing the Haar (db-1) mother wavelet specified in Equation 4.1. Equation 4.2 is used to construct the wavelet transform $W_H(a,b)$ of the generating power signal $P(t)$ using the Haar mother wavelet $\psi_{a,b}$.

$$\psi(t) = \begin{cases} 1 & 0 \leq t < \frac{1}{2} \\ -1 & \frac{1}{2} \leq t < 1 \\ 0 & \text{else} \end{cases} \tag{4.1}$$

$$W_H(a,b) = \frac{1}{\sqrt{a}} \int_{-\infty}^{\infty} P(t)\psi_{a,b}(t)dt \tag{4.2}$$

The wavelet transform is applied to the power signal for a period of 10 days that was previously studied in Section 4.2 and the resulting wavelet transform values are given as a scalogram in Figure 4.8. In the analysis, the scale parameter a is set to a value between 0 and 64. It can be seen that the dark blue and red with a high magnitude in the plot correspond to stronger changes in the power signal for example on days 6 and 9.

However, it is unclear which magnitude of W can be considered a ramp and distinguish it from changes in power which are non-ramp events. Although it may be possible to visually distinguish a few ramps by comparing the scalogram and the original power signal, it is not possible to detect all the ramps in the power signal.

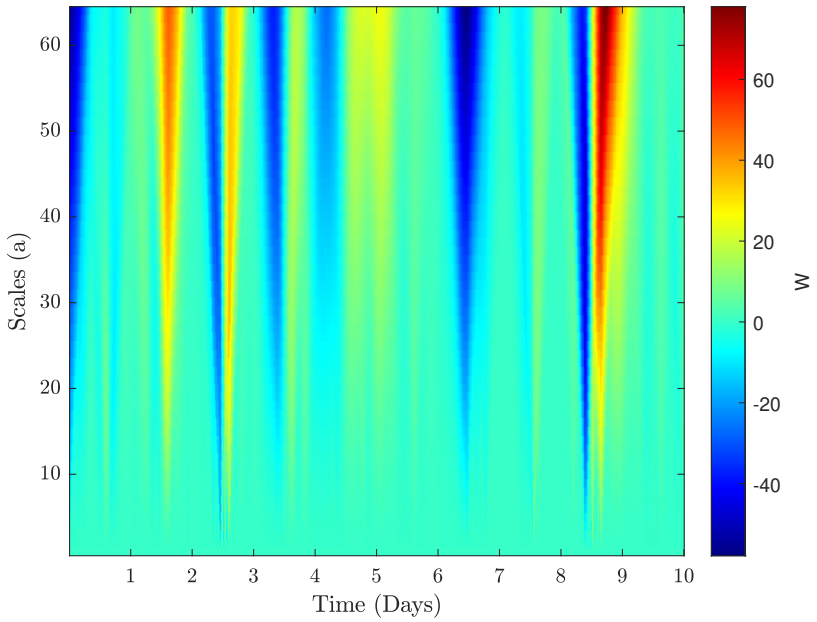

Figure 4.8: Wavelet coefficient scalogram of generation signal

4.3.2. Randomly shuffled surrogate models

The method distinguishes ramp events from non-ramp events by using randomly shuffled surrogate models of the original power signal. Random shuffling is a method for generating surrogate data from the original time series that preserves only the distribution of the original data. The auto-correlation within the time series is removed.

The wavelet transform of one surrogate power time series is shown in Figure 4.9 using the same criteria as for the original power signal. As seen in Figure 4.8, the higher scale value structures or the lower frequency structures have vanished in the case of the surrogate power signal. The wavelet spectrum's power is more evenly distributed across all scales.

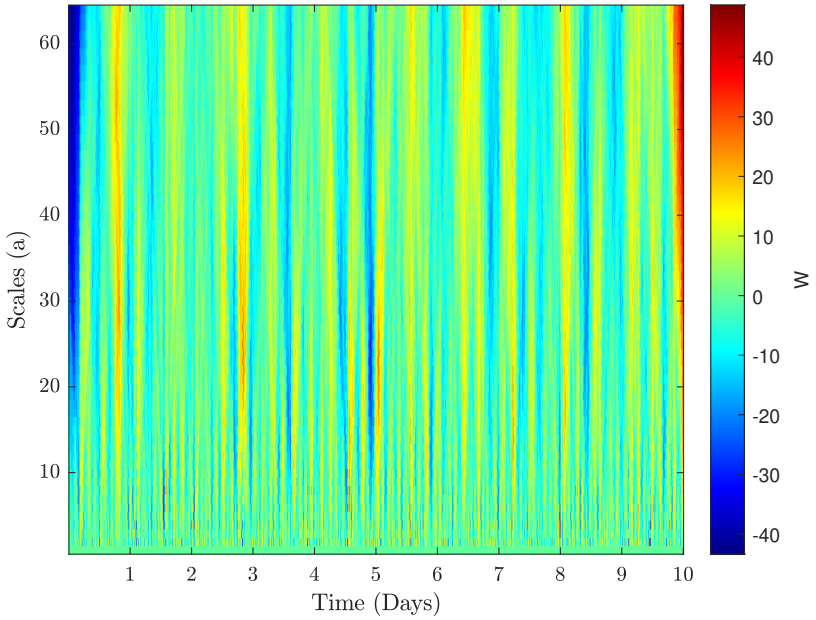

Figure 4.9: Wavelet coefficient scalogram of surrogate signal

A total of 100 such surrogate signals are generated based on the ten-day period, $P_i^*(t)$, where i = 1 to 100. Each of the surrogate signals is subjected to the wavelet transform such that the coefficient values are given by $W_i^*(a,b)$. Following that, distributions of the coefficient values of the b values for all the 100 surrogates of each scale parameter a are generated using these coefficient values. These distributions are then to be compared with the distribution of the wavelet transform coefficients $W(a,b)$ of the original data.

In Figure 4.10, the solid red line represents the distribution of coefficient values for the original signal W at a = 40, whereas the dotted lines represent the distribution of coefficient values for all surrogates, W^* at a = 40. The threshold W_T^* for discriminating ramp events is set to the greater 10% of the $|W^*|$ magnitude of the distribution of the wavelet transform of the surrogates [33]. The yellow region beneath the dotted line contains the largest 10% of the magnitude of the wavelet coefficients at scale a = 40 of the surrogate data. The W values are then discriminated by this W_T^* value such that the yellow region beneath the solid line contains the values of the discriminated coefficients.

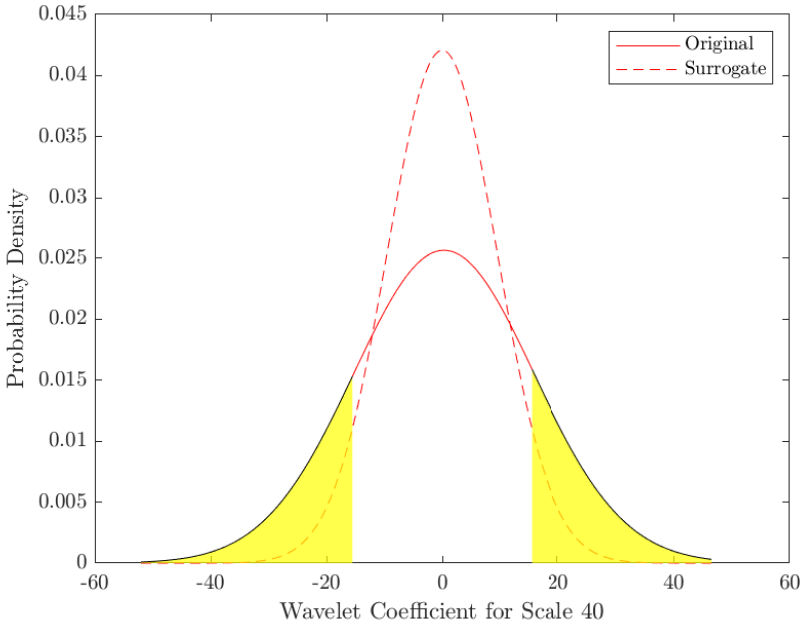

Figure 4.10: Distributions of W and W^* for the scale 40

This method of detection is carried on for all scales of W such that for each scale a, the scale-dependent threshold value $W_T^*(a)$ is computed. In a case that the $|W_H(a,b)|$ value is lower than the $W_T^*(a)$, a null hypothesis is accepted and assumed to not be a ramp. On the other hand, if the value of $|W_H(a,b)|$ is greater than $W_T^*(a)$ at the specific scale, the event is assumed to be a ramp event.

The scalogram obtained by applying this method to discriminate the ramps at each scale is shown in Figure 4.11. When compared to Figure 4.8, the plot is similar, but the values below the threshold values are removed and shown as zero. The remaining values, indicated by other colors, are those that meet the criteria and are thus considered ramp events.

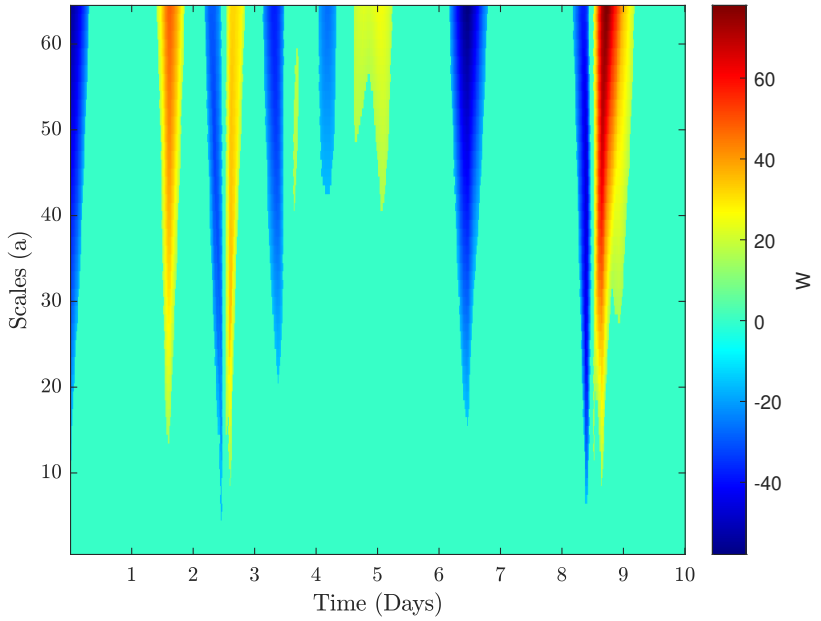

Figure 4.11: Wavelet coefficient scalogram after detection

4.3.3. Detection of ramp events

Once the detection of the ramp and non-ramp events is computed using the above-mentioned method, the mean power ramps $R(t)$ can be calculated using Equation 4.3. The ramps detection using wavelet transform will be referred to as **Wavelet Method** in the report.

$$
\begin{aligned}
&R(t) = \frac{1}{a_{\max}} \sum_{a=1}^{a_{\max}} W_{\mathrm{R}}(a,b), \\
&\text{where} \\
&W_{\mathrm{R}}(a,b) = W(a,b) \quad \text{when} \quad |W(a,b)| \geq W_{\mathrm{T}}^{*}(a) \\
&W_{\mathrm{R}}(a,b) = 0 \quad \text{when} \quad |W(a,b)| < W_{\mathrm{T}}^{*}(a)
\end{aligned}
\tag{4.3}
$$

The mean ramps for each time period are calculated as a fraction of the sum of the wavelet transform values for all scales and the scale parameter's maximum value, which in this case is 64. As mentioned in the previous section, the $|W_H(a,b)|$ values lower than the $W_T^*(a)$ value are assigned a value of 0.

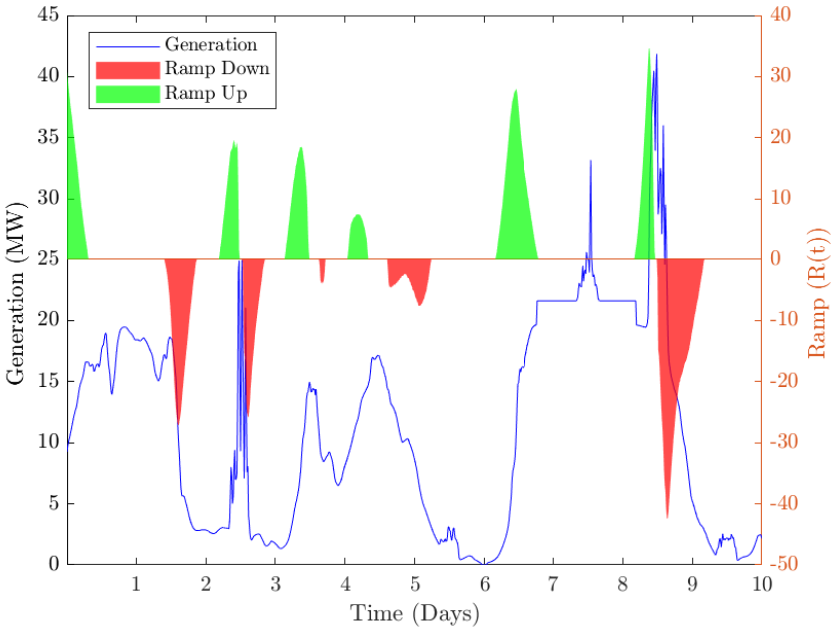

Figure 4.12: Ramp detection with wavelet transform

Figure 4.12 gives the power signal of the 10 day period that is considered superimposed with the ramp values $R(t)$. Figure 4.12 depicts the power signal for the ten-day period superimposed with the ramp values $R(t)$. The green areas denote the ramp up events, while the red areas denote the ramp down events. The magnitude and duration of the ramps can be easily determined by processing data from the start and end points of detected ramp events. The number of ramps is calculated as the count of all magnitudes of the ramps that are above zero. Figure 4.13 gives the overview of the ramp detection method using wavelet transform.

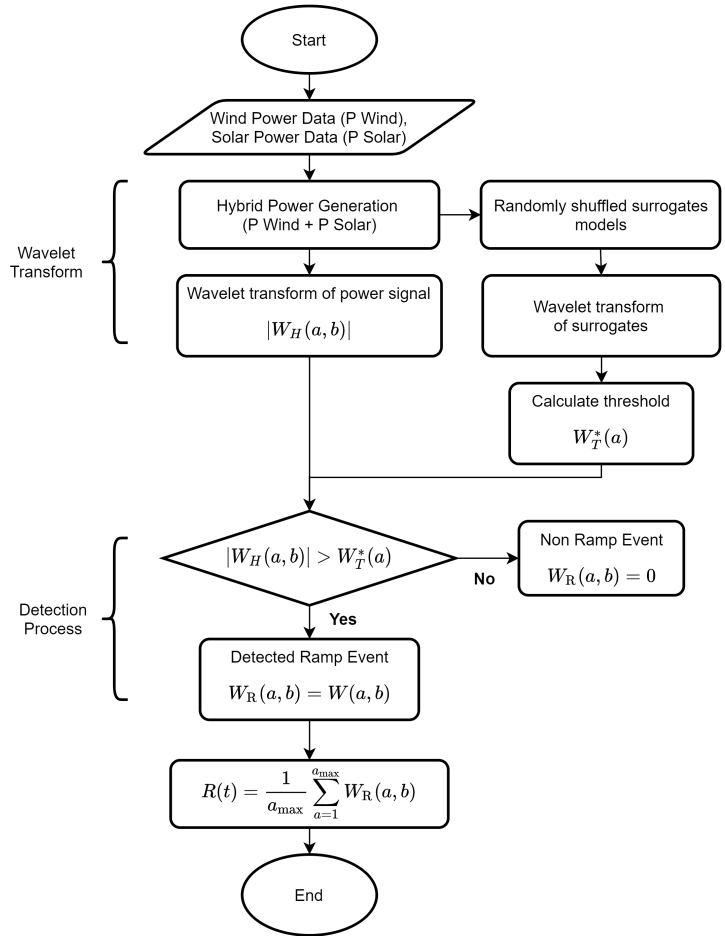

Figure 4.13: Overall framework of ramp detection using wavelet method

4.4. Ramp detection using demand correlation

This section describes a methodology for detecting ramp events that incorporates information from the load side in order to identify and discriminate ramp events in conjunction with the previous methods. The previous methods of detecting ramps were based solely on power output, ignoring the constantly changing demand discussed in Section 2.4. To address the lack of detection methods that combine information from the source and load sides, this section introduces the concept of significant ramps.

4.4.1. Trends in demand

In one scenario, generation from the farm may decrease abruptly and is detected as a ramp down using one of the previously discussed methods, while demand also decreases during the same period, as illustrated in Figure 4.14. In another scenario, as illustrated in Figure 4.15, there could be a ramp down in generation while demand continues to rise throughout the duration of the ramp event.

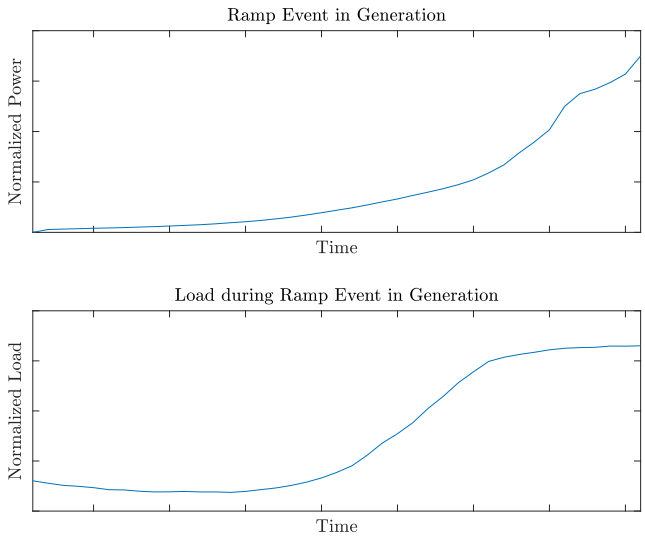

Figure 4.14: Same direction change in both load and generation (Not a significant ramp event)

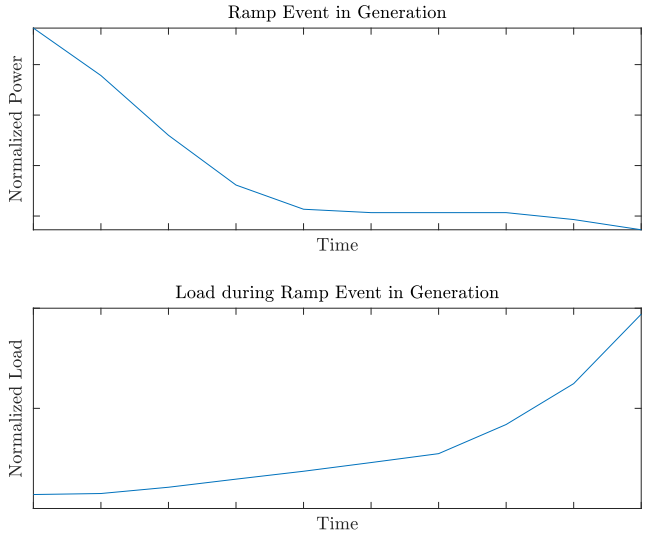

Figure 4.15: Opposite direction change in both load and generation (Significant Ramp)

The former case would result in a less disruptive and significant ramp down event than the latter. In the first case, because generation decreases as demand decreases, the requirement for balancing generation and demand through reserves and backup generation is avoided. Similarly, a ramp-up event that occurs as demand increases does not have to be curtailed. Due to the fact that these ramp events may be desirable [34], they are not considered significant. However, in the second case, the ramp down in generation must be resolved using reserve generators, as demand increases concurrently with the reduction in generation.

The ramp events that prove to be unfavorable are those in which the generation trend is in opposition to the demand trend. As a result, these ramp events are deemed more significant than ramps that follow the same trend as the load. The ramps that are detected by combining data from the source and load will be referred to in the report as **Significant Ramps**.

In this method, the plant-level power ramps are compared with the national load. There is a possibility that the ramps would not be significant and would be easily dealt with by other generators spread out over the nation. However, as the share of variable renewable energy generators increases, since the weather conditions would be similar over the country most of the power plants would ramp up and down at almost the same periods with some delay. Solar PV generation for one would have the same large ramp up and down events occurring at the same period around the country owing to the diurnal nature of solar energy.

4.4.2. Detection of ramp events

The ramp events are initially detected using the Binary method or the Wavelet method discussed in the previous sections. Then the demand curve of the nation, in this case, the Netherlands is examined. The normalized demand curve as discussed in Section 3.4 from the ENTSO-E Transparency Platform [37] is used to determine the significance of the events.

$$r_{sign} = \frac{\sum_{i=T_{start}}^{T_{end}} \left(G_i - \bar{G}\right)\left(L_i - \bar{L}\right)}{\sqrt{\sum_{i=T_{start}}^{T_{end}} \left(G_i - \bar{G}\right)^2} \sqrt{\sum_{i=T_{start}}^{T_{end}} \left(L_i - \bar{L}\right)^2}} \tag{4.4}$$

Once the ramp event is identified using the binary or wavelet method, the start and end times of the ramps are recorded and the corresponding demand from the start to end is checked. The correlation coefficient between the demand and the generation during the duration of the event is calculated using Equation 4.4. The generation and load are denoted by G and L respectively while the ramp start and end time are given by T_{start} and T_{start}.

If the correlation between the two is close +1, the correlation is very strong and the trend is in the same direction and hence the significance of these ramp events is less. On the other hand, if the correlation is close

to -1, the generation and load during the period are highly anti-correlated and have a high significance. The scores of the significance of the ramps are determined in two methods given below.

- **Simple score**

  A simple scoring technique examines only the sign of the correlation coefficient between generation and load during the event. If the value is negative, the event is assigned a value of one and is considered as a significant ramp. Alternatively, if the value is positive, the event is assigned a significance score of zero, indicating that it is not significant.

- **Weighted score**

  Different weights are given to the ramp events based on the correlation coefficient values of the generation and demand. The highest weight is given to a ramp event with a correlation of -1 and the least is given to a correlation of +1. Events with a high score that is for correlation below -0.3 are considered as significant and the remaining are eliminated. This strategy can be improved further by taking into account ramps of varying significance and using different strategies to deal with them depending on the significance.

Figure 4.16 gives the power signal of the 10 day period superimposed with the significant ramps detected using demand correlation after detection with the binary method.

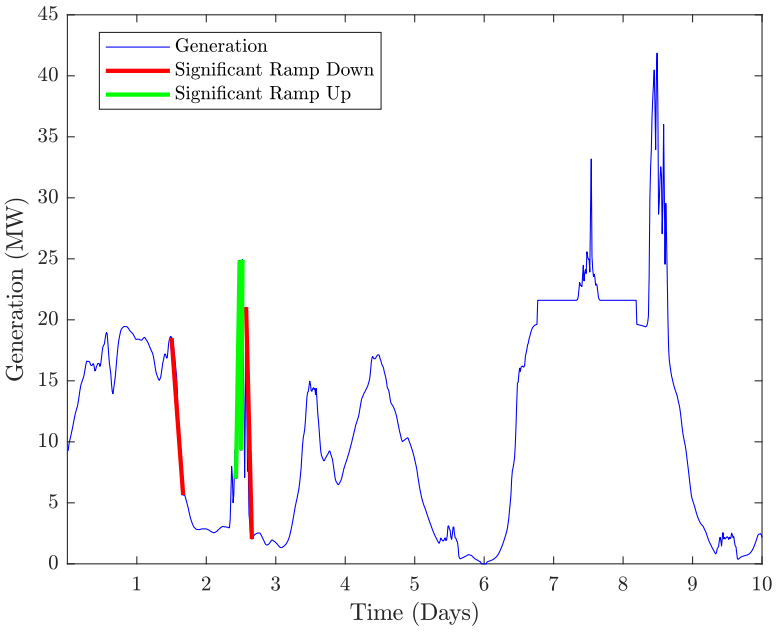

Figure 4.16: Significant ramps with demand correlation

A fraction of the ramp events are eliminated due to the corresponding load values and hence the number of ramps is lower compared to the previous methods. This can be noticed in Figure 4.17 which depicts the average daily profile of the periods when ramp events exist with and without implementing the significant method. The solid lines are the ramps that are detected using the wavelet method while not considering the trend in the load. The dashed lines depict the significant ramps that are detected with the wavelet method and processing the load information. As discussed, the number of ramps is lesser in the significant method. The second plot gives the typical averaged load profile of the Netherlands. The load follows an increasing trend from 2:00 to about 18:00, during this time the ramp events that are in the same direction (ramp ups) are not considered significant anymore which can be noticed in the reduction in the number of ramp ups during that period. Similarly, the ramp down events during 18:00 to 2:00 are eliminated since the load is decreasing at the same time.

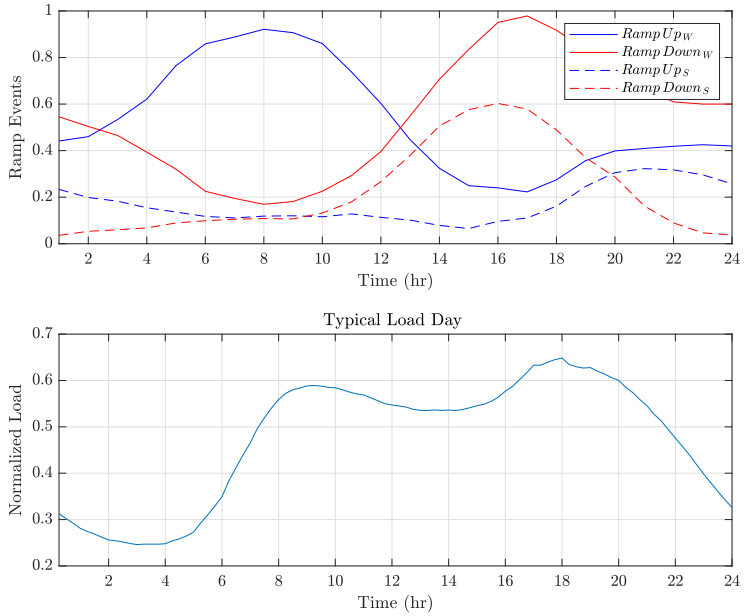

Figure 4.17: Time of occurrence of ramp events with and without significant method and average daily load profile

The method is applied to all of the ramp events discovered by the preceding approaches, and the significance of the events is determined. The duration and magnitude of these events can be extracted simply by checking the values corresponding to the start and end times. The overall framework of the significant ramp detection is illustrated in Figure 4.18.

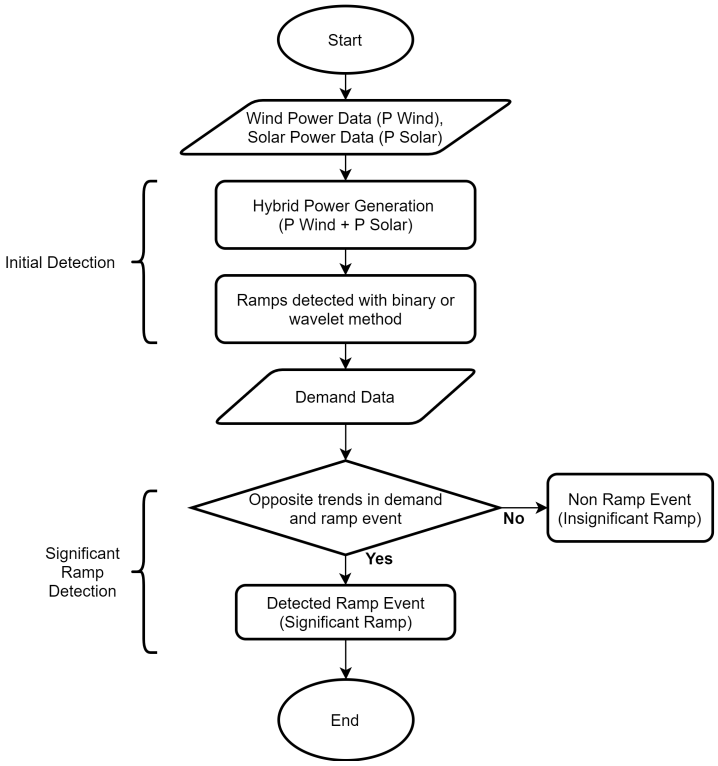

Figure 4.18: Overall framework of ramp detection using significant method

4.5. Evaluation of methods

One of the objectives of the research is to find the most effective metric to characterize the ramp features of a hybrid power plant. This section gives an overview of the differences in ramp detection methods and their comparison. The most suitable method is selected at the end of the chapter.

The detection of ramps using the basic method as presented in Section 4.1 takes into account a set time interval and threshold value that affect the identification of ramps in the power signal. The threshold values and time interval values vary across the literature. These definitions are considered to be basic classifications because the ramps are claimed to have the same predetermined time duration and so do not include ramps with different time resolutions. Ramp events are under-reported because their duration is not necessarily defined and can range from 15 minutes to 10 hours. This method also detects noise in the signal as ramp events and hence is not accurate.

The binary method for detecting ramps is defined by a set of thresholds that varies across the literature, and no particular binary definition is universally accepted. The ramp detection with the binary method is very sensitive to the definition used. Due to a lack of consensus and consistency in the binary definitions of a ramp, picking the best method would be very difficult to achieve.

The binary method can be used in the detection of ramp events in the case of wind farms as suggested in the literature. However, when it comes to the detection of ramps of a hybrid power plant with both wind and PV, the detection is not as accurate and dependable. All the definitions use thresholds which are defined as a percentage of the rated capacity of the farm. In the case of wind farms, wind turbines have a higher capacity factor and operate at their rated capacity more often than solar PV panels.

In case A, a wind farm of 50 MW, the ramp up definition of 20% of installed capacity would mean a change in the generation of 10 MW or above would be classified as a ramp up. The farm will operate at 50 MW for a considerable fraction of the year. A 20% definition for a ramp up in case B with a Hybrid power plant with 50 MW wind and 30 MW solar would mean that the threshold would be set to 20% of 80 MW which is 16 MW. However only in few instances, the farm operates at the rated capacity of 80 MW.

A ramp up event occurs in the first case with a magnitude of 12 MW and the same event occurs in the second case at the same time and magnitude due to the wind capacity being the same assuming solar irradiation is zero during the event. In the first case, the ramp event is detected as it is greater than the threshold of 10 MW while in the second case it is not detected owing to the greater threshold of 16 MW. When there is a mix of both wind and PV in the hybrid power plant, determining the threshold based on the total installed capacity would result in overestimating the value. The threshold values are set high due to the PV capacity which usually does not generate at its maximum capacity. The ramp events are under-reported using this method.

One method of detecting solar ramps using the binary method and SDA is presented by Cui et al. [41]. In this method, the ramps are first detected for the power generated with the original irradiation for the particular location. Next, the ramps are detected for the power that would be generated assuming clear sky conditions. The ramp events that are detected in both cases are eliminated since these would be caused due to the diurnal nature of the solar irradiation. Only events that occur due to the passing clouds are considered and deemed important as the diurnal nature is present every day and is always known to occur. However, this method can not be applied to a hybrid power plant since the generation is a mix of both wind and PV. Once the wind and PV generation are combined, the diurnal ramps of solar become less recognizable. Although the diurnal ramp of solar are known to exist, they can not be eliminated since the PV generation adds up to the wind to either create larger ramps or prevent wind ramps.

The wavelet method on the other hand does not depend on predefined thresholds and rather on statistically determined thresholds. These thresholds can easily be determined if there is sufficient historical data of the wind speeds and solar irradiation for the particular location. The randomly shuffled surrogate models of the historical data can be easily modeled and the thresholds for each scale factor as discussed in Section 4.3 can be calculated and defined. The detection of ramps is not based on the installed capacity of the hybrid power plant which removes the issue of overestimation of the threshold. Instead, the detection is done based on the statistical thresholds from the site data. This prevents the overlooking of ramp events that occur in the binary method.

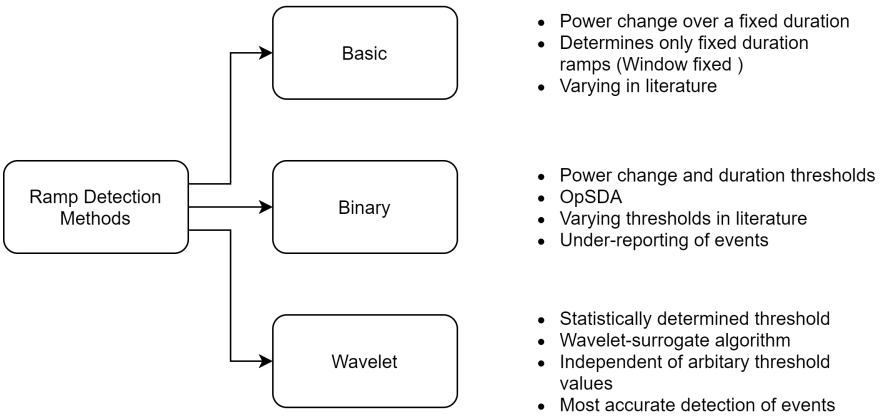

Figure 4.19: Different methods of ramp detection

4.5.1. Comparison of detection methods

Table 4.1 gives the comparison of the ramp features with binary and wavelet ramp detection methods. Different definitions with different threshold values for the binary method are presented in the table. The grid capacity of 50 MW is considered while the installed capacity is 59.6 MW. First, the ramp events are detected with the binary method with both ramp up and ramp down threshold of 20% of the grid capacity for the reference case. Second, the binary method is used with a ramp up of 20% and a ramp down of 15% of the grid capacity. Next, the same method as the previous case is used but the thresholds are a percentage of the installed capacity. Finally, the wavelet method is used to detect the ramp events for the same power signal as all three.

While comparing the first and second cases in the ramp downs, it can be noticed that the number of events has increased with the second definition. In the first definition, the event is detected as a ramp down when the magnitude is higher than 20% of the grid capacity (50 MW) which is 10 MW. However, in the second definition, the ramp down is detected if the magnitude is greater than 15% of the grid capacity which is 7.5 MW. Since the threshold is lower, more events are detected as ramp down events.

Now looking at the second and third cases, the threshold percentage remains the same for ramp ups and ramp downs. However, the second definition considers a threshold calculated as a percent of the grid capacity while the third definition considered a percent of the installed capacity. The ramp up in second definition is detected if the magnitude change is greater than 20% of the grid capacity (50 MW) that is 10 MW. And in the third definition, the change must be greater than 20% of the installed capacity (59.6 MW) which is 11.92 MW. Lesser ramp events are detected in definition three since the threshold value is higher than the second definition and hence the changes below the thresholds are ignored.

Ramp Up							
					Largest Ramp		
Method	No. of Events	Total time of year (%)	Average Duration (hours)	Average Magnitude (MW)	Magnitude (MW)	% of Installed Capacity	Duration (hours)
1. Binary (20, 20, Grid Cap)	351	33.6 %	8.4	21.7	48.7	81.7 %	13.7
2. Binary (20, 15, Grid Cap)	351	33.6 %	8.4	21.7	48.7	81.7 %	13.7
3. Binary (20, 15, Installed)	326	31.6 %	8.5	22.1	48.7	81.7 %	13.7
4. Wavelet	370	39 %	9.3	23.5	47.7	80 %	11.75
Ramp Down							
					Largest Ramp		
Method	No. of Events	Total time of year (%)	Average Duration (hours)	Average Magnitude (MW)	Magnitude (MW)	% of Installed Capacity	Duration (hours)
1. Binary (20, 20, Grid Cap)	330	29 %	7.9	20.6	47	78.8 %	13.5
2. Binary (20, 15, Grid Cap)	347	30 %	7.6	18.3	47	78.8 %	13.5
3. Binary (20, 15, Installed)	343	29.7 %	7.6	20	47	78.8 %	13.5
4. Wavelet	369	39 %	9.3	22.8	47.9	80.3 %	12.5

Table 4.1: Comparing ramp detection methods

It can be seen that the ramp detection using the binary method is extremely sensitive to parameters such as the magnitude thresholds, the duration thresholds and capacity to be considered. There are no verified and accepted threshold values for the ramp detection and hence the results are inconsistent. As mentioned in Section 4.2, a few definitions use duration thresholds which limits the duration of an event which can be considered as a ramp. With different duration threshold values, the ramp detection fluctuates. The capacity to be considered varies in literature and as demonstrated, the ramp events detected are sensitive to the capacity that is considered.

The issue that arises, in this case, is that the installed capacity may fluctuate over time. Additional turbines or solar panels could be installed or current ones improved. With increased installed capacity, a ramp event that was identified previously would no longer be detected as one, as the capacity has been raised, and thus the threshold has been increased. When capacity is lowered, on the other hand, due to maintenance, smaller magnitude ramps are generated, which may be managed by the operator but are mistakenly identified. However, the difficulty of handling ramps of the same magnitude would be the same in both cases.

The issue of under-detection of ramp events due to overestimating the threshold values in binary definitions as discussed earlier can be noticed by comparing the wavelet method and binary methods. The number of ramps detected using the binary method is lower compared to the wavelet method for both ramp up and ramp down events. The wavelet method prevents the under-detection of ramp events by not considering predetermined thresholds. The largest ramp events are given for all the cases and the largest events are much the same for both binary and wavelet methods. The total time of the year that the ramp events occur also depict that the binary definitions detect a lower number of ramp events compared to the wavelet method.

	Up Ramps				Down Ramps			
Method	No. of Events	Total time of year (%)	Average Duration (hours)	Average Magnitude (MW)	No. of Events	Total time of year (%)	Average Duration (hours)	Average Magnitude (MW)
Wavelet	370	39 %	9.3	23.5	369	39 %	9.3	22.8
Wavelet Significant	76	5.8 %	6.7	11	218	22 %	8.9	24

Table 4.2: Detection with significant method

The significant ramp detection as introduced in Section 4.4 is used in conjunction with the wavelet method and the results are presented in Table 4.2. The ramp events in the significant method are reduced since a few are eliminated owing to the same direction of the generation and load during an event. The ramp ups are reduced considerably as the ramp ups in generation coincide with the ramp up in load which occurs during the day. The portion of the year covered by ramp up events decreases by around 85% in the case of significant ramp events. The ramp downs are reduced but not as much as the ramp ups, since the ramp down in generation does not coincide regularly with ramp downs in demand.

4.5.2. Selected definition

As previously stated, the wavelet transform method has two distinct advantages over the binary method. One benefit is that the detection does not rely on arbitrary threshold values, and two, the problem of under-reporting hybrid wind-PV ramp events becomes less severe.

The wavelet transform requires historical data of the wind and solar irradiation at the site. This data is easily obtainable and the thresholds can easily be determined statistically. The wavelet-surrogate method is more elaborate and relatively computationally complex. However, this method yields a better detection of ramp events than other methods that depend on simpler fixed threshold based definitions.

As discussed earlier, the ramps can be classified based on the behavior of the demand during the occurrence of a ramp event. The significant method of detecting ramp events combines both the generation and demand data to determine the significance of the events. Since the ramp events with the same trend as the demand would be desirable and need not be removed, this method of detection gives a finer idea on the events that are of importance to the grid operation.

Considering all the issues presented in this section, the ramp detection with the wavelet method to characterize ramp features of a wind-based hybrid power plant is more suitable compared to basic and binary methods. The problem of not considering information from the load side, introduced in Section 2.4, for ramp event definitions is addressed with the significant ramp method. The significant method in combination with the wavelet method is thus selected as the preferred detection method for wind-based hybrid power plants in this study.

5

Complementarity

This chapter gives an overview of the complementarity concepts and a comparison of different time scales and spatial dispersion. Section 5.1 covers the general idea and need for calculating the correlations between sources. Next, Section 5.2 covers the reduction in variability over a national scale with distributed generation locations. Further, the complementarity of wind and solar power over different time scales for the reference case and the nation are presented in Section 5.3. Finally, the complementarity on different time scales and ramp events are compared in Section 5.4.

5.1. Complementary nature of wind and solar

Wind and solar energy are both intermittent sources with timescales varying from a few minutes to years due to their reliance on weather conditions, which presents the grid operators with issues [42]. Solar power follows diurnal and annual patterns that are driven by the movement of the earth around the sun and is disrupted by cloud coverage. On the other hand, wind energy is dependent on fluctuations in local wind speeds induced by moving weather fronts [10]. The variations of wind and solar do not follow the same characteristics and it is possible to attain a partially smoothed total hybrid output generation [9]. In the future with a significant portion of the energy mix taken up by the wind and solar power, it is important to study the correlation between different power sources in order to meet the demand and optimize the reserve generation.

Complementarity in terms of wind and solar generation is the capability of the two sources to compensate for each other to give put a smoother output. Complementarity can be observed both in time and in space domains [7]. Temporal complementarity is observed between two or more sources in the same location such that the sources exhibit periods of availability that are complementary in the time domain. Spatial complementarity is observed between many sources of generation of the same type or different where the sources complement each other over a particular area. The lack of a particular source in one region is complemented by the availability in another region.

Wind-based hybrid power plants aim to increase the overall system reliability and reduced the cost of energy. The hybrid power plants are based on the principle of exploiting the complementary nature of wind and solar to provide a comparatively steady output. Hence, an analysis of the complementarity of the wind and solar is required as presented in section 2.1. The correlation between the two sources is calculated using the Pearson correlation coefficient. In the case of the hybrid power plant, a negative correlation or an anti-correlation is desirable as it indicates that the two sources are complementary in nature [43]. The Pearson correlation coefficient between the data sets of wind (W) and solar (P) is calculated using Equation 5.1

$$r_{Wind\,PV} = \frac{\sum_{i=1}^{n}\left(W_i - \bar{W}\right)\left(P_i - \bar{P}\right)}{\sqrt{\sum_{i=1}^{n}\left(W_i - \bar{W}\right)^2}\sqrt{\sum_{i=1}^{n}\left(P_i - \bar{P}\right)^2}} \tag{5.1}$$

5.2. Spatial complementarity

The more spread out the generation units are, the smoother the combined output is. This reduces the requirements of reserves, reduces forecast errors and allows conventional plants to run at higher efficiency. Several studies have concluded that dispersion causes a reduction in variations and increased availability of power [44] [8]. Increased deployment of renewable energy would improve the system reliability. For wind energy, the correlation is strong with farms that are nearby and it decreases as the distance increases between the farms [10]. The weather fronts do not occur and affect the entire nation at the same time and hence, a lower correlation. Solar power on the other hand is almost consistent throughout the country since solar power is based on the diurnal pattern of solar energy.

In Figure 5.1a the normalized ramps for each month is shown for both the site and nation scale generation. It can be seen that the number of ramp events is much lower on the national scale owing to the dispersion of the wind farms all over the nation which leads to a reduction in fluctuations and hence ramp events.

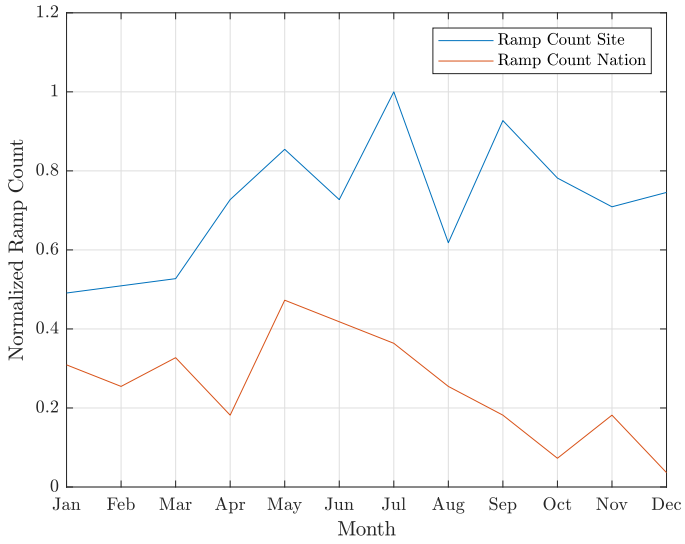

(a) Normalized ramp counts for nation and site wind generation

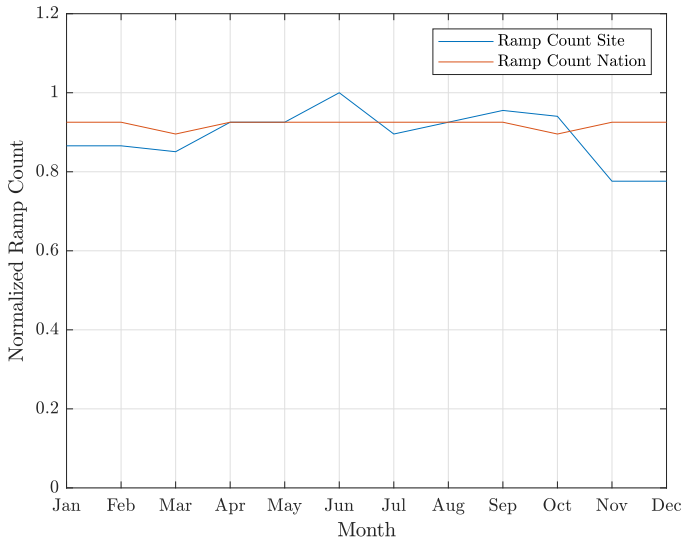

(b) Normalized ramp counts for nation and site PV generation

Figure 5.1: Normalized ramp counts for nation and site for every month

Figure 5.1b gives the normalized ramp events for the solar generation for the scale and the nation generation. There is not much difference in the ramp events since the solar power follows the same diurnal patterns on a daily basis and will not vary much over a long region and hence very less reduction in ramp events or fluctuations will occur.

5.3. Temporal complementarity

Temporal complementarity is a phenomenon when variable sources such as wind and solar have an availability such that they are complementary in the time domain. The Pearson correlation coefficient is applied to the data set of the wind and solar at different time scales. The different time scales are looked at with the hourly totals, the daily totals, and monthly totals of the data. Figure 5.2 gives the variability and correlations of wind and solar power in the reference site on different time scales. In Figure 5.2a, there exists a strong anti-correlation or negative correlation of -0.74 for monthly totals of wind and solar power. This suggests that the sunny months are less windy and similarly the windy months are less sunny. The daily total time scale shows a weaker yet negative correlation of -0.38. On the hourly scale, wind and solar power have a weak negative correlation of -0.04. It can be seen from the daily profile in Figure 5.2c that the wind does not follow a strictly diurnal pattern that the solar follows.

The negative correlations in the monthly, daily and hourly scale suggest that the wind and solar could even out fluctuations in power on longer scales. However, it is not clear if the fluctuation or ramp events in smaller time scales of hours can be removed. As mentioned, fluctuations and ramps exist on both diurnal and seasonal timescales, it is possible to study the seasonal complementarity on both hourly and daily scales. Table 5.1 gives the correlation coefficients for each month in both the daily and hourly scales with the daily and hourly totals. The correlations on the hourly scale are very weak and almost zero. However, the majority of the daily scale values are not very strong but are still anti-correlated and suggest that sunny days are generally less windy and windy days are generally less sunny.

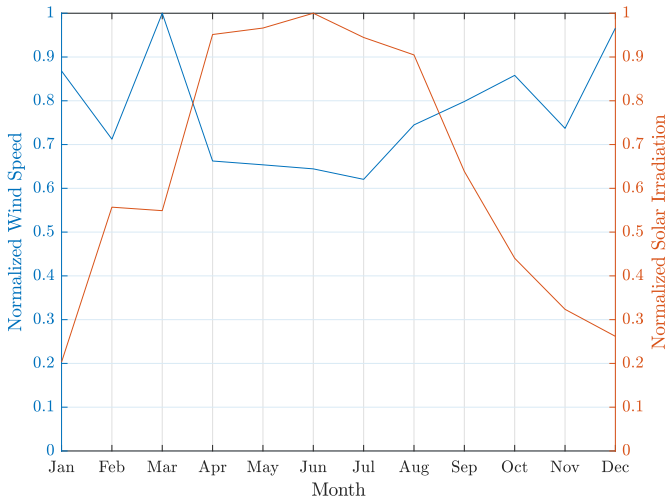

(a) Monthly totals ($r_{Wind\,PV} = -0.74$)

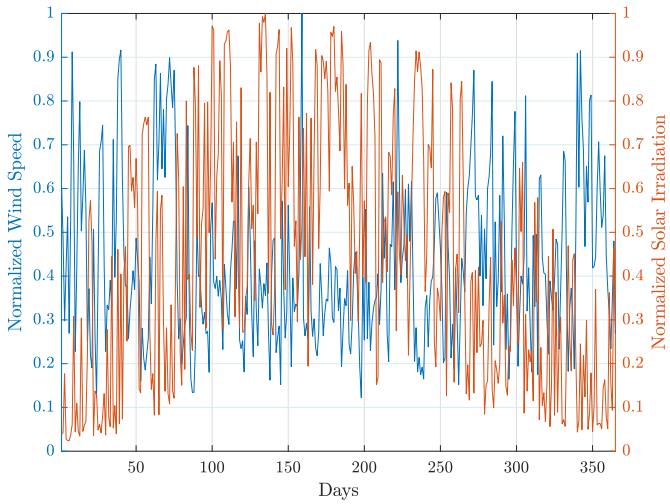

(b) Daily totals ($r_{Wind\,PV} = -0.38$)

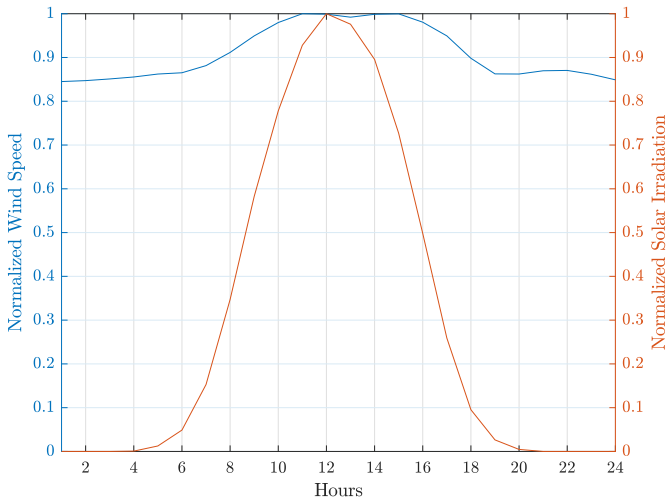

(c) Hourly totals ($r_{Wind\,PV} = -0.04$)

Figure 5.2: Variability and correlation coefficients between site wind and solar power on different time scales

Month	Correlation Coefficient	
	Hourly Totals	Daily Totals
January	-0.11	-0.39
February	-0.04	-0.42
March	-0.05	-0.37
April	0.22	0.13
May	0.19	-0.05
June	0.04	-0.22
July	0.12	-0.39
August	-0.02	-0.49
September	-0.02	-0.49
October	0.13	0.07
November	-0.12	-0.43
December	-0.06	-0.38

Table 5.1: Correlation between the hourly and daily totals of wind power and solar power at the site for each month

The same calculations for correlation coefficients are done for national scale wind and solar power data that is obtained from the ENTSO-E Transparency Platform [37] for the year 2019. A stronger anti-correlation given in Table 5.2 for the monthly scale exists compared to the site alone implying a stronger complementary between the wind and solar on the national scale. The hourly correlation for the nation is -0.2 which is weak but is still stronger than the site hourly correlation value of -0.09.

Time Scale	Correlation Coefficient
Monthly	-0.85
Daily	-0.42
Hourly	-0.2

Table 5.2: Correlation coefficients between national wind and solar power on different time scales

5.4. Ramps and complementarity

The ramp events occur on different time scales typically ranging from less than an hour up to 15-16 hours. The hybrid power plants are stated to have a stable power output owing to their complementary nature. However, the complementarity varies on different time scales and, as presented in Section 5.3, the anti-correlations are strong only on monthly and less strong on daily scales. The monthly and daily scales are much larger than the duration of the largest ramp events. Further, on the hourly scale, which would be better suited for studying the ramps, the correlation is very weak. Figure 5.3 gives the normalized ramp counts for each month with two cases of the hybrid power plant. The first case is the reference case for the site with 22 MW of wind power and 38 MW of solar power and the second case is a case with 40 MW of wind and 20 MW of solar power. Although the installed capacity is the same, the mix is different and hence the number of ramps detected is different in both cases. The dashed red line gives the correlation coefficient between the wind and solar at the site. For the two cases, it can be seen that the ramp events follow a general trend where the number of ramps is higher during the months with a positive correlation and fewer ramps when the wind and solar are negative. However, in the month of October, the correlation is higher than the previous month and the ramps are expected to go up in October. This assumption is true in Case 1 with the 22 MW wind and 38 MW solar where the number of ramps increased from September to October. But in Case 2, the number of ramps instead decreases. A similar problem occurs in July with case 1.

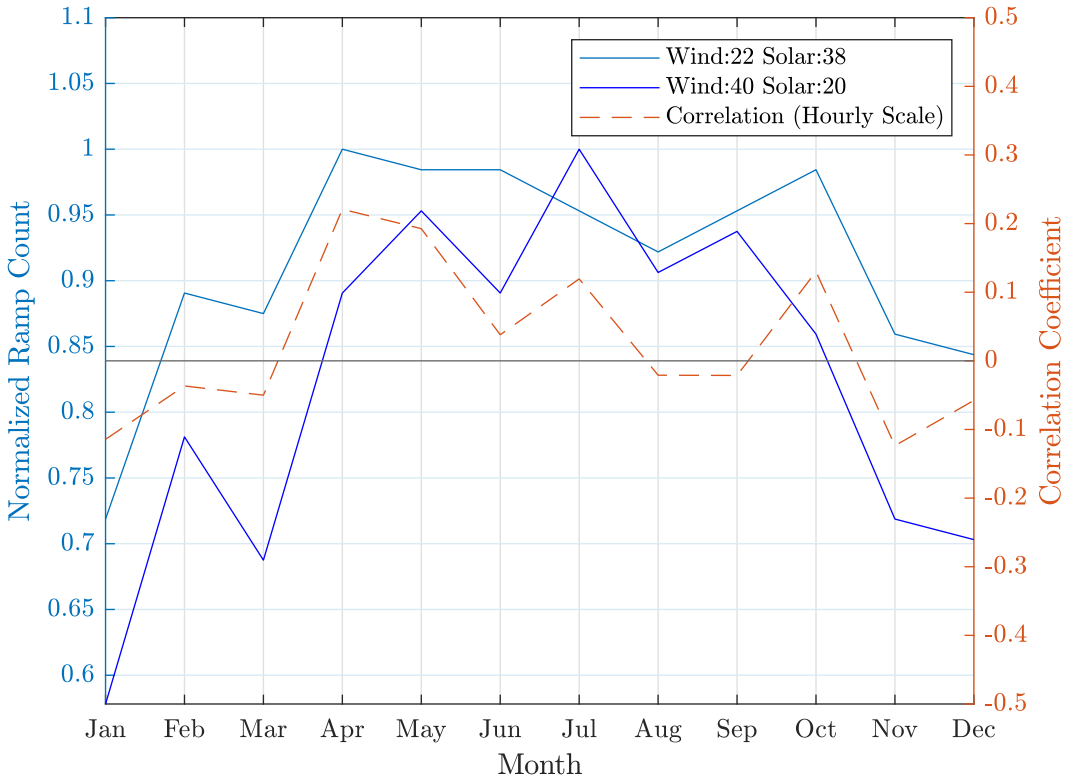

Figure 5.3: Correlation coefficients and normalized ramp count for 40 MW Wind and 20 MW PV

The complementarity alone can not perfectly give information on the ramp events that would occur. The regularity of ramp events does follow the correlations on the hourly scale up to a certain extent. However, this will not hold well when the hybrid power plant has one major and one minor source of energy. If the PV capacity would be very low around 2 MW while the wind capacity is 48 MW, the ramp events would be dominated by wind and the correlation between the wind and solar would be of no importance in predicting the ramp events in the generation.

Wind and solar power do not fluctuate on the same time scales. Irrespective of the weather conditions, solar irradiation always increases from zero to high irradiation in a few hours during dawn and decreases to zero in a few hours at dusk. The wind speeds generally fluctuate over longer time scales unlike the diurnal fluctuations of solar. Hence, although a negative correlation is seen over a year for different time scales, the short duration changes in solar power are not balanced by changes of the opposite direction in wind power. Thus having a high fraction of solar installed capacity as part of the hybrid plant would lead to a higher number of ramp events.

An evened-out distribution of the generation occurs on a larger monthly scale due to the seasonal behavior. Higher wind power is generated during the winter while more solar power can be produced in the summer. In a hybrid wind-PV plant, the overall availability over the year is higher as the dependency on a seasonal single source such as only wind or solar is reduced.

6

Hybrid Power Plant Sizing

This chapter discusses the many elements to consider during the sizing and selecting the wind-PV mix for the hybrid wind-PV farm in terms of ramp count, capacity factor, and internal rate of return. The chapter aims to answer the question of *what role the installed wind to PV capacity plays on the ramp events of the hybrid plant* and to determine the impact on the system. The optimal sizing for the hybrid wind-PV plant to minimize the number of ramps is presented in Section 6.1. The concept of over-planting and its effect on the ramp events is discussed in Section 6.2. The economic analysis of wind-based hybrid power plant along with the capacity factor is discussed in Section 6.3. A method of penalizing ramp events and internalizing them in the economic analysis is introduced in Section 6.4

6.1. Optimal sizing for ramps

The reference site uses 22 MW of wind and 38 MW of solar energy. However, this mix of wind and solar is not the best in terms of reducing the ramp events. A change in the wind and PV installed capacities is required to ensure a minimal number of ramps while providing being able to provide the capacity of the grid connection.

Since, this study concentrates on the ramp events in the hybrid power plant, the optimal sizing of the plant would require the least number of ramp events to occur. As the wind to PV ratio is varied, the total number of ramps changes since the magnitudes of the changes in power vary. An increase in solar generation in a scenario with very low solar installed capacity would not be detected as a ramp event owing to its low magnitude. However, during the same period, a higher installed capacity of PV could be classified as a ramp up event since the increase in generation would be severe. An increase in generation from solar could add up to a pre-existing increase in generation from wind turbines and cause a ramp event.

An optimization problem is devised such that the optimal Wind and PV installed capacity is calculated such that the ramps are minimized. The optimization is carried out with the same wind turbines and PV panels as presented in Chapter 3. A non-linear optimization problem is designed with an objective function to minimize the total number of ramp events that occur during the year.

6.1.1. Optimization problem formulation

The formulation of an optimization problem involves defining the objectives and requirements of the project and translating them into well defined mathematical expressions [45]. The formulation of an optimization problem includes deciding the objective function, choosing the design or optimization variables and determining the constraints.

Objective function: minimize the total number of ramp events

The objective of the model is to minimize the total number of ramps that occur over the one year that is considered in this study given in Equation 6.1. In the objective function, the number of ramps is calculated using the significant wavelet method that was explained in Section 4.3. The load information for determining

the significance is taken from the demand for the year 2019. The total number of ramps is given as the sum of significant ramp up and ramp downs. The significant ramp up count is given by the number of events with a magnitude above zero after removal of insignificant ramps of the same direction as load. Similarly, the ramp down count is determined by the number of significant events with a magnitude below zero.

$$\text{Minimize : Total number of ramps } (Cap_{wind}, Cap_{PV}) \tag{6.1}$$

Decision variables

The optimization is free to optimize the sizing of the hybrid power plant that is the wind and PV capacities. The decision variables are the wind installed capacity (Cap_{wind}) and the PV installed capacity (Cap_{PV}). The decision variables are bounded by a minimum and a maximum capacity value given in Equation 6.2.

$$\begin{aligned} 0 \leq Cap_{wind} \leq Cap_{wind,max}, \\ 0 \leq Cap_{PV} \leq Cap_{PV,max} \end{aligned} \tag{6.2}$$

Power flows and curtailment

The total installed capacity of the hybrid power plant is given by Equation 6.3. The total power generation from the hybrid power plant at any instance of time, t, is given in equation 6.4 where the wind power and PV power are calculated as the product of the respective installed capacities and the generation per MW of the units at the time. The power generation is capped at the grid capacity as given in Equation 6.5 and the rest is curtailed.

$$Cap_{total} = Cap_{wind} + Cap_{PV} \tag{6.3}$$

$$P_{total}(t) = P_{wind}(t) + P_{PV}(t) \tag{6.4}$$

$$P_{curtail} = P_{total} - P_{grid\ cap} \tag{6.5}$$

Grid connection

Given that the hybrid plant's grid connection is expected to be fixed, the sum of the two variables (Installed Capacity of the farm) must be greater than or equal to the grid capacity and may not exceed 100 MW.

$$P_{total} \geq P_{grid\ cap} \tag{6.6}$$

6.1.2. Optimization results

The optimization model is programmed in MATLAB programming language using the fmincon function from the optimization toolbox. The $Cap_{wind,max}$ and $Cap_{PV,max}$ values for the optimization are taken as 100 MW. As discussed in the reference case, the grid connection is considered to be 50 MW.

The significant wavelet method gives an optimal with wind capacity of 50 MW and PV capacity of 0 MW. The ramp events with wind energy only are limited to extreme events and are typically not so frequent. However, the solar ramps are frequent, steep and repetitive almost daily and hence result in a higher number of ramp events. Thus the solution prefers a complete filling of the grid capacity with wind energy.

6.1.3. Sensitivity of results

This subsection will detail the procedure that is used to check the sensitivity of the results to different conditions. The method consists of performing a series of optimizations with different constants and different method of ramp detection.

- **Varying constants**

  The optimization process is repeated with changed grid capacity values to check if the optimization model still prefers the filling of the grid connection with only wind energy. A grid connection of 30 MW and 100 MW are tested in the same model. The solutions in both cases give a wind capacity that fills the grid connection with solar capacity as 0 MW.

- **Ramp detection method**

  The ramp detection method for the total number of ramp events is changed and checked with the significant binary method, wavelet method and binary method. The solutions in all the cases prefer the grid capacity to be filled by wind turbines.

6.2. Over-planting

The study's reference case is based on the Haringvliet Energy Park, which has a grid connection or grid capacity of 50 MW. That is, the farm is expected to provide a maximum of 50 MW at any given time, with any extra power being curtailed or stored in batteries. Battery storage will be discussed in subsequent chapters. Over-planting is a strategy in which surplus generation sources such as wind turbines or solar panels are installed in the farm in excess of the grid capacity. This is done to increase generation during periods of low wind and low irradiation by adding more generation units. Over-planting with wind or solar energy may be a possible approach for enhancing the use of the electric infrastructure [46].

The optimal mix of wind and PV from Section 6.1 is taken as the base and two scenarios are considered, one over-planting with wind turbines and the second with PV over-planting. The overall ramps are examined first, followed by the individual ramp up and ramp down events.

The hybrid power plant is over-planted with wind and solar in two scenarios from 0 MW to 20 MW with steps of 0.5 MW. Figure 6.1 depicts the normalized number of ramps detected with the significant wavelet method at each step for both the wind and solar over planting scenarios. As seen in the blue line, the variation in the number of ramps is quite small and rather consistent in the wind over-planting scenario.

This can be attributed to the fact that since a major fraction of the base sizing is wind, the wind over-planting does not result in major changes in the overall profile of the generation. Above the grid capacity, the generation is either curtailed or stored. No new ramp events are added to the generation. On the other hand, the number of ramps increases considerably with the increase in PV over-planting. The addition of PV through over-planting introduces new ramps in the generation and as the capacity increases, the magnitude of the changes increases.

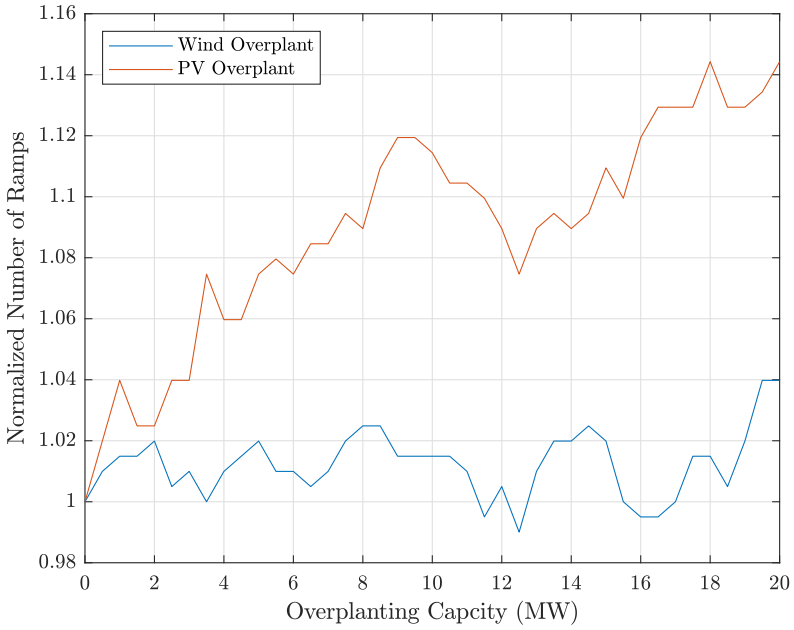

Figure 6.1: Number of significant ramp events with over-planting

Figure 6.2 gives the ramp up and down events with both the over-planting scenarios. In the wind scenario, as discussed previously only a few new ramps are introduced or old ramps are removed with over-planting and hence the number of ramp ups and downs is stable.

In the PV scenario, the number of up ramps decreases slightly with increasing PV installed capacity. The solar compensates for a few ramp ups in wind by filling up the gaps. The ramp up events due to PV coincide with the increase in load during the day and are no longer considered significant as discussed in 4.4.

The down ramps however increase with the increase in PV over-planting. The magnitudes of the power drops in generation increase as the over-planting increases and hence more ramp down events are detected. A majority of these ramp down events due to PV generation do not coincide with the decrease in load and hence are classified as significant ramps.

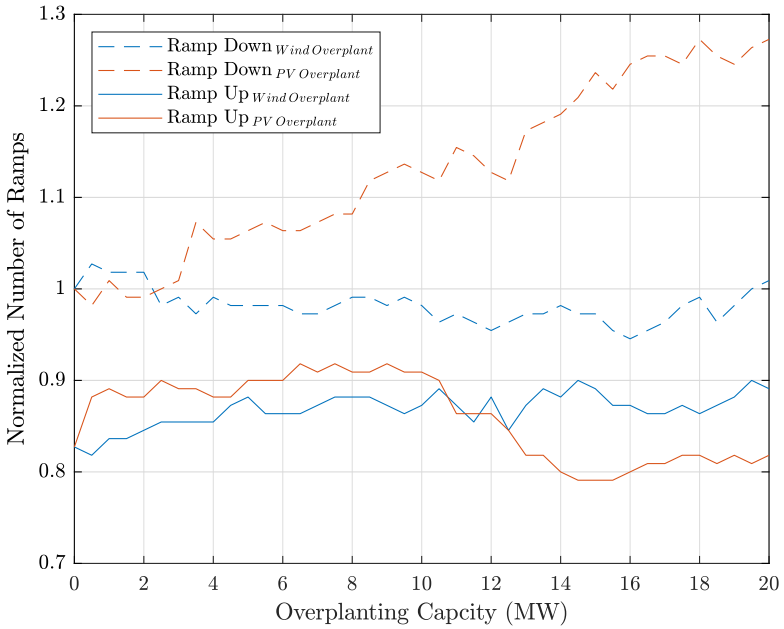

Figure 6.2: Number of significant ramp up and ramp down events with over-planting

6.3. Economic analysis

Over-planting results in an increase in the energy park's capacity factor. A commonly discussed advantage of hybrid power plants is the higher yearly capacity factor [47]. Any generation that exceeds the grid capacity is curtailed and/or stored, and so the capacity factor is defined as the ratio of annual energy production (AEP) to the product of grid capacity and the number of hours in a year, as specified in Equation 6.7.

$$\text{Capacity Factor} = \frac{\text{Annual Energy Production } (MWh)}{P_{grid\ cap}(MW) \times \text{ Time } (h)} \tag{6.7}$$

In the case of over-planting, the numerator, AEP of the energy park increases while the denominator remains the same since the grid capacity is fixed at 50 MW. This trend can be noticed in Figure 6.3 as the capacity factor increases as the farm is over-planted with either wind or solar up to 100 MW of rated capacity of the hybrid power plant. The increase in capacity factor for wind over-planting is higher than solar over-planting. Over-planting with wind would mean a more efficient utilization of the grid connection point in terms of capacity factor or the annual energy yield.

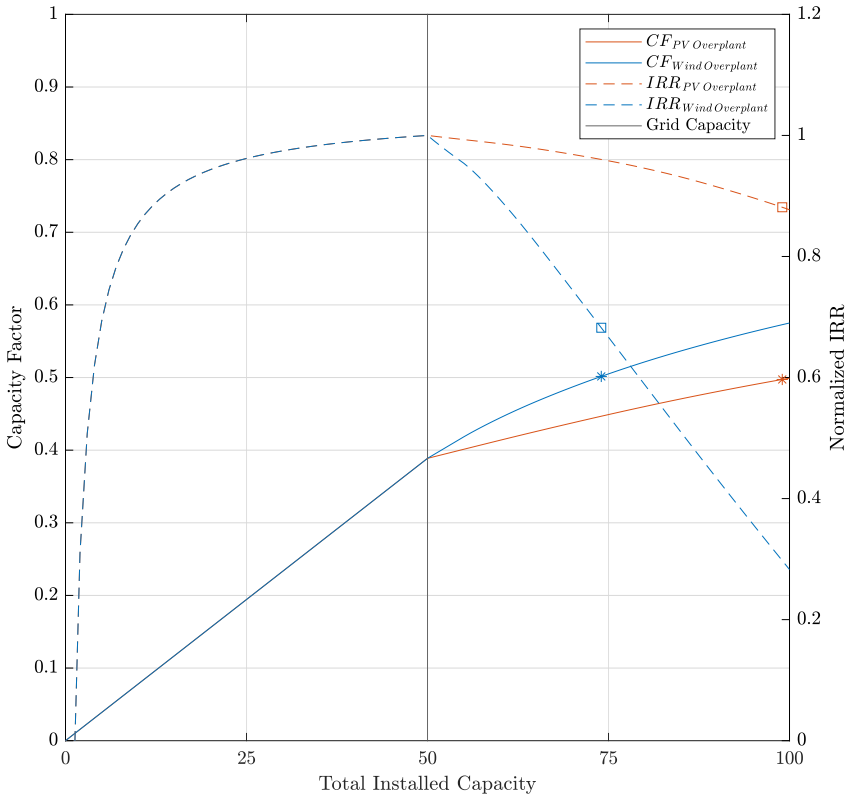

Figure 6.3: Capacity factor and IRR for over-planting with wind and solar

Internal rate of return (IRR) is a financial metric used to estimate the profitability of future investments when external factors are excluded. IRR is the discount rate at which the investment's net present value (NPV) of all cash flows equals zero. The IRR is determined using the NPV calculation specified in Equation 6.8. C_t denotes the net cash inflow for the year t, whereas C_0 denotes the total investment costs. IRR is popularly used for comparing the profitability of different projects. Investors can determine the estimated rate of return on a project by performing this calculation.

$$0 = \text{NPV} = \sum_{t=1}^{T} \frac{C_t}{(1+IRR)^t} - C_0 \tag{6.8}$$

Figure 6.3 depicts the normalized IRR that is calculated for the two scenarios of over-planting with wind or solar. A period of 20 years is assumed as the lifetime of the plant and IRR is calculated for the lifetime. The initial total investment cost is calculated as a sum of the total capital for turbines, capital for PV panels, the balance of system, and the grid connection tariff. The turbine costs are taken as €1300 per kW [48], PV capital cost of €750 per kW [49], connection tariff of €1.5m [50]. The same annual energy production and electricity price is assumed for the lifetime of the plant. The electricity price for the year 2019 is obtained from the ENTSO-E transparency platform [37].

It can be noticed that in both cases the IRR drops with over-planting however the drop is much higher and noticeable in the wind over-planting case. For a capacity factor of 0.5, the normalized IRR for wind over-planting is seen as 0.68 while for the same capacity factor, the solar over-planting normalized IRR is 0.88. This can be attributed to the excess curtailment of power with wind over-planting during times of high wind.

The wind power at higher wind speeds adds up to the existing power which has already hit the maximum value, grid capacity, at the same time period. The solar over-planting case fills up the gaps in generation with wind energy. Solar over-planting results in better utilization of the sources in terms of returns. Comparing the capacity factor and IRR changes with over-planting with either solar or wind, it is evident that although the increase in capacity factor is lower with solar, the drop in IRR is slower than with wind over-planting.

6.4. Economic analysis (with ramps)

A grid code is a technical specification that specifies the criteria that must be met by a generating unit connected to a public electric grid in order for the system to operate safely, securely, and economically. Certain grid codes restrict the rate of change of active power from the plant by mandating maximum ramp up and ramp down rates [51]. At the moment, grid codes have no specific regulations on the ramp rates of wind-PV hybrid power output. However, the power ramp rates for wind and photovoltaic output in many grid codes are commonly set to 10% to 20% of rated power per minute, which can be considered a reference for hybrid power plants. For the Netherlands, the maximum active power gradient is 20% of the rated capacity per minute [52].

However, these ramp rate limits are based on a short time scale (minutes) and are implemented in order to prevent large voltage steps and in-rush current during wind farm startups and shutdowns. The restrictions are not intended to control the ramp events that occur during the operation of the farm which are of interest in this study. The current ramp events caused by renewable energy sources on a national scale are minor and easily adjusted by controllable generating units. The issue of ramps will become considerably more critical in the future, as variable renewable energy sources will replace the majority of conventional generating units.

New restrictions on the ramp events in generation need to be introduced for the future with the intent to alleviate the impact of the power fluctuations caused by the variable nature of wind and solar energy. An incentive could be introduced by the system operators or included in the grid codes in order to encourage energy producers to control the severity of ramp events.

As part of this study, a simple penalty function based on the magnitude of the ramp is introduced. Initially, the ramp events are detected in the power signal for both the over-planting scenarios discussed in the previous sections. A penalty price with the units €/ MW is selected and multiplied by the magnitude of each of the ramp events. The total penalty for the year is calculated as a sum of all such individual penalties for both ramp up and ramp down events as given in Equation 6.9 where R_{M_i} is the ramp magnitude.

$$\text{Total Penalty} = \sum_{i=1}^{n} \text{Penalty Price} * R_{M_i} \tag{6.9}$$

The total penalty is internalized in the IRR calculations from the previous section for the two scenarios of over-planting. The total penalty is included in the yearly costs while calculating the IRR of the hybrid power plant. Figure 6.4 gives the IRR with the ramp penalties internalized for the over-planting scenarios considering a penalty price of €200 per MW. It can be seen that the IRR with the wind over-planting decreases with almost the same slope as earlier since the number of ramps does not change much. However, in the solar over-planting scenario the IRR decreases at a faster rate than when the penalties are not internalized. This behavior can be attributed to the increasing ramp events with solar planting. Yet the IRR decrease for solar is still slower and favorable over over-planting with wind after penalizing ramps. At a capacity factor of 0.5 given by the blue and red stars, the IRR for wind is lower than the IRR for the solar over-planting.

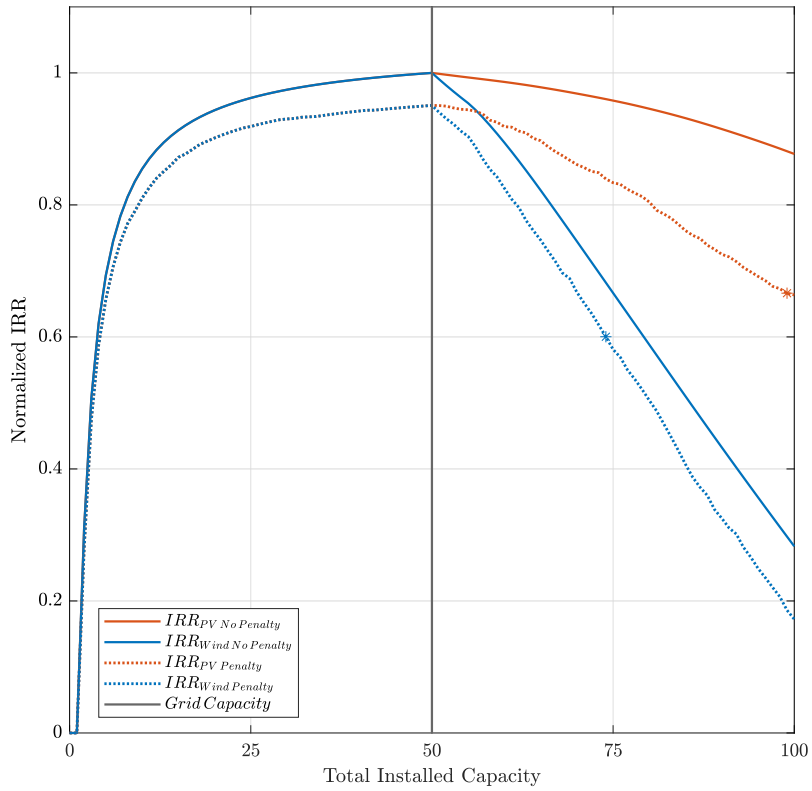

Figure 6.4: IRR for over-planting with penalized ramps

With different penalty prices for the ramp events, the IRR calculated with the internalized ramp costs changes. There will be a driving price of the penalty that determines the selection of over-planting with either wind or solar. For example at the capacity factor of 0.5, a penalty price of €300 per MW or higher would cause the IRR for the solar over-planting case to be lower than the IRR for the wind over-planting as shown in Figure A.4. Hence by internalizing the ramp event costs by giving them an economical value, the sizing decisions of the hybrid power plant are influenced.

7

Battery Storage

This chapter describes the control for the battery storage component to reduce the ramp events in the hybrid power plant. The objective of this chapter is to develop insights into *how the inclusion of battery storage in wind-based hybrid power plants affects ramp events.* Firstly, the optimization problem for the battery charging and discharging is presented in section 7.1. Next, the battery functionality with the hybrid wind-PV power plant for a period of 10 days is presented in section 7.2. Finally, the utility of a battery storage system to remove ramp events is discussed in Section 7.3.

Previously, it was determined that combining solar or over-planting with solar power capacity would increase the number of ramp events in the generation. As a result, while wind and solar complement each other on different scales, solar power generates greater ramps in a wind-based power plant. Currently, the ramp events are not penalized and the producers have no incentive to reduce ramps. However, were this to change in the future, the inclusion of battery storage would provide opportunities to increase the revenue. Battery storage can be controlled by the users and can be used to reduce the ramp events in the generation, unlike solar power which can not be controlled.

The storage technology considered in this study is a Li-ion battery based on the 42.2 kWh BMW-i3 battery shown in Figure 7.1 which is identical to the battery used in the electric cars. The battery capacity is 120 Ah while the nominal voltage of the battery is 352 V [53]. The battery is considered as a one-hour battery, that is it can charge from zero to maximum capacity or discharge from maximum capacity to zero within a period of one hour. Many such battery packs are combined to make up the battery system of the hybrid power plant.

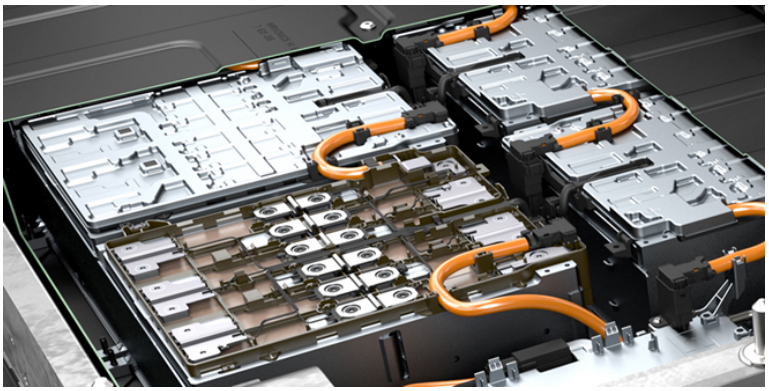

Figure 7.1: BMW i3 42.2 kWh Battery [54]

7.1. Optimization of the battery control strategy for ramps

In this study, a simple methodology is presented to show the functionality of a battery storage system which is used primarily to reduce the ramp events in the generation. The battery control for the hybrid power plant is computed through an optimization problem defined to reduce the intensity of the ramp events as well as smoothen the output generation to the grid.

The operation of the battery is mainly focused on the reduction of the ramp events through charging and discharging of the battery. The wind and solar generation from the power plant are summed up and the total hybrid generation is taken in as the input for the optimization. Figure 7.2 gives an outline of the battery integrated hybrid power plant model. The demand information from the grid in order to predict the significant ramp events is also taken as an input for the battery optimization. The battery is charged or discharged based on the predicted information of the wind power, solar power as well as demand. The battery energy can also be further designed to participate in the balancing market as a source of revenue other than reducing the ramps. A nonlinear optimization problem is defined to minimize the change in magnitude between two consecutive time intervals while satisfying the constraints of eliminating significant ramp events.

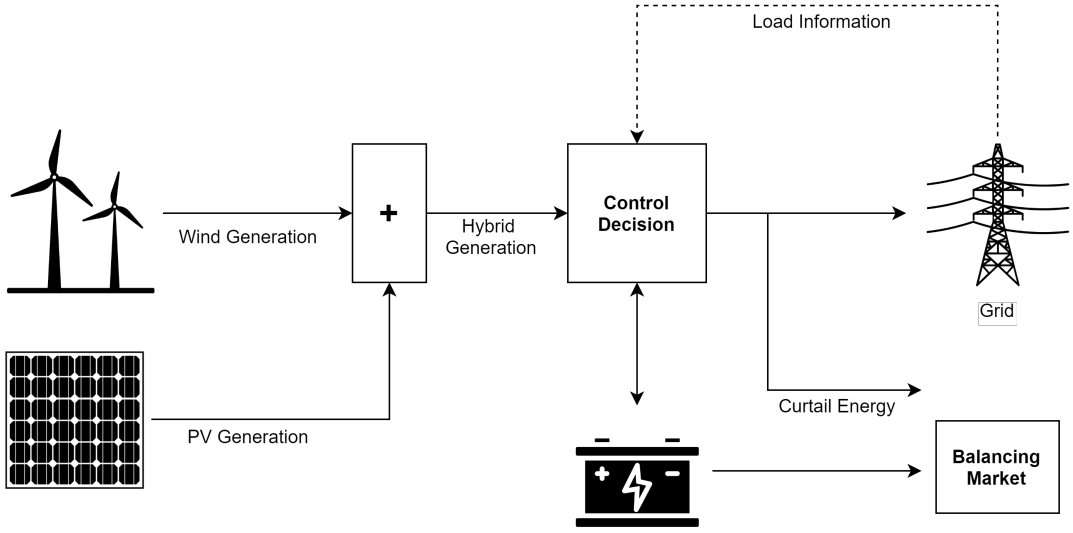

Figure 7.2: Battery integrated system model

7.1.1. Objective: minimize the magnitude change

The objective function of the optimization problem is to minimize the magnitude change in the power between two consecutive time intervals from the total generation. The objective function is given by Equation 7.1 where $f(x)$ gives the magnitude change between the power at point $i+1$ and i. This objective function is defined such that the total power profile after the use of a battery storage system is smoother and consists of comparatively lesser power fluctuations. The objective function is normalized by dividing the optimized output over the original power magnitude change in the power generation without battery storage.

$$\text{Minimize}: f(x) = \frac{|(P(i+1) - x(i+1)) - (P(i) - x(i))|}{|P(i+1) - P(i)|} \tag{7.1}$$

7.1.2. Decision variables

The decision variable in this optimization is the battery power that is either being charged or discharged at each time interval denoted by x_i. The battery power is bounded by the maximum and minimum power that can be put in or removed from the battery given in Equation 7.2. The maximum depends on the nominal energy of the battery in MWh and the time it takes to completely charge or discharge the battery. Similarly, the minimum power is the same value with a negative direction.

$$x_{min} \leq x_i \leq x_{max} \tag{7.2}$$

7.1.3. Constraints

The optimization is bound by constraints in order to maintain the energy being charged or discharged within the limits with the maximum and minimum state of charge as mentioned in Section 3.3. The state of charge constraint is given by Equation 7.3 such that the SOC has to lie between SOC_{min} and SOC_{max}.

$$SOC_{min} \leq SOC_i \leq SOC_{max} \tag{7.3}$$

The SOC is calculated through the battery energy that is either charged E^c_{i+1} or discharged E^d_{i+1} from the battery given by Equations 7.4 and 7.5. The state of charge is calculated as the energy being charged or discharged over the nominal energy of the battery. Hence the battery power x which is the decision variable needs to satisfy the SOC constraints. Further, in the case that the generation is above the grid capacity and the SOC has not reached its maximum value, the excess power beyond the grid capacity is charged in the battery.

$$E^c_{i+1} = E_i + \frac{x_i \eta_c}{4 * E_{nom}} \tag{7.4}$$

$$E^d_{i+1} = E_i - \frac{x_i}{4 * E_{nom} \eta_d} \tag{7.5}$$

The ramp event constraints are given such that the ramp events that occur in the initial generation are either eliminated or the magnitude is reduced by the charging or discharging of the battery. The event detection in this study is done with the significant binary method since the iterations for the optimization with wavelet methods are not computationally feasible. The ramp event constraint is given in Equation 7.6, where R_M is the event magnitude given as the difference between the power at the end and start time of the ramp event. The ramp definition of 20% of the grid capacity is used as the definition for the binary ramp detection method. The power with the battery model is given as G which is equal to the battery power x subtracted from the original generation P and hence the events are detected on this power signal. The events are detected using the optimized swinging door algorithm or the OpSDA discussed in 4.2.2.

The event magnitude R_M is calculated as the difference in power between the end time and start time of the event as given in Equation 7.7. The constraint on the event magnitudes requires the optimized generation to not consist of events of greater than 20% of the grid capacity as given in Equation 7.6. Since the generation is variable, there would be changes in magnitude above the 20% that occur over a longer time duration such as a day. These events would cause the constraint to be violated. Hence, the events shorter than 15 hours are considered events of importance to calculate the magnitudes. A duration of 15 hours is chosen as the maximum since the largest ramps seem to occur in the order of 12 - 14 hours as seen in Table 4.1.

The ramps are detected using the significant binary definition and the load information from the grid is taken as well for determining the significance of the event. The events that are considered are the events that occur with the opposite trend to the load at the same interval and hence significant and the correlation coefficient r_{GL} between the generation and load is less than 0.

$$R_M < 20\%\ P_{grid\ cap} \tag{7.6}$$

$$\begin{aligned} &R_M = |G_{R,end} - G_{R,start}| \\ &\text{where,} \\ &R_D = t_{end} - t_{start} \leq 15\text{h} \\ &r_{GL} = \frac{\sum_{i=T_{start}}^{T_{end}} \left(G_i - \bar{G}\right)\left(L_i - \bar{L}\right)}{\sqrt{\sum_{i=T_{start}}^{T_{end}} \left(G_i - \bar{G}\right)^2} \sqrt{\sum_{i=T_{start}}^{T_{end}} \left(L_i - \bar{L}\right)^2}} < 0 \end{aligned} \tag{7.7}$$

7.2. Battery functionality

The optimization is carried out for the reference site of the Haringvliet energy park used in the previous sections. A wind capacity of 50 MW and solar capacity of 30 MW is taken as an example to better depict the ramp events and the operation of the battery. A one-hour battery storage system of 50 MWh is considered in this section. The maximum and minimum battery power of the battery system is 50 MW and -50 MW. The SOC_{min} and SOC_{max} are taken as 20% and 100%.

Figure 7.3 gives the functioning of the battery storage system strategy to remove ramp events in the generation for a period of 10 days. The blue curve gives the original generation without the battery. It can be seen that there are sudden changes in magnitude on days 4 and 5 for example. On days 8 and 9, the generation is more than the grid capacity of 50 MW and in the case without the battery system, the excess energy would have to be curtailed. The black curve gives the optimized generation with the battery system. It can be noticed that the new power signal is much smoother and has fewer fluctuations in the signal. On day 3, the sudden changes in power are caused by the solar generation with possible interruption by clouds. This event is smoothened out and the sudden fluctuations are eliminated through the usage of the battery. Figure 7.4 gives the SOC of the battery system for the 10 day period. The state of charge varies between the minimum and maximum SOC values based on whether the battery is being charged or discharged. In this procedure, a perfect prediction of the wind and solar resources is assumed to plan the battery strategy.

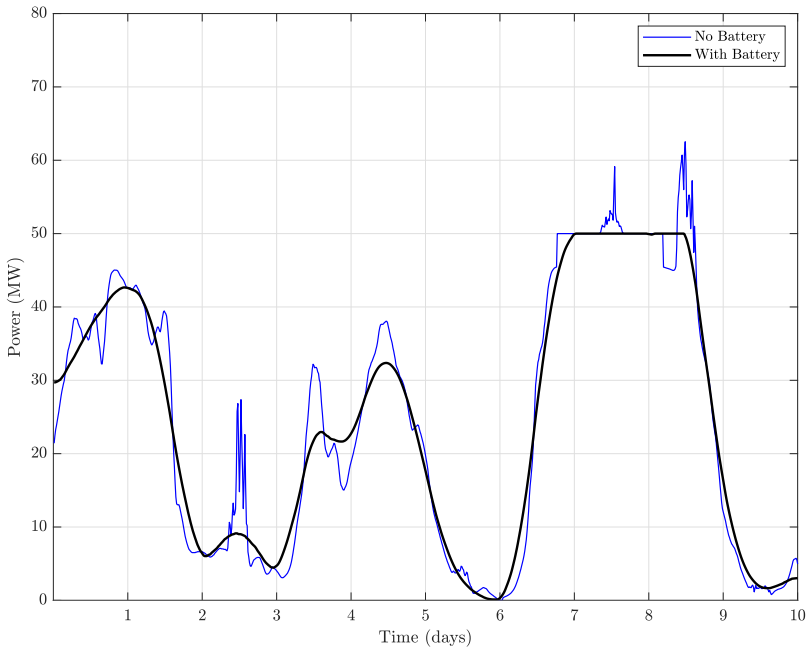

Figure 7.3: Hybrid power plant output with and without battery

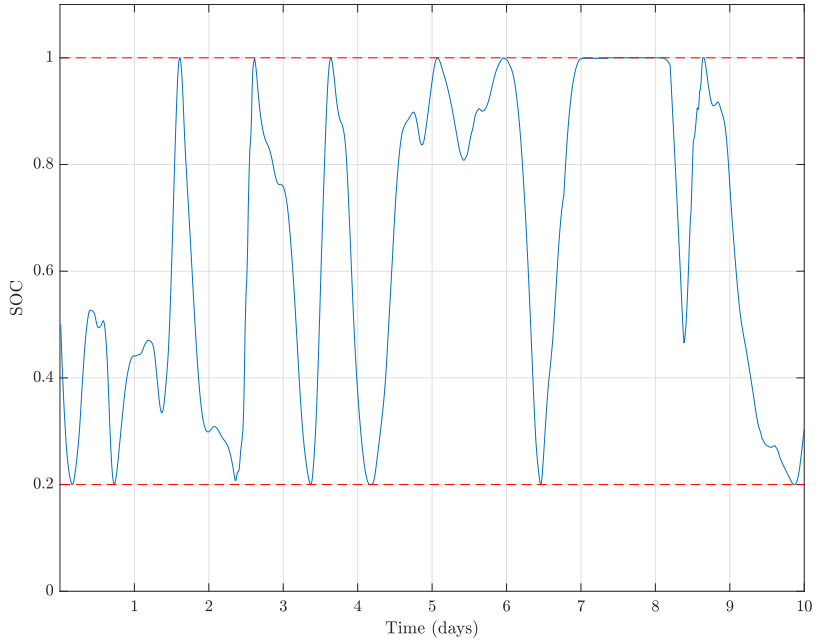

Figure 7.4: State of charge of the battery

Significant ramp events in the original generation are given in Figure 7.5 such that ramp ups occur on days 3 and 4 while ramp downs occur on days 2, 3 and 4. In the new power signal with battery, the ramp up event and ramp down event on day 2 are eliminated by charging the battery during the events. The magnitude of the ramp up event on day 4 is reduced such that it is under the threshold value. The ramp down events on days 2 and 4 are spread out over a longer duration of almost a day. These events would no longer be significant owing to the longer duration. The ramp detection is run again on the new power signal and the number of ramps detected is zero. As a result, the battery smooths the power output while removing the ramp occurrences in the power signal.

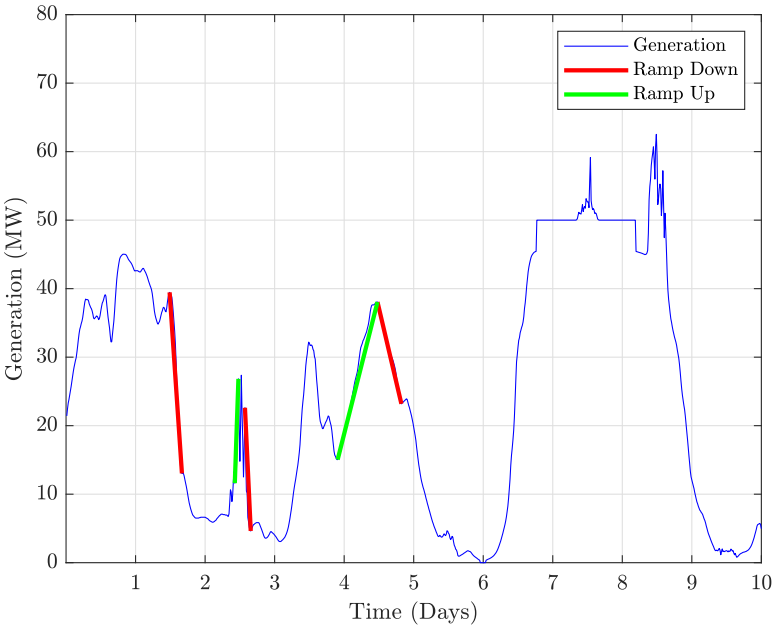

Figure 7.5: Significant ramps in the 10 day period

In the earlier case, the information of the entire 10 day period is assumed to be available perfectly to plan the battery charging and discharging. Figure 7.6 illustrates the battery included hybrid generation where only the daily information is available. The battery control strategy is such that the ramp events and fluctuations are removed on a daily scale. This method removes the ramp events by tending to flatten the output when possible. However, this causes ramp events between each day in a duration of less than one hour. In this strategy, the output tends to be flatter which may also be beneficial for selling the energy in electricity markets.

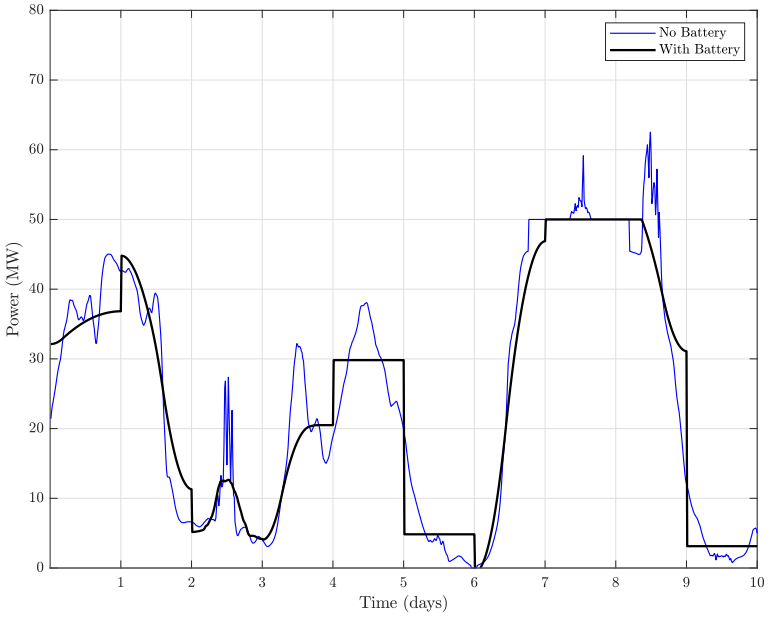

Figure 7.6: Battery operation with daily information

In order to validate the optimization model, the battery sizing is changed to 1000 MWh. The resulting total generation signal with the battery is a flat curve over the time period that is considered. This is expected since the battery sizing gives the freedom to charge and discharge all the energy such that the power changes are tending towards zero and the ramp events are completely eliminated.

7.3. Ramp mitigation with batteries

The magnitudes of the ramp events are reduced or the events are spread out over a longer time to eliminate the significant ramp events using the battery. The functionality of a simple battery strategy to eliminate ramp events is presented in Section 7.2. The model is based on several assumptions and simplified calculations. However, it can be summarized that a battery system could be used in a wind-based hybrid power plant in order to alleviate the effect of fluctuations and ramp events. In the case without the battery system, the generation above the grid connection is curtailed.

If the grid connection of the hybrid power plant is filled with wind energy and over-planted with solar owing to the better IRR, there will be many instances when the solar generation adds up to the wind generation which is at its rated generation. The excess solar generation in such cases can be stored in the battery and discharged in the future to deal with the ramp events. Furthermore, the over-planting with solar energy could be replaced by a storage system. Since the ramp events as presented earlier increase with the share of solar power, removing or reducing the installed solar capacity and replacing it with storage could be more effective in terms of reducing ramp events.

8

Conclusions

8.1. Summary and Discussion

This research investigated how to best characterize ramp events caused by electricity generation from a wind-based hybrid power plant and used the findings to study the impact of system design with respect to ramp mitigation and profitability considering solar and/or batteries to form the hybrid. The detection of ramp events is a challenge in terms of determining how to distinguish ramps from incoherent fluctuations in the power. Several methods of characterizing the ramps based on the magnitudes and duration were explored. Adopted from Bedassa et al. [33], a method employing wavelet transforms to obtain surrogate models for detecting ramp events was used, developed further and applied in this research. The main findings are summarized in the following:

- Owing to the dependency on the ramp definitions, which are varying throughout literature, and the disadvantages of calculating thresholds as a percentage of the capacity, it was shown that binary ramp definitions are very case dependent in their usefulness and lead to under-detection. The wavelet method, on the other hand, uses statistically determined threshold values to extract ramp events and the problem of under-detection is reduced.
- The method of significant ramps, proposed here, helps to identify which ramp events are of importance and which ramp events would be much less disruptive and may be ignored. The proposed "significant wavelet ramp method" is, hence, selected as the metric to characterize ramp events of a wind-based hybrid power plant.
- It was shown that the anti-correlation of wind and solar resources alone does not yield complete information on ramp events. It is necessary to have complementarity (or anti-correlations) at shorter time resolutions such as 15 minutes or an hour. A seasonal anti-correlation may be beneficial for national system adequacy, but not for daily ramping events.
- In order to minimize the ramp events, it is preferred to fill up the grid capacity with wind power as solar power would cause additional ramps. In the wind over-planting case, very few new ramps are detected whereas with solar over-planting the number of new ramps increases significantly as the solar capacity increases.
- The capacity factor in both over-planting cases increases with wind having a faster increase while the IRR drop is less steep in the solar over-planting case. The analysis shows that the choice of wind or solar over-planting could be driven by a penalty price that internalizes the ramp events.
- Compared to solar over-planting, the inclusion of a battery control strategy to reduce the ramp events could be more effective and/or more economical.

The main objective of the research was to *characterize the ramping behavior and system impact of wind-based hybrid power plants*. The complementarity analysis of the site alone is not sufficient to promise a smoother output from the wind - PV power plants which is often assumed in the literature. The significant wavelet method of extracting ramp events results in the most conclusive characterization of the ramp events in the hybrid power plant. For a future with a high market share of variable renewable energy sources, it is recommended to consider the demand information while defining ramps events. More importance must be given to the power ramp events either through penalizing ramps or having stricter grid codes as the ramp events become more frequent and threatening. Unless ramp events are handled through storage systems, it will be challenging to phase out the dependence on conventional generation units. The ramp events need to be considered during the initial sizing and development with possible inclusion of a ramp-reducing battery strategy. A comprehensive study of ramp events in hybrid power plants is helpful in understanding the importance of reducing and handling ramp events for both the system operator as well as the producer.

8.2. Recommendations

This research provides insight into the characterization of ramp events and the impact of the ramp events on the system design. However, there are several limitations to the methods used which are discussed in this section.

- The analysis is considered on a single location and the results could vary for a different site where the anti-correlation is very strong or weak. It is recommended to perform further studies for locations with different conditions.
- The scoring of the significance of the ramp events is achieved primarily on the sign of the correlation of the generation and load during the occurrence of the event. Different significance could be given to different ramps based on the severity by scoring the correlations. For future research, it is recommended to incorporate this method of discriminating different ramp events.
- The penalty cost due to ramp events included in the yearly costs is based on a constant price which is multiplied by the magnitude of the ramp. In future research, a dynamic penalty can be introduced which changes based on both the magnitude as well as the duration of the ramp event.
- The battery model for reducing the ramp events is based on crude calculations as this was sufficient to demonstrate the possible utilization of a storage system in alleviating the effect of ramp events. More detailed modeling of the battery with this strategy is recommended for future research. It was also assumed that the battery would not provide any balancing or ancillary services. The balancing and ancillary services market could be an added source of income for the hybrid power plant. Therefore, developing a battery capable of performing balancing functions would be an intriguing subject for future research.
- The wind, solar and demand data used for the analysis are for a single year for 2019. This information is sufficient to compare different ramp definitions and detection methods but the same data is assumed for the lifetime of the plant in the IRR analysis. Further, the electricity prices are taken for a single year. This method excludes the possible increase or decrease in prices in the future due to the increased market share of variable renewable energy. Therefore more extensive modeling of the future prices and weather conditions is recommended for future study.

This research shows the methods to detect ramp events and analyze the impacts on the system sizing and decisions. It provides a valuable method of significant ramp detection that could be used for any type of variable renewable generation. The work introduces possible economic value to the reducing ramps in the production which would be helpful to the system operator and ultimately the reliability of the grid.

Bibliography

[1] Katherine Dykes, Jennifer King, Nicholas Diorio, Ryan King, Vahan Gevorgian, Dave Corbus, Nate Blair, Kate Anderson, Greg Stark, Craig Turchi, Patrick Moriarty, Katherine Dykes, Jennifer King, Nicholas Diorio, Vahan Gevorgian, Dave Corbus, Nate Blair, Greg Stark, Craig Turchi, and Patrick Moriarty. Opportunities for Research and Development of Hybrid Power Plants. *Nrel/Tp-5000-75026*, 5 2020. doi: 10.2172/1659803.

[2] Rashid Al Badwawi, Mohammad Abusara, and Tapas Mallick. A Review of Hybrid Solar PV and Wind Energy System. *Smart Science*, 3(3):127–138, 2015. doi: 10.1080/23080477.2015.11665647.

[3] Mingjian Cui, Jie Zhang, Cong Feng, Anthony R. Florita, Yuanzhang Sun, and Bri Mathias Hodge. Characterizing and analyzing ramping events in wind power, solar power, load, and netload. *Renewable Energy*, 111:227–244, 2017. ISSN 18790682. doi: 10.1016/j.renene.2017.04.005.

[4] Mingjian Cui, Bri-Mathias Hodge, Anthony Florita, and Jeffrey Freedman. Ramp forecasting performance from improved short-term wind power forecasting over multiple spatial and temporal scales. *Energy*, 122:528–541, 2017. ISSN 03605442. doi: 10.1016/j.energy.2017.01.104.

[5] Mingjian Cui, Jie Zhang, Anthony R. Florita, Bri Mathias Hodge, Deping Ke, and Yuanzhang Sun. An optimized swinging door algorithm for wind power ramp event detection. *IEEE Power and Energy Society General Meeting*, 2015-Septe(August), 2015. ISSN 19449933. doi: 10.1109/PESGM.2015.7286272.

[6] Vasiliki Klonari, Daniel Fraile, Raffaele Rossi, and Michael Schmela. Exploring the Viability of Hybrid Wind-Solar Power Plants. *4th International Hybrid Power Systems Workshop*, pages 1–7, 2019.

[7] J. Jurasz, F. A. Canales, A. Kies, M. Guezgouz, and A. Beluco. A review on the complementarity of renewable energy sources: Concept, metrics, application and future research directions. *Solar Energy*, 195: 703–724, 2020. ISSN 0038092X. doi: 10.1016/j.solener.2019.11.087.

[8] Abhnil A. Prasad, Robert A. Taylor, and Merlinde Kay. Assessment of solar and wind resource synergy in Australia. *Applied Energy*, 190:354–367, 2017. ISSN 03062619. doi: 10.1016/j.apenergy.2016.12.135.

[9] Franciele Weschenfelder, Gustavo de Novaes Pires Leite, Alexandre Carlos Araújo da Costa, Olga de Castro Vilela, Claudio Moises Ribeiro, Alvaro Antonio Villa Ochoa, and Alex Maurício Araújo. A review on the complementarity between grid-connected solar and wind power systems. *Journal of Cleaner Production*, 257:120617, 2020. ISSN 09596526. doi: 10.1016/j.jclepro.2020.120617.

[10] Joakim Widén. Correlations between large-scale solar and wind power in a future scenario for Sweden. *IEEE Transactions on Sustainable Energy*, 2(2):177–184, 2011. ISSN 19493029. doi: 10.1109/TSTE.2010.2101620.

[11] Chandrika Kamath. Using simple statistical analysis of historical data to understand wind ramp events. 1 2010. doi: 10.2172/972427.

[12] Cristobal Gallego-Castillo, Alvaro Cuerva-Tejero, and Oscar Lopez-Garcia. A review on the recent history of wind power ramp forecasting. *Renewable and Sustainable Energy Reviews*, 52:1148–1157, 2015. doi: 10.1016/j.rser.2015.07.154.

[13] Miguel Angel Gonzalez-Salazar, Trevor Kirsten, and Lubos Prchlik. Review of the operational flexibility and emissions of gas- and coal-fired power plants in a future with growing renewables. *Renewable and Sustainable Energy Reviews*, 82:1497–1513, 2018. ISSN 1364-0321. doi: https://doi.org/10.1016/j.rser.2017.05.278.

[14] California ISO. Energy and environmental goals drive change. *Technical Report*, page 4, 2016.

[15] C Ferreira. A Survey of Wind Power Ramp Forecasting. 05(04):368–372, 2011. ISSN 1949-243X. doi: 10.4236/epe.2013.54b071.

[16] Chandrika Kamath. Understanding wind ramp events through analysis of historical data. *2010 IEEE PES Transmission and Distribution Conference and Exposition: Smart Solutions for a Changing World*, 2010. doi: 10.1109/TDC.2010.5484508.

[17] Nicholas Cutler, Merlinde Kay, Kieran Jacka, and Torben Skov Nielsen. Detecting, categorizing and forecasting large ramps in wind farm power output using meteorological observations and WPPT. *Wind Energy*, 10(5):453–470, 2007. ISSN 10954244. doi: 10.1002/we.235.

[18] Jeffrey Freedman, Michael Markus, and Richard Penc. Analysis of west texas wind plant ramp-up and ramp-down events. *Technical report AWS Truewind*, 01 2008.

[19] AWS Truewind. Aws truewind's final report for the alberta forecasting pilot project. *Wind Power Forecasting PILOT Project*, 66, 2008.

[20] Cameron W. Potter, Eric Grimit, and Bart Nijssen. Potential benefits of a dedicated probabilistic rapid ramp event forecast tool. *2009 IEEE/PES Power Systems Conference and Exposition*, pages 1–5, 2009. doi: 10.1109/PSCE.2009.4840109.

[21] Beatrice Greaves, Jonathan Collins, Jeremy Parkes, and Andrew Tindal. Temporal forecast uncertainty for ramp events. *Wind Engineering*, 33(4):309–319, 2009. doi: 10.1260/030952409789685681.

[22] PL Barbour, S Casey, and SN Walker. Evaluation of bpa vendors wind plant'wind ramp event'tracking system. *Energy Resources Research Laboratory*, 2010.

[23] Craig Collier, Jeremy Parkes, Jon Collins, Lars Landberg, and GL Garrad Hassan. Improved ramp event forecasting using upstream wind measurements. *European Wind Energy Conference*, 2010.

[24] Kristen T Bradford, RL Carpenter, and Brent Shaw. Forecasting southern plains wind ramp events using the wrf model at 3-km. *AMS Student Conference*, 2010.

[25] Arthur Bossavy, Robin Girard, and Georges Kariniotakis. Forecasting uncertainty related to ramps of wind power production. *European Wind Energy Conference and Exhibition 2010, EWEC 2010*, 2:9–pages, 2010.

[26] Q. Yang, L.K. Berg, M. Pekour, J.D. Fast, R.K. Newsom, M. Stoelinga, and C. Finley. Evaluation of wrf-predicted near-hub-height winds and ramp events over a pacific northwest site with complex terrain. *Journal of Applied Meteorology and Climatology*, 52(8):1753–1763, 2013. doi: 10.1175/JAMC-D-12-0267.1.

[27] Ángela Fernández, Carlos M. Alaíz, Ana M. González, Julia Díaz, and José R. Dorronsoro. Diffusion methods for wind power ramp detection. *Advances in Computational Intelligence*, pages 106–113, 2013. doi: 10.1007/978-3-642-38679-4_9.

[28] A Suzuki, J Parkes, P Shaw, C Collier, and L Landberg. Use of offsite data to improve short term ramp forecasting. *European Wind Energy Association Conference Proceedings*, 2012.

[29] Pål Preede Revheim and Hans Georg Beyer. Using random forests for wind power ramp forecasting. *European Wind Energy Conference*, 03 2014.

[30] Cristóbal Gallego, Álvaro Cuerva, and Alexandre Costa. Detecting and characterising ramp events in wind power time series. *Journal of Physics: Conference Series*, 555(1), 2014. ISSN 17426596. doi: 10.1088/1742-6596/555/1/012040.

[31] Hengxu Zhang, Yongji Cao, Yi Zhang, and Vladimir Terzija. Quantitative synergy assessment of regional wind-solar energy resources based on MERRA reanalysis data. *Applied Energy*, 216(February):172–182, 2018. ISSN 03062619. doi: 10.1016/j.apenergy.2018.02.094.

[32] Mingjian Cui, Jie Zhang, Anthony R. Florita, Bri Mathias Hodge, Deping Ke, and Yuanzhang Sun. An optimized swinging door algorithm for identifying wind ramping events. *IEEE Transactions on Sustainable Energy*, 7(1):150–162, 2016. ISSN 19493029. doi: 10.1109/TSTE.2015.2477244.

[33] Bedassa R. Cheneka, Simon J. Watson, and Sukanta Basu. A simple methodology to detect and quantify wind power ramps. *Wind Energy Science*, 5(4):1731–1741, 2020. ISSN 23667451. doi: 10.5194/wes-5-1731-2020.

[34] Jie Wan, Yanjia Wang, Guorui Ren, Jinfu Liu, Wei Wang, and Jilai Yu. An integrated evaluation method of the wind power ramp event based on generalized information of the source, grid, and load. *Energies*, 13 (24), 2020. ISSN 1996-1073. doi: 10.3390/en13246503. URL https://www.mdpi.com/1996-1073/13/24/6503.

[35] David Faiman. Assessing the outdoor operating temperature of photovoltaic modules. *Progress in Photovoltaics: Research and Applications*, 16(4):307–315, 2008. doi: https://doi.org/10.1002/pip.813.

[36] A. Smets, K. Jäger, O. Isabella, R. van Swaaij, and M. Zeman. *Solar Energy: The Physics and Engineering of Photovoltaic Conversion, Technologies and Systems*. UIT Cambridge, 2016. ISBN 9781906860325.

[37] ENTSO-E. Transparency Platform. URL https://transparency.entsoe.eu/load-domain/r2/totalLoadR2/show.

[38] The Wind Power. Nordex N117/3600 - Manufacturers and turbines. URL https://www.thewindpower.net/turbine_en_1362_nordex_n117-3600.php.

[39] JA solar. 345W Module Datasheet. pages 9–10. URL http://www.jasolar.com/html/en/2018/en_smodule/11.html.

[40] Li Han, Yan Qiao, Mengjie Li, and Liping Shi. Wind Power Ramp Event Forecasting Based on Feature Extraction and Deep Learning. *Energies*, 13(23), 2020. ISSN 1996-1073. doi: 10.3390/en13236449.

[41] Mingjian Cui, Jie Zhang, Anthony Florita, Bri-Mathias Hodge, Deping Ke, and Yuanzhang Sun. Solar Power Ramp Events Detection Using an Optimized Swinging Door Algorithm. (August), 2015. doi: 10.1115/detc2015-46849.

[42] Sheng Zhou, Yu Wang, Yuyu Zhou, Leon Clarke, and James Edmonds. Roles of wind and solar energy in china's power sector: Implications of intermittency constraints. *Applied Energy*, 213:22–30, 03 2018. doi: 10.1016/j.apenergy.2018.01.025.

[43] Pedro Bezerra Leite Neto, Osvaldo R. Saavedra, and Denisson Q. Oliveira. The effect of complementarity between solar, wind and tidal energy in isolated hybrid microgrids. *Renewable Energy*, 147:339–355, 2020. ISSN 18790682. doi: 10.1016/j.renene.2019.08.134.

[44] Hannele Holttinen. Hourly wind power variations in the nordic countries. *Wind Energy*, 8(2):173–195, 2005. doi: https://doi.org/10.1002/we.144.

[45] M. Asghar Bhatti. *Optimization Problem Formulation*, pages 1–45. Springer New York, New York, NY, 2000. ISBN 978-1-4612-0501-2. doi: 10.1007/978-1-4612-0501-2_1.

[46] Kaushik Das, Anca D Hansen, Matti Koivisto, and Poul E Sørensen. Enhanced Features of Wind-Based Hybrid Power Plants. *4th International Hybrid Power Systems Workshop*, (May), 2019.

[47] WindEurope. Renewable Hybrid Power Plants Exploring the benefits and market opportunities. *Position papers*, 2019.

[48] WindEurope. Financing and investment trends: The European wind industry in 2019. *WindEurope*, pages 37–39, 2020.

[49] Ran Fu, David Feldman, Robert Margolis, Mike Woodhouse, Kristen Ardani, Ran Fu, David Feldman, Robert Margolis, Mike Woodhouse, and Kristen Ardani. U.S. Solar Photovoltaic System and Energy Storage Cost Benchmark: Q1 2020. *National Renewable Energy Laboratory*, pages 1–120, 2021.

[50] TenneT. Costs of a grid connection. URL https://www.tennet.eu/electricity-market/connecting-to-the-dutch-high-voltage-grid/costs-of-a-grid-connection/.

[51] Constantinos Sourkounis and Pavlos Tourou. Grid Code Requirements for Wind Power Integration in Europe. *Conference Papers in Energy*, 2013:1–9, 2013. doi: 10.1155/2013/437674.

[52] Regeling Wetten.nl. Netcode elektriciteit - BWBR0037940. 2021. URL https://wetten.overheid.nl/BWBR0037940/2021-07-03.

[53] BMW. Technical specifications. BMW i3 (120 Ah). 2018. URL https://www.press.bmwgroup.com/global/article/attachment/T0284828EN/415571.

[54] Charged EVs. BMW establishes retirement plan for EV batteries . URL https://chargedevs.com/newswire/bmw-establishes-retirement-plan-for-ev-batteries/.

A

Appendix

A.1. Daily average profiles at reference site

Figure A.1 and A.2 give the average daily profiles for each month of the year for the reference site. As mentioned in Section 3.4, it can be clearly seen that wind speeds in the winter months are higher while the solar irradiance is low.

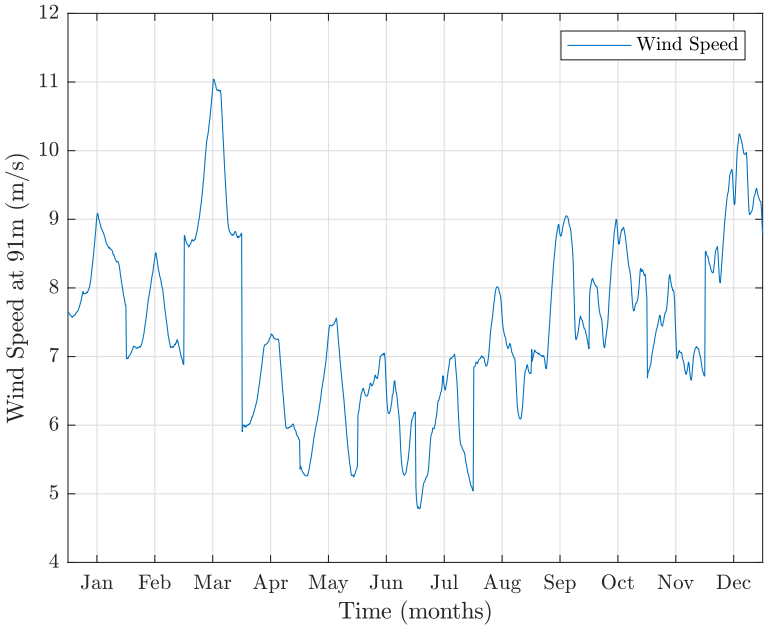

Figure A.1: Monthly average wind profiles

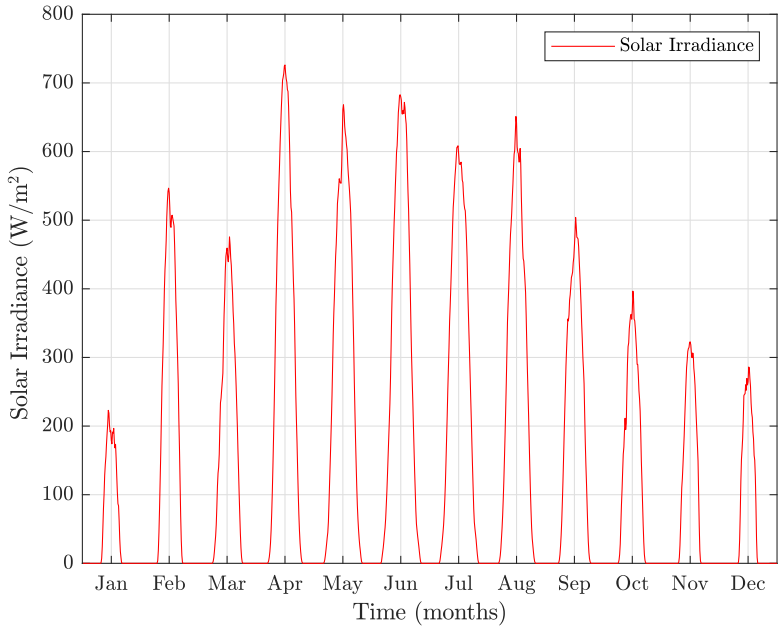

Figure A.2: Monthly average solar profiles

A.2. National wind and solar correlation

Table A.1 gives the correlations between the national wind and solar power on the hourly and daily scale. It can be noticed that there exists a week negative correlation on an hourly scale while the daily totals have a strong negative correlation.

Month	Correlation Coefficient	
	Hourly Totals	Daily Totals
January	-0.16	-0.47
February	-0.23	-0.49
March	-0.15	-0.35
April	-0.03	0.41
May	-0.16	-0.36
June	-0.09	-0.24
July	-0.03	0.04
August	-0.06	-0.32
September	-0.16	-0.49
October	-0.13	-0.16
November	-0.14	-0.42
December	-0.06	-0.16

Table A.1: Correlation between the hourly and daily totals of national wind power and solar power for each month

Figure A.3 gives the variability and correlations of wind and solar power of the nation on different time scales. In Figure A.3a, there exists a strong anti-correlation or negative correlation of -0.85 for monthly totals of the wind and solar power. The daily total time scale shows a weaker yet negative correlation of -0.42. On the hourly scale, the wind and solar have a weak negative correlation of -0.2.

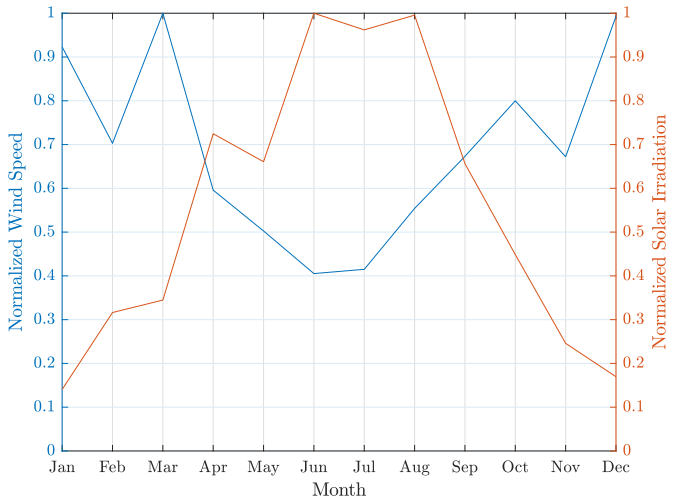

(a) Monthly totals ($r_{Wind\,PV} = -0.85$)

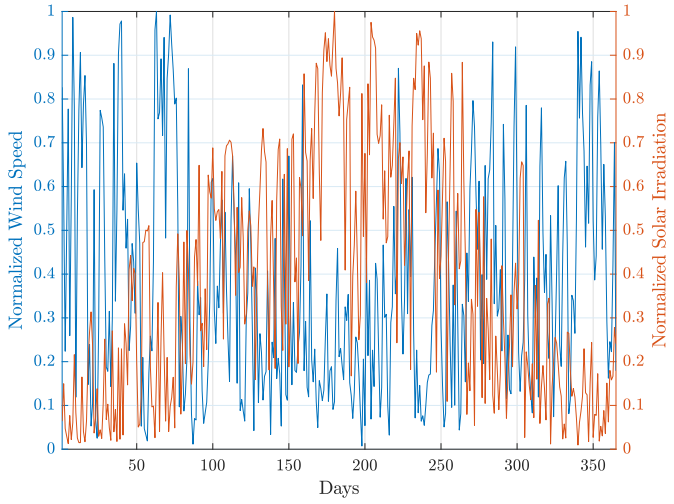

(b) Daily totals ($r_{Wind\,PV} = -0.42$)

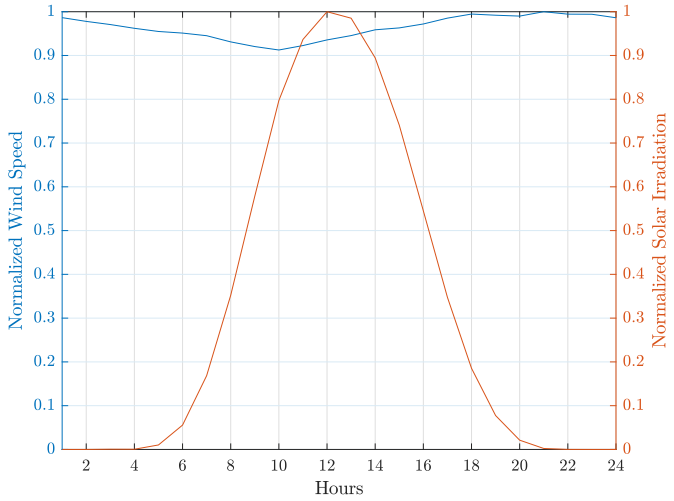

(c) Hourly totals ($r_{Wind\,PV} = -0.2$)

Figure A.3: Variability and correlation coefficients between national wind and solar power on different time scales

A.3. Economic analysis

Figure A.4 depicts the IRR with the ramp penalties internalized for the over-planting scenarios with a penalty price of €300 per MW. It can be seen that at the capacity factor of 0.5 the IRR for the solar over-planting case is lower than the IRR for the wind over-planting. The solar over-planting in this case becomes less favourable as the penalty price goes beyond this tipping point.

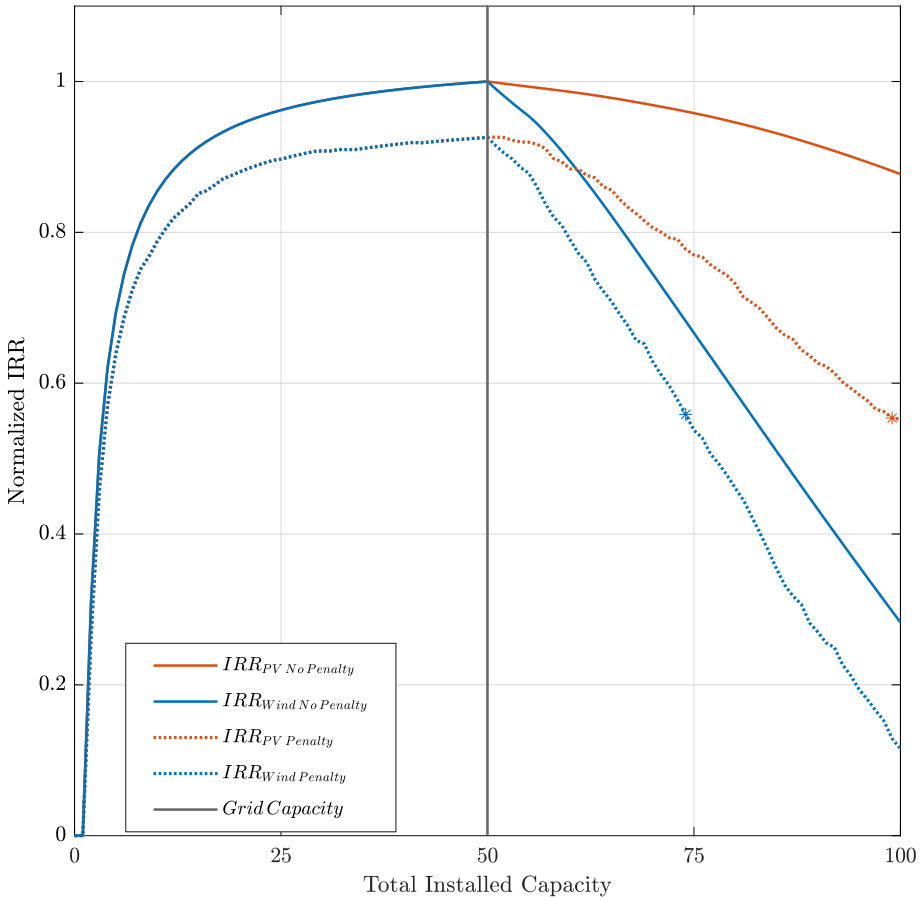

Figure A.4: IRR for over-planting with penalized ramps with 300 €/MW